A METHODOLOGY TO REDUCE DIMENSIONALITY OF A COMMERCIAL SUPERSONIC TRANSPORT DESIGN SPACE USING ACTIVE SUBSPACES

A Thesis
Presented to
The Academic Faculty

by

Nathan Thomas Crane

In Partial Fulfillment
of the Requirements for the Degree
Master of Science in the
Guggenheim School of Aerospace Engineering

Georgia Institute of Technology
May 2020

A METHODOLOGY TO REDUCE DIMENSIONALITY OF A COMMERCIAL SUPERSONIC TRANSPORT DESIGN SPACE USING ACTIVE SUBSPACES

Approved by:

Dr. Dimitri Mavris, Advisor
School of Aerospace Engineering
Georgia Institute of Technology

Dr. Jimmy Tai
School of Aerospace Engineering
Georgia Institute of Technology

Dr. Chung Lee
School of Aerospace Engineering
Georgia Institute of Technology

Date Approved: April 16, 2020

To the future of aerospace; may we one day speed across the sky again.

ACKNOWLEDGEMENTS

I would like to start by thanking my parents and brothers for always encouraging and believing in me, even when all of my engineering talk may not make sense. Thank you for listening and trying to understand anyway.

Additional acknowledgement needs to go to Dr. Mavris, Dr. Tai, and Dr. Lee for guiding me throughout this process and continuing to point me in the correct direction. Thank you for your help with this paper and with everything throughout my limited time at ASDL.

Finally, I would like to thank all of those who have helped me personally through this process. I could not have finished this without your constant support and belief in me even when I may have had doubts.

Thank you all.

TABLE OF CONTENTS

LIST OF TABLES

LIST OF FIGURES

LIST OF SYMBOLS AND ABBREVIATIONS

AS	Active Subspace
CAD	Computer Aided Drafting
CFD	Computational Fluid Dynamics
C_D	Coefficient of Drag
C_L	Coefficient of Lift
DoE	Design of Experiments
DV	Design Variable
ESP	Engineering Sketch Pad
LE	Leading Edge
Mid	Mid Airfoil Section
nm	Nautical Miles
OS	Oversampling
Root	Root Airfoil Section
t/c	Thickness to Chord
Tip	Tip Airfoil Section
VSP	Vehicle Sketch Pad

SUMMARY

As the commercial aviation industry continues to grow, the next technological leap is speed. Commercial supersonic transports are reappearing from multiple companies focused on different areas in the commercial aviation sector. Even though this problem has been solved before by Concorde and the TU-144, the design problem is still difficult. Supersonic design is highly interdisciplinary, lacks historical data, and requires additional design considerations earlier in the design cycle. With a larger number of design variables and the need to use higher fidelity analysis in the design process, due to lack of historical data to generate empirical equations, supersonic design computational cost can rapidly grow. High computational cost leads to point designs or limited design space exploration. To address this issue, the dimensionality of the design space needs to be reduced without removing the effects from the design variables. A recent technique called Active Subspaces has been shown to accomplish this goal by rotating a design space into the most active direction and taking surrogates in this active direction. Through rotation, the effects of each design variable are still present, but less impactful directions can be removed from the surrogate model. This research applies this method to a commercial supersonic design space and asks additional questions about gradient oversampling needed for good active subspace fits, if a better active subspace could be found in a partition of the full design space, and how the goodness of an initial surrogate affects the active subspace surrogate if gradients are taken from the original surrogate. Finally, the research compares computational cost between creating a traditional surrogate of a design space compared to integrating an active subspace.

The research questions were addressed through a data collection flow starting at a design of experiments of 20 planform variables. These configurations were fed into Engineering Sketch Pad to generate the geometry. The geometry was then fed into CART3D to perform analysis on the cruise performance of each configuration. Finally, the aerodynamic coefficients were taken from the CFD results and tabulated. These results were post processed, and the design space was analyzed. A traditional surrogate was created. From this surrogate, gradients were taken to develop active subspace variables, and these variables were used to generate a sweep of active subspace surrogates starting with 1 active subspace variable continuing until the surrogate was made of all 20 variables. Using this data to answer the research questions, it was found that oversampling gradients beyond the published range does not decrease error, and undersampling increases error but not at the significance which was expected. An active subspace in a local partition of a design space did reduce error initially but the error reduction decreased as more variables were included in the active subspace surrogate. The number of cases per design variable of an initial surrogate used to calculate gradients was significant and error of an active subspace surrogate decreased until the number of cases reached 50 cases per design variable. After this number, the decrease in error plateaued. Finally, active subspaces saw a large potential to reduce computational time, as a small reduction in dimensionality could greatly reduce cases needed, especially if gradients could be found within a tool. Using these results, a design methodology was presented incorporating active subspaces into the design loop.

CHAPTER 1. INTRODUCTION AND BACKGROUND

1.1 Introduction and Motivation

The commercial aviation industry has united the world, allowing people to travel to places infeasible on foot or even by automobile. The industry is consistently growing and is expected to continue growing well into the future. Figure 1 shows the projected growth is attributed to a major growth in air travel in China, South Asia, and the Middle East. This expansion is occurring as large emerging economies increase in tourism and overall GDP growth enables access to air travel for a larger portion of the world population [1][2].

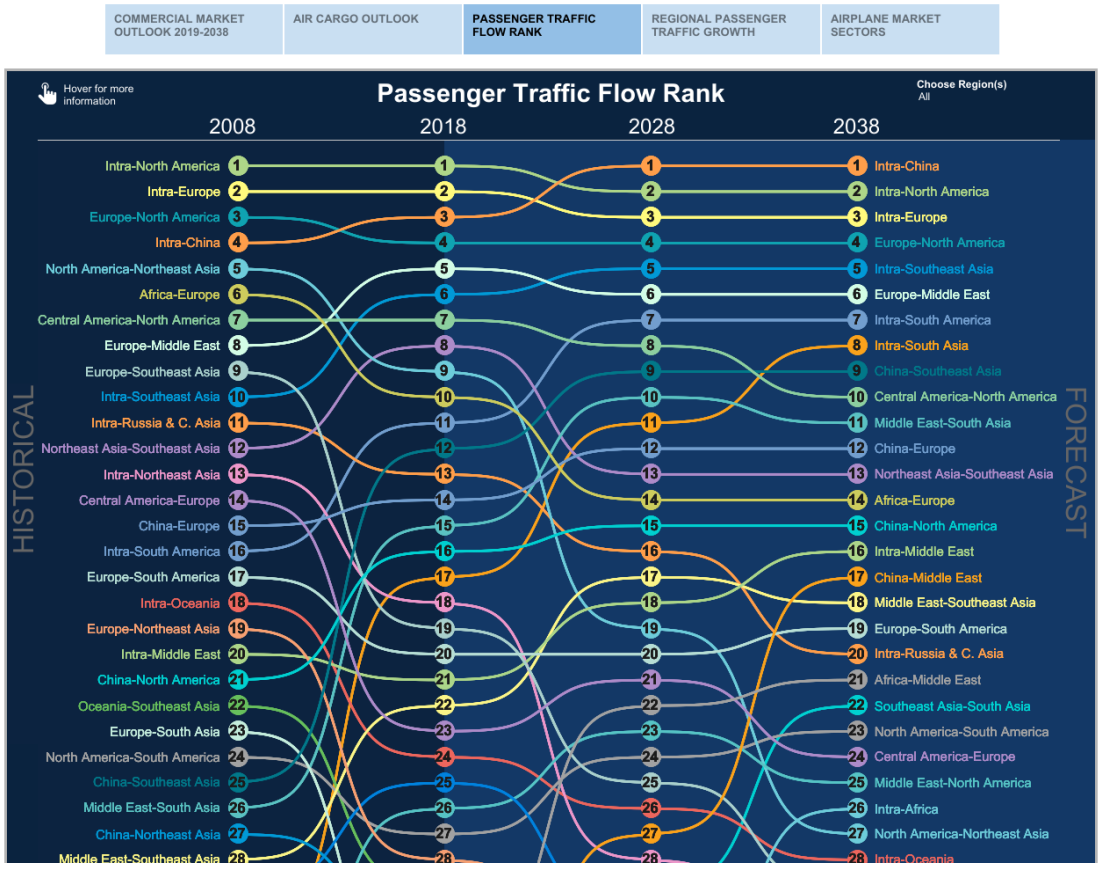

Figure 1: Boeing Passenger Traffic Flow Rank from 2008 to 2038 [1]

From this continuous growth, Figure 2 shows that the number of passengers is expected to double between 2018 and 2033.

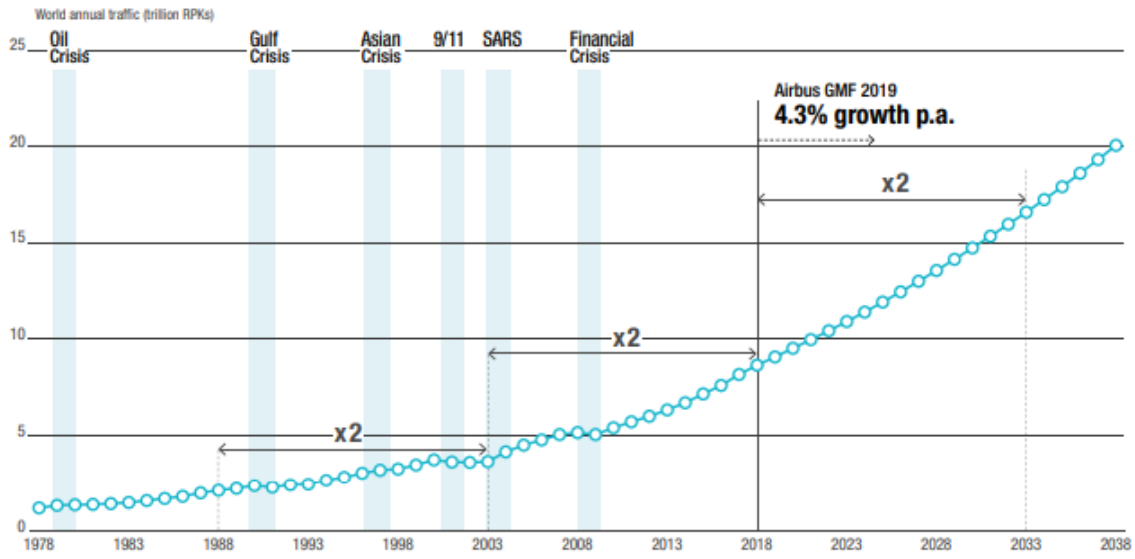

Figure 2: Airbus Projected World Annual Traffic [2]

To accommodate these passengers, Figure 3 and Figure 4 show that the fleet is projected to grow by 39,210 to 44,040 aircraft units by 2038. From both of these figures, it can be seen that the majority of the prospective deliveries occur in the small, single aisle family of aircraft with many of these aircraft filling new, short-haul flights.

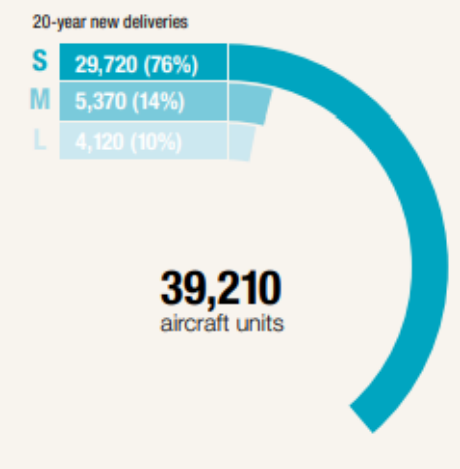

Figure 3: Airbus 20 Year Outlook [2]

The emergence of many short-haul flights shows that the airlines are rapidly growing point-to-point routes in addition to the aviation mega city routes [2].

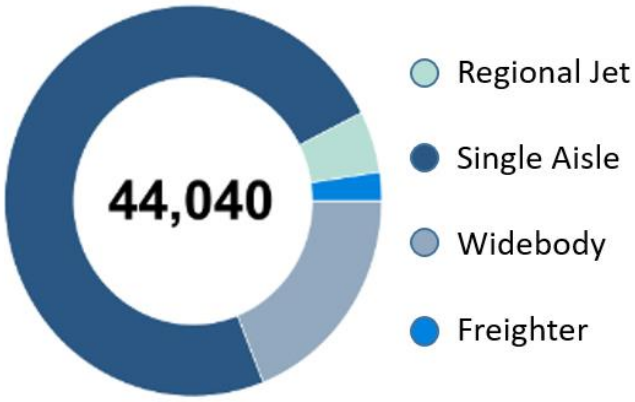

Figure 4: Boeing 20 Year Outlook [1]

While the growth of small aircraft is increasing, jumbo aircraft are beginning to be phased out from many airlines. The Airbus A380 will cease production in 2021, and the Boeing 747 has only had 47 passenger 747 orders since 2005 [3]. The industry is switching to large twin-engine, twin-aisle aircraft because according to Randy Tinseth, Boeing's vice

president of marketing, “The twin-engine, twin-aisle economics of [the Boeing 777] just beats the big four-engine aircraft, and it’s just the reality of the market” [3]. Jumbo jets are good for clearing airport congestion, but the longer range and more frequent flights of aircraft like the 777 and 787 are preferred over the jumbo aircraft [3]. The change in desire for jumbo jets to twin-engine, twin-aisle can be seen in the Airbus and Boeing 2019 orders and deliveries. Figure 5 shows that there have only been cancelations in A380 orders and no new 747-8 orders. The backlog for each of these aircraft is only 51 and 20 aircraft respectively while the companies twin-engine, twin-aisle cumulative backlog of 883 aircraft for Airbus and 1,115 aircraft for Boeing [4].

Boeing, Airbus: 2019 Orders & Deliveries Through August 31

Deliveries	Airbus	A220	A320	A330	A350	A380	TOTAL
		26	374	30	65	5	500
	Boeing	737	747-8	767	777	787	TOTAL
		116	4	28	27	101	276
Net Orders	Airbus	A220	A320	A330	A350	A380	TOTAL
		-26	128	5	19	-31	95
	Boeing	737	747-8	767	777	787	TOTAL
		-183	0	10	36	52	-85
Gross Orders	Airbus	A220	A320	A330	A350	A380	TOTAL
		19	170	10	63	0	262
	Boeing	737	747-8	767	777	787	TOTAL
		36	0	10	36	63	145
Backlog	Airbus	A220	A320	A330	A350	A380	TOTAL
		428	5,810	270	613	51	7,172
	Boeing	737	747-8	767	777	787	TOTAL
		4,595	20	93	440	582	5,730

Figure 5: Airbus and Boeing Orders and Deliveries through August 2019 [4]

With the positive projections in air travel, the market is primed for supersonic aircraft to reemerge in the commercial sector, and many companies believe this thought. There are currently multiple corporations working to develop supersonic aircraft either for commercial operations or as flight demonstrators. But since Concorde's entry to service in 1976 there have been no new commercial supersonic aircraft, so why are these companies pursuing a seemingly failed venture [5]?

Commercial supersonics have had advocates since before Concorde was operational through today. In 1975, NYU Director of Division of Applied Science, Antonio Ferri, presented a Dryden Research Lecture on the possibilities and goals for future supersonic transports. In this lecture Ferri outlines technologies needed to develop a large, long range supersonic transport. He concludes by stating that:

> "[A supersonic] airplane capable of carrying 300 passengers for ranges on the order of 7000 miles appears to be within the capability of advanced technology. Only a few of the several predictable technological advancements are required to reach such a goal" [6]

Supersonic commercial travel has the ability to significantly decrease travel time enabling day trips across seas and allowing further destinations to be weekend trips. Business trips can be reduced to a single day with Washington DC to London being reduced to only three and a half hours [7]. In addition to time savings, modern technology allows for more efficient and quieter supersonic aircraft. With improvements in advanced materials, vision systems, more efficient engines, and low boom design, supersonic aircraft are at a critical point of feasibility in the market.

Even with many engineers believing that a supersonic transport is well within our technical expertise, a new commercial supersonic transport has not entered into service since Concorde because designing commercial supersonic aircraft is difficult. Traditional design methods use historical data to develop empirical equations to define the major geometry of an aircraft. While some of these empirical equations still apply, there are only two major data points for commercial supersonic aircraft: the TU-144 and Concorde. The TU-144 had a limited lifetime, but even with the TU-144 included, two data points is not significant to develop trends. Another issue developed from the lack of historical data is the lack of a consistent reference geometry for commercial supersonic aircraft. Nearly all commercial subsonic aircraft have a long tube with medium-high aspect ratio, swept wings, a conventional or T horizontal tail, and single vertical tail. There is not a common concept for supersonic aircraft. Does the wing need to be highly swept, delta wing, double delta, ogive, or something else? The range of supersonic configurations are shown in Figure 6, which gives 25 of the 40 configurations that were studied in the NASA supersonic commercial air transport (SCAT) program [8].

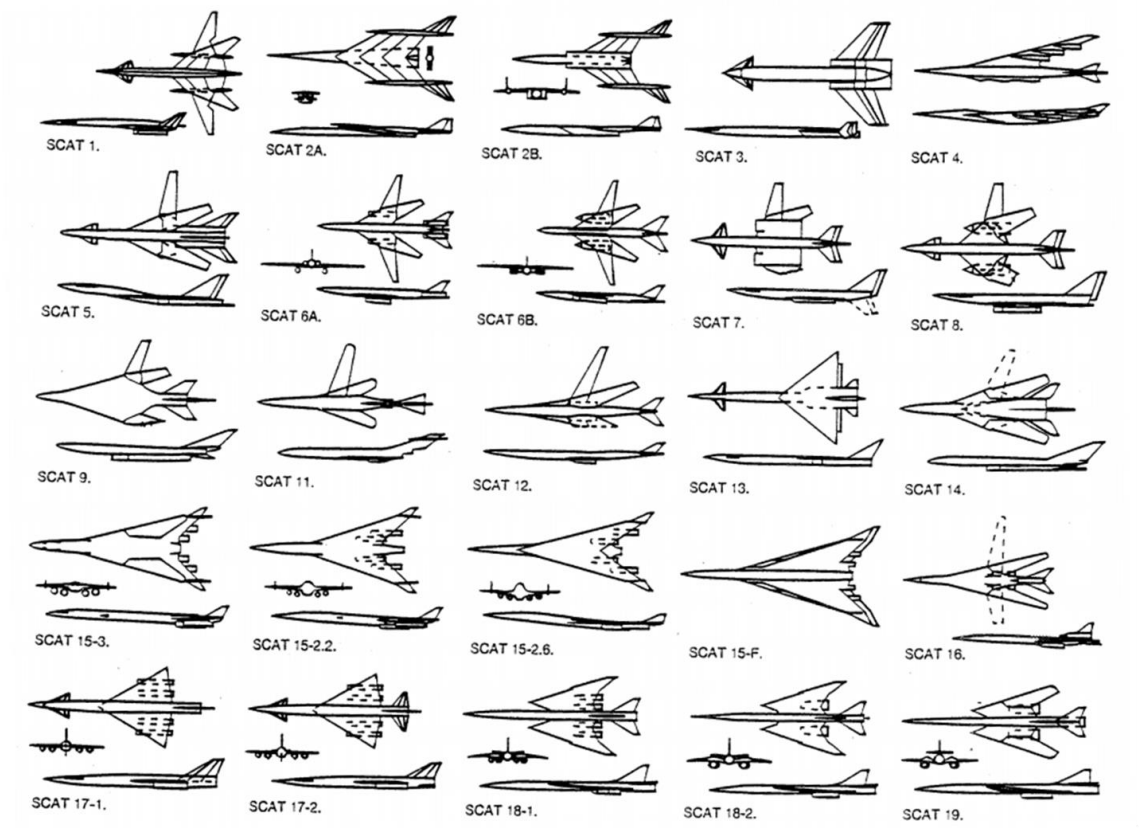

Figure 6: SCAT Supersonic Configurations [8]

There have been many other supersonic studies after the SCAT program, but few have moved past the paper stage. One of the largest programs was the National SST program in the United States from 1963 to 1971 where aerospace companies pursued 300 passenger, 7000 nm range supersonic aircraft. Given in Figure 7 and Figure 8, there was still not an underlying concept as the two selected configurations from Lockheed Martin and Boeing were vastly different [8].

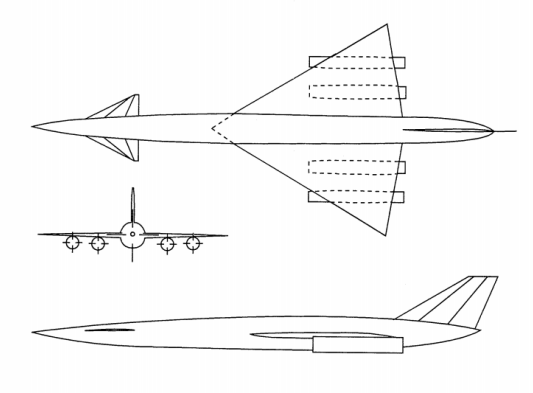

Figure 7: Lockheed Martin HSCT Proposal [8]

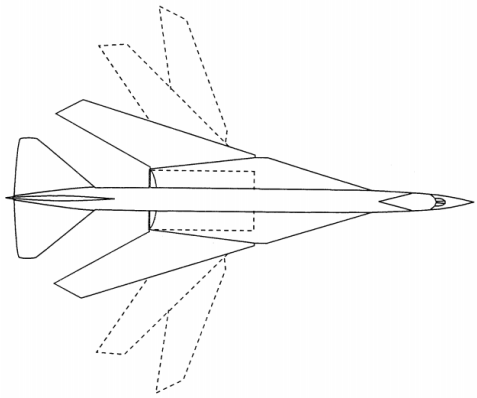

Figure 8: Boeing HSCT Proposal [8]

The Boeing configuration was chosen due to the variable sweep capabilities and named the B2707. Even with major funding, the design incurred many problems from weight and stability until the Boeing 2707-200 design was established with four engines mounted on a large horizontal tail. But supersonic design is difficult, and this concept still had weight and stability issues, and Boeing transitioned the 2707-200 into the conventional fixed-wing aft-tail 2707-300 as shown in Figure 9. Even with the major push from the United States, in March 1971, the US SST program was canceled [8].

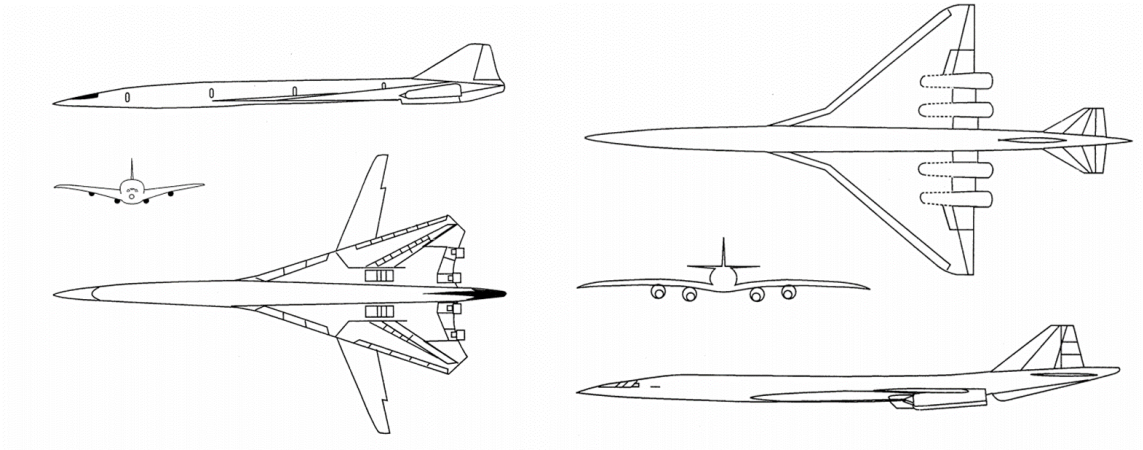

Figure 9: Boeing 2707-200 (Left) and 2707-300 (Right) [8]

The drastic, complete design changes can be seen in the current companies pursuing supersonics too. There are three major players in the commercial supersonic space today: Aerion Supersonic and Spike Aerospace focusing on the business jet market and Boom Technology focusing on public commercial travel. These companies are very enthusiastic about reentering into the commercial supersonic space, but all have experienced the difficulties of supersonic design since their initiations.

1.1.1 Current Supersonic Companies

1.1.1.1 Aerion Supersonic

Aerion was the first major supersonic company to announce they were building a supersonic business jet. Their first configuration shown in Figure 10, named the AS1, used supersonic natural laminar flow to enable efficient supersonic flight [9].

Figure 10: Aerion AS1 Configuration [9]

As seen throughout history, this configuration did not last very long, and Aerion grew the aircraft to reduce emissions. The next concept was called the AS2 and added a third engine to the AS1 configuration. This aircraft is seen in Figure 11. This configuration was eventually updated with a T tail as well.

Figure 11: Aerion AS2 Initial Configuration [10]

In 2017, GE Aviation partnered with Aerion to define a supersonic engine for the AS2, and later that year, Lockheed Martin and Aerion joined together to explore the feasibility of a joint development of the AS2 [11]. This partnership led to another configuration change in the AS2. With Lockheed Martin involved, the wing changed from a low wing to a high wing, and the two side engines were moved forward and under the wing. The fuselage was also much more area ruled with this configuration which is shown in Figure 12.

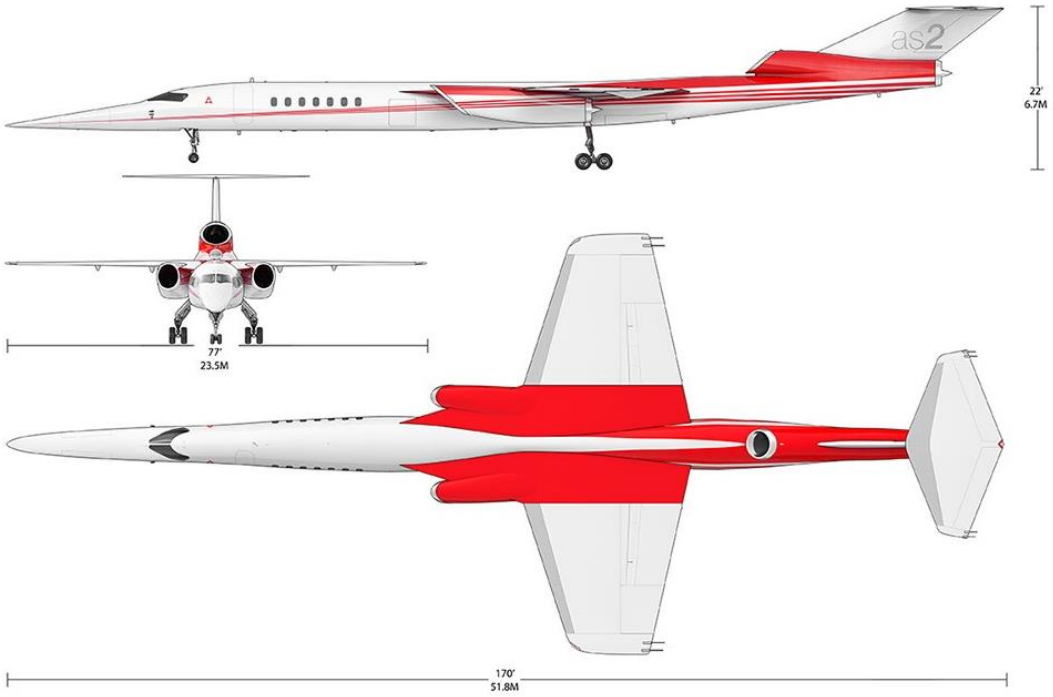

Figure 12: Aerion AS2 and Lockheed Martin Configuration [10]

In February 2019, Lockheed Martin left the partnership with Aerion, but Aerion replaced this partner with another large company: Boeing [12]. In this partnership, Boeing provides engineering, manufacturing, and flight test resources, and Boeing also invested a

substantial sum of money into the program [13]. With this new partnership, the configuration has remained the same, but since the merger the Aerion website has removed all technical specifications of their aircraft, and states that they are "in stealth mode…[while] working behind the scenes on fully maturing the design" [10].

1.1.1.2 Spike Aerospace

Spike Aerospace launched in 2013 to design a supersonic business jet. The first iteration of their configuration, called the S-512, had a similar planform to Aerion's AS2. This concept is given in Figure 13 and is designed to carry 18 passengers at Mach 1.6 [14].

Figure 13: Spike S-512 First Concept [14]

The company decided to pursue low boom for their configuration, and in 2015, the S-512 was updated with a modified delta wing configuration shown in Figure 14 [9]. Since the announcement of this new configuration, the company has been very sparse with updates.

Figure 14: S-512 Low Boom Configuration [14]

1.1.1.3 Boom Technology

The last current day major player in the supersonic industry is pursuing the commercial passenger market. Boom Technology was founded in 2014, and in 2016 Virgin partnered with the start-up [15]. Boom plans to fly 55-75 passengers in their aircraft called Overture, and the company is also designing a scaled demonstrator aircraft called XB-1 [16]. When the start-up began, the aircraft had a similar configuration to Concorde except it had two engines instead of four under the wing, and this initial configuration is show in Figure 15.

Figure 15: Initial Boom Configuration [15]

Early in the design a third engine was added to the configuration; Figure 16 shows the triple engine aircraft with the initial configuration of the demonstrator aircraft [17].

Figure 16: Boom Airliner and XB-1 [17]

As of the date of writing this paper, Boom XB-1 has a new configuration with three engines, and the airliner has slightly changed with the overall configuration remaining similar. The current XB-1 is shown in Figure 17 and airliner in Figure 18.

Figure 17: Triple Engine XB-1 [17]

Figure 18: Boom Overture [16]

Each of these companies show the difficulties associated with supersonic design. While the major configuration of a subsonic aircraft remains set after the conceptual design phase, all three companies announced their aircraft and then performed a major configuration change either changing the type of wing planform, adding additional engines, or both. From the produced flight vehicles, many studies, and prospective vehicles, it is seen that supersonic design is a complex and interdisciplinary task, but what contributes to producing a vehicle that flies above Mach 1 so difficult? Concorde entered into service over 40 years ago, and the basic performance of a supersonic transport aircraft could easily be met with current technologies [18]. The prevalence of late cycle design changes requires additional research and design analysis earlier in the design process. This is not easy with supersonic aircraft, though, as supersonic design is highly interdisciplinary which increases the number of design variables needed. In addition, without historical data, high fidelity analysis is needed to estimate performance. High dimensionality combined with high fidelity analysis leads to very high computational time. The following sections outline some difficulties specific to supersonic aircraft that increase design complexity.

1.1.2 Supersonic Design Complexities

Supersonic design is a difficult problem due to the interdisciplinary nature and the lack of historical data. Supersonic aircraft must meet the same regulations as subsonic aircraft while being able to in a different regime of speed. The following sections provide brief outlines of some challenges of supersonics which lead to the problem being highly interdisciplinary.

1.1.2.1 Environmental Impact

The environmental impact of a supersonic aircraft is twofold: global environment and local environment. The global environment is what crosses the mind when environmental impact is mentioned. The emissions considered here are greenhouse gases and emissions from supersonic aircraft. A major concern for supersonic aircraft is the cruise altitude, which is significantly higher than subsonic counterparts. At these altitudes, deep in the stratosphere, the emissions directly deplete the ozone while also leaving high altitude vapour trails which can stay at altitude for weeks [9]. In addition to these supersonic specific issues, supersonic aircraft have to meet current subsonic emission regulations. Figure 19 shows that aircraft emissions are trending down, and many organizations have set goals and hard limits to further reduce aviation emissions in the future [19]. Any new engines that are being developed after 2012 must meet CFR 32.23 which limits nitrogen and carbon monoxide emissions [20].

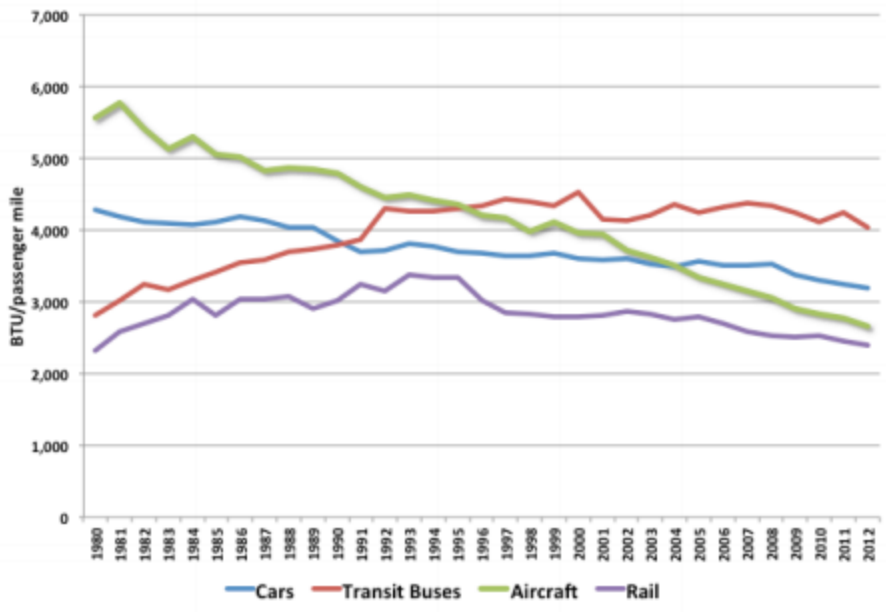

Figure 19: Comparison of Vehicle Fuel Efficiency [19]

The second environmental impact is local impact or noise level. During Concorde operations, the aircraft was so loud that many new takeoff, climb-out, and landing noise standards were developed. Since these operations, the noise restrictions have evolved to become stricter, and supersonic aircraft are required to meet all subsonic noise restrictions [9]. As of 2006, all commercial aircraft must meet the Stage 4 noise requirements, and all newly certified aircraft must meet Stage 5. Also, after December 2017, any aircraft with a takeoff weight greater than 121,254 pounds has to be certified to Stage 5 noise limitations which are defined by ICAO Annex 16.1.14 [20]. The stages are given in Figure 20. Even as the overall noise decreases, noise remains a major issue for the local communities around airports as the number of aircraft landing and departing is continuing to increase [21].

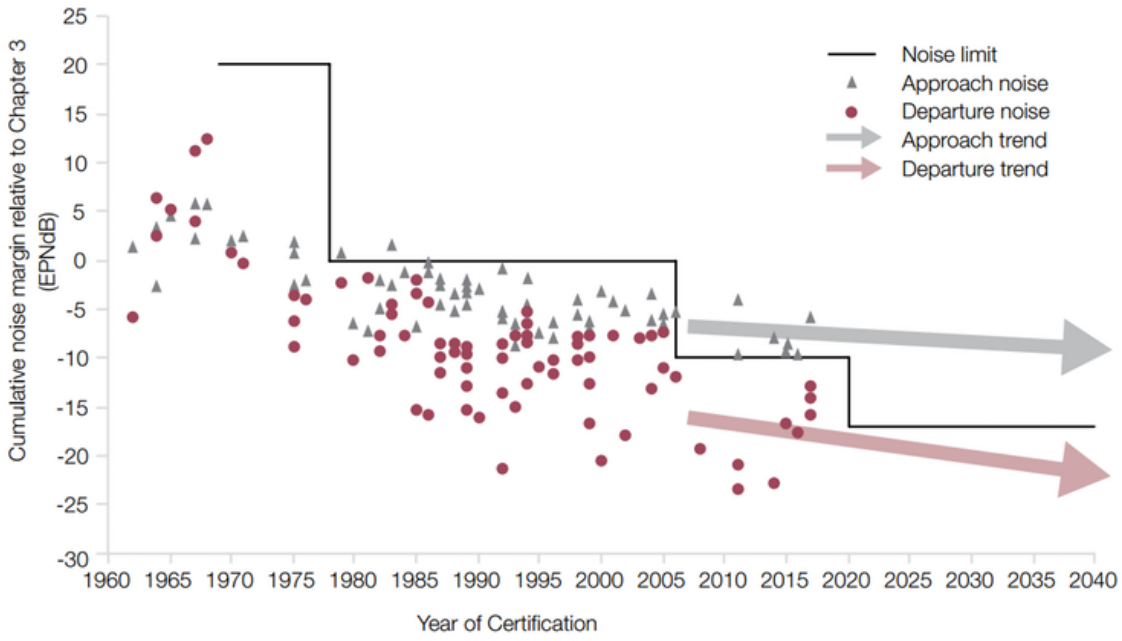

Figure 20: Historic and Future Trends in Certified Aircraft Noise Levels [21]

Sonic boom is another local impact that is innate with supersonic designs. CFR 91.817 states that in the United States, supersonic flight is banned over land to prevent sonic booms from reaching the United States [20]. Because of this, there have been many efforts to reduce the boom, and the X-59 QueSST flight demonstrator is currently being manufactured to flight test a low boom configuration [22]. While strides have been made in low boom design, the research has shown that the technology does not scale well, and it is clear that smaller aircraft have a great advantage over large aircraft as size and weight have a first-order effect on boom strength [23]. Figure 21 shows a comparison of the ground boom signatures of a 300 passenger HSCT design, the Concorde, a supersonic business jet, and two quiet supersonic business jet designs.

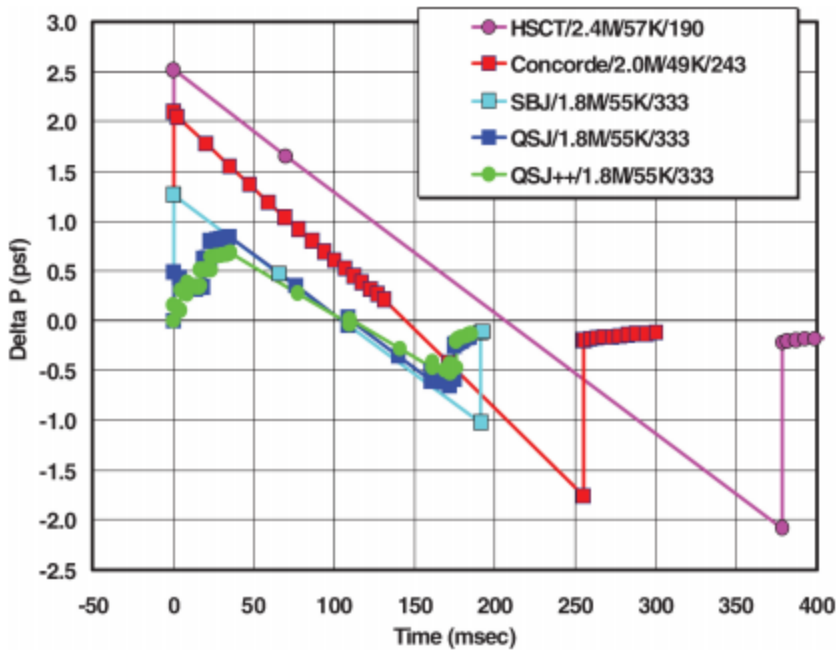

Figure 21: Ground Boom Signatures from Multiple Supersonic Concepts [23]

Environmental impact is separated into emissions and noise where noise is broken into traditional certification noise and boom noise. These components contain two of the major aerospace disciplines: aerodynamics and propulsion. Propulsion is the cause of emissions as the engine generates all particulates emitted during the flight. Propulsion is also a major factor in noise during certification operations for takeoff and landing. Aerodynamics play a major role in sonic boom but also impact landing and takeoff noise when flaps and landing gear are deployed.

1.1.2.2 Economic Viability

Due to the greater amount of fuel needed and the higher performance, supersonic aircraft will always be larger and heavier than their subsonic counterparts; therefore, to be economically viable, these aircraft need to provide significant value to passengers in terms

of time savings while minimizing excess cost [18]. Speed and time savings not only benefit the passenger as they can travel farther in less time, but this speed benefits the operator increasing number of trips per day for a given aircraft. Although innate costs associated with supersonic aircraft are higher, “it is not the technology, it is the fleet flight rate that determines payload costs” [24].

While economic viability is not typically stated as an engineering discipline, every discipline is involved in this section. The aircraft cost, fuel efficiency, and maintenance cycle all greatly impact the economic viability of the aircraft. As seen from many projects of the past, even a well-designed aircraft can crumple if not economically viable.

1.1.2.3 Supersonic Performance

Supersonic aircraft need low drag to be as efficient as possible in the supersonic regime where they spend the most time. The main difficulty with designing strictly for supersonic cruise is that the aircraft must still meet the aviation regulations and mission requirements [9]. The aircraft must be able to adapt to subsonic flight, specifically cruising over land, and the aircraft must have good flying qualities throughout the entire flight envelope including subsonic, supersonic, and transonic [25]. Sun outlines an example of performance balancing in Figure 22. Supersonic aircraft want highly swept wings to improve supersonic performance; however, higher swept wings perform poorly at low speeds. Performance balancing is highly dependent on propulsion, aerodynamics, and structures. Propulsion must have enough thrust to cruise at supersonic conditions while also maintaining performance at subsonic speeds. The aerodynamics needs to be efficient at high speeds but has to enable low speed performance for landing and maneuvering.

Structures must counteract the aerodynamics to ensure the aircraft is sufficiently strong and does not flutter at high speeds.

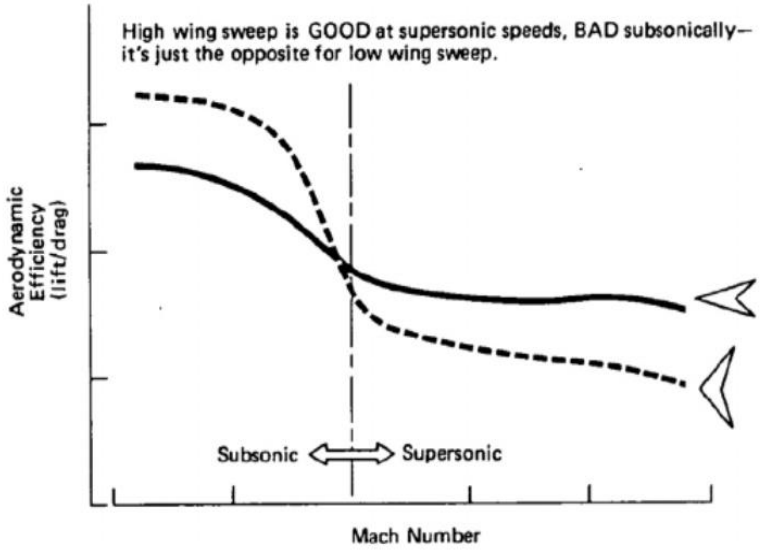

Figure 22: Wing Sweep Balancing for Subsonic and Supersonic Conditions [9]

1.1.2.4 Interdisciplinary Design

As seen in the past complexities, supersonic design is highly interdisciplinary. Small changes in geometry can drastically change the performance of the aircraft. This leads to an initial outer mold line having great input from aerodynamics, structures, propulsion, and controls engineers. The propulsion is highly integrated with aerodynamics as an engine is designed for high speed cruise conditions. In subsonic design, the different disciplines typically work independent from each other and systems are eventually integrated together, but supersonic design must contain additional design variables from the other disciplines.

1.1.2.5 Supersonic Analysis and High Dimensionality

With little historical data and no baseline configuration for commercial supersonic aircraft, design methodologies cannot use historical based, empirical equations or tools without corrections. This leads to many methodologies integrating high fidelity tools into conceptual design or correcting the empirical tools using high fidelity methods. These high fidelity tools combined with the higher dimensionality required from the interdisciplinary nature of supersonic design greatly increases the computational cost of supersonic design. With a large computational cost, design spaces cannot be fully explored or designs do not include enough variables early in the design process. Without design exploration, the late design changes as seen in history and currently occur. Many methodologies have been created to address supersonic design, and these are presented in the next section.

1.2 Background and Literature Review

This section presents current supersonic design methodologies, and the limitations of these current methods. Following, active subspace theory will be presented alongside literature where active subspaces were used to reduce dimensionality. Finally, active subspace theory will be outlined.

1.2.1 Supersonic Design Methodologies

Many different studies have presented supersonic designs since the Concorde was created, but most design methods can be separated into two major categories: Low fidelity, historical data-based design and high fidelity, physics-based design. Most design space exploration methodologies begin with a Design of Experiments which is fed into either low

or high fidelity analysis. With this data, trends in the results can be seen and optimal points in the design space can be investigated.

1.2.1.1 Low Fidelity, Historical Data and Empirical Equation Based Design

This design methodology is derived from the traditional subsonic design methods. While these equations may seem like oversimplifications, especially in the supersonic regime, many improvements can be integrated with the lower fidelity calculations to calibrate the results closer to the true answer. Traditional supersonic design follows the steps presented in Roskam [26]. This method creates constraint equations to find feasible areas in the design space, a design point is chosen, and mission analysis is run to ensure the aircraft can accomplish the given mission [27]. Along the process, additional details are included, but initial performance is calculated through empirical equations developed using historical trends.

When envisioning lower fidelity methods, one may think of a pen and paper going through step-by-step, but these methods are also widely used to investigate the trends in a given design space using advanced modelling environments. While the tools still rely on the same underlying empirical equations, these methodologies, such as those presented by Hamel [28] and Johnson [29], can intelligently generate full design spaces enabling design exploration. Many of these tools allow design space exploration, so even if the exact performance figures are not correct, if the error is consistent, the trends will still be relevant. Other examples of low fidelity design methodologies are found in [30] and [31].

Low fidelity analyses are typically used in conceptual design due to a lower computational cost, but as computers increase in performance and more complex, unknown

designs are created, high fidelity analysis is becoming more prevalent in the earlier design stages. The goal of conceptual design is to estimate the aircraft's performance and ensure the given design can meet the requirements [32]. Even with many low fidelity analyses, high fidelity tools are used to check the solutions at some point in the design process, especially if the configuration is outside of the typical design space. Designers do not want to extrapolate from a design space, and especially with the low amount of historical data within the commercial supersonic design, to use many trends a designer must extrapolate from either subsonic or supersonic military aircraft.

1.2.1.2 High Fidelity, Physics Based Design

Many modern studies use some form of high fidelity, physics-based design methodology. These include high fidelity codes to perform analysis on the concepts, but these methodologies quickly fall into the curse of dimensionality and require large amounts of computational power. Typically, these methodologies are not able to explore a large design space, or they explore a design space but need massive amounts of computational time and power to complete a study.

NASA Langley presented a conceptual design methodology which incorporates multidisciplinary design and optimization through the use of multiple modules in ModelCenter. To reduce some cost, their aerodynamic analysis section uses low fidelity tools when optimizing and only uses CFD as verification to these low fidelity tools. This method has been successful within NASA, but integrating CFD and high fidelity structural analysis still has created issues [33]. This method uses VSP to model the geometry, and while this allows a baseline geometry, certain nuisance variables may be disregarded. Also,

this method will still suffer from very high dimensionality if the user is optimizing multiple components of a given geometry.

In addition to NASA, Stanford has developed many high fidelity supersonic design methods. In 2009, Choi, Alonso, and Kroo published a multi-fidelity approach to supersonic design. Using a hierarchy of tools starting with low fidelity and moving to higher fidelity produced a significant improvement compared to only using the low fidelity tools; however, this method simplifies aircraft geometry and the switching criteria for the hierarchy from low to high fidelity analysis needs careful study before applying this method to a real design problem [34].

Many other design and optimization methodologies have been developed with higher fidelity analysis in the loop. Multiple studies have been aimed at developing a multi or mixed fidelity approach, similar to the two presented before. This type of approach allows the faster design studies to use lower fidelity analysis with the final designs being checked with high fidelity analysis. Additional examples of both high fidelity and mixed fidelity design and optimization approaches are given by [35], [36], [37], [38], and [39].

Both high fidelity and mixed fidelity design methods are limited by the high computational cost associated with running high fidelity tools in the design loop. Even if points are checked using high fidelity, enough high fidelity cases need to be run to properly calibrate the low fidelity tools, and these calibration runs can grow quickly when the dimensionality of the design space is large.

1.2.1.3 Low-Boom Design

An extension of high fidelity, physics-based design is low-boom design. A low-boom design still produces a shockwave, but the aircraft are shaped in a specific way to lessen the overpressure and produce a quieter sonic thump at the ground instead of a sonic boom. The end goal for these aircraft is to prove to the regulating agencies that supersonic flight can be feasible over land as long as the aircraft are designed properly [40]. The X-59 QueSST demonstrator is currently being built by NASA and Lockheed Martin to prove low boom capabilities [22].

Low-boom design has been a major focus in recent supersonic studies to prove that aircraft can fly supersonic over land without creating a disturbance, so there are many design methodologies specifically focused on reducing overpressure. These methodologies typically see performance fall out of the design instead of designing specifically for the performance. While these aircraft can significantly reduce sonic boom, few studies include performance as a driving metric, so overall vehicle performance suffers compared to other supersonic configurations [33].

Low-boom design methodologies include an even larger variable space than traditional aircraft design as every part of the aircraft contributes to the sonic boom signature. These design methodologies even further include high fidelity tools as many use off-body pressure distributions to measure the boom signature, and many off-body pressure distributions need to be measured at multiple aircraft lengths from the aircraft. When pressure distributions need to be measured that far off the body, the grid sizes get extremely large, further increasing computational time.

1.2.1.4 Supersonic Design Methodology Summary

While most references develop their own way to design a supersonic aircraft, the primary methods are split into two major categories: historical data, empirical equation-based design and high fidelity, physics-based design. While both of these can successfully be used as conceptual design methods, they both have their limitations. Low fidelity methods were originally created to design subsonic aircraft, and with little historical data on commercial supersonic aircraft, these design methods will need to be corrected and calibrated using physics-based analyses. High fidelity methods model the performance with high accuracy but require much higher computational time. This high computational time can limit the size of the design space investigated or the number of design variables studied. Because of the interdisciplinary nature of supersonic design, the impact of each design variable needs to be captured, so pure design variable removal is not feasible. This creates the question of how to reduce dimensionality, therefore reducing computational cost, without removing the impact of design variables.

1.2.2 Active Subspaces for Dimensionality Reduction

Even with corrected low fidelity methods, a large number of design variables can limit the range of design variables and the number of configurations investigated. A novel technique called Active Subspace Theory, originally published by Paul Constantine in 2011, has recently seen applications to many problems. This technique takes a design space and identifies the important directions in the space of the inputs, which are the weights defining a linear combination of the design variables. The design space is then rotated into the most active directions removing the impact of the least important directions [41]. Surrogates are

made within this rotated design space, and without the least important directions, dimensionality is reduced while the impact from each original design variable is still accounted for in the surrogate.

This theory has been applied to many different problems proving to reduce dimensionality while maintaining good surrogates. These problems range from hydrologic models [42], solar cells [43], and most importantly for this research, aerospace applications. Two major aerospace applications have been published using active subspaces. The first was one of the earliest applications of active subspaces in the 2011 paper published by Constantine where an active subspace surrogate was created for hypersonic flight data [44]. This initial paper utilized Bayesian inverse analysis and reduced order modelling to analyse data from hypersonic Reynolds-averaged Navier-Stokes CFD cases of a hypersonic engine. This problem was readdressed using active subspaces in a 2015 paper from Constantine, where active subspace theory was used to perform uncertainty quantification on the hypersonic data [45]. The active subspace enabled a dimension reduction from seven parameters to a single active subspace variable. From this dimensionality reduction, the uncertainty quantification needed only 68 simulations to perform calculations [45].

The second major aerospace application was published in 2014 by Lukaczyk where active subspaces were applied to a transonic wing shape optimization of an ONERA-M6 transonic wing [46]. Lukaczyk parameterized the ONERA-M6 wing using 50 design variables and used active subspaces to model the wing with fewer dimensions. Active subspace surrogates were created for lift and drag, and Figure 23 shows the training error of each active subspace surrogate given the number of active subspace variables. It can be

seen that the active subspace surrogates have very low training error with less than half of the original number of design variables.

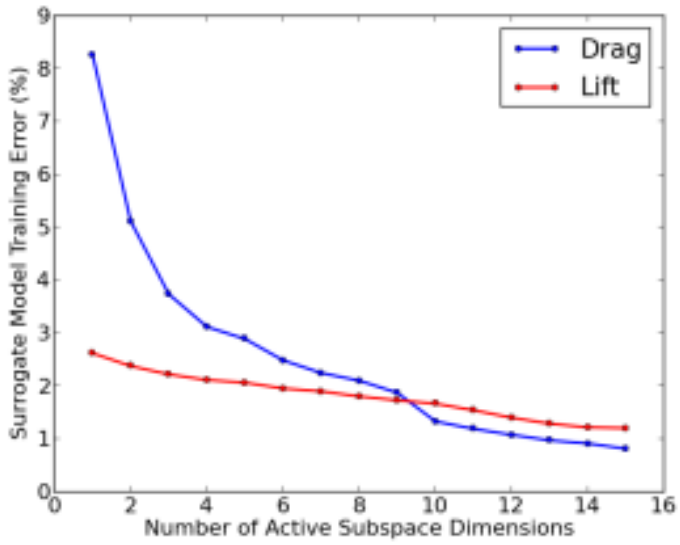

Figure 23: Training Error for Active Subspace Surrogates [46]

From this data, Lukaczyk then used the active subspace surrogates to optimize the drag of the ONERA-M6 wing. The large dimensionality reduction presented in that paper encouraged this research to investigate the incorporation of active subspace methods into a supersonic design space. If a dimensionality reduction could be found in such a design space, then larger design studies can be incorporated earlier in the design process. In order to implement this method, the theory behind active subspaces will be presented.

1.2.2.1 Active Subspace Theory

This section addresses the theory to find an active subspace developed from Constantine [41]. Although research has shown successful application to many problems, an active subspace is not present in every problem. An active subspace must be discovered in a problem, and even if discovered, it may not show substantial dimensionality reduction [41]. The process to identify an active subspace, developed by Constantine, is further presented:

To begin, define a function f with m continuous inputs of a column vector x where x ranges from -1 to 1. Function f's gradient is also oriented as a column vector.

$$f = f(x), \quad \nabla_x f = \nabla_x f(x), \quad x \in [-1,1]^T$$

The number of gradients needed has been defined as a range by Constantine. This range is presented in Equation 1 where M is the number of runs needed, α is the oversampling rate which Constantine defines as between 2 to 10, k is the number of gradients needed, equal to the number of active subspace variables desired, and m is the number of original design variables [41].

$$M = \alpha * k * \ln(m) \qquad \textbf{Equation 1}$$

Define the symmetric, mxm matrix C, which is defined as the average of the outer product of the gradient with itself, and each element of C is the average of the product of partial derivatives. C is the uncentered covariance matrix of the gradient.

$$C = \int (\nabla_x f)(\nabla_x f)^T \rho dx\,, \qquad C_{ij} = \int \left(\frac{\partial f}{\partial x_i}\right)\left(\frac{\partial f}{\partial x_j}\right)\rho dx\,, \qquad i,j = 1,\dots,m$$

In practice, the elements of C can be approximated using a random sampling of gradient values in the design space, and this approximated covariance matrix is defined as

$$C \approx \frac{1}{M}\sum_{i=1}^{M}(\nabla_x f_i)(\nabla_x f_i)^T$$

Because the active subspaces method needs gradient evaluations throughout a design space, in practice adjoint solvers can be used to directly calculate the gradient at a point, but finite difference methods and response surface modelling of the design space can also be used.

The C matrix is symmetric, so it has a real eigenvalue decomposition. The eigenvalues can be exploited to reduce dimensionality by identifying the important directions in the design space.

$$C = W \Lambda W^T$$

where W is a mxm column matrix of eigenvectors, and Λ is a diagonal matrix of eigenvalues.

The smaller the eigenvalue, the less the results change along that design variable. The eigenvalues are arranged in descending order and the sets of eigenvalues and eigenvectors are separated into two sets to reduce dimensionality. The separation is a judgement call by the user, but the decision can be informed by viewing the decay of the eigenvalues.

After a selection of dimensions is chosen, the eigenvalues and eigenvectors can be partitioned as,

$$\Lambda = \begin{bmatrix} \Lambda_1 & \\ & \Lambda_2 \end{bmatrix}, \qquad W = [W_1 \ W_2]$$

where Λ_1 is the diagonal matrix with the first n design variables, and W_1 contains the first n eigenvectors.

With the new basis identified, the design space is mapped into the active subspace,

$$y = W_1^T x$$

and $f(x)$ can be approximated in the new active subspace,

$$f(x) \approx g(W_1^T x) = g(y)$$

With $f(x)$ approximated in the active subspace, a surrogate model can be developed in the active subspace using points $g_1, \ldots, g_N$.

CHAPTER 2. PROBLEM FORMULATION

This chapter takes the background research and literature review and formulates research questions to guide the studies. Hypotheses are also developed for each research question, and these hypotheses will be revisited and compared once results have been collected. The first section in this chapter addresses the objectives of the research while the second section outlines the research questions and respective hypotheses.

Supersonic design is a very interdisciplinary task, and the interdisciplinary nature necessitates high dimensionality in the conceptual design space. With high dimensionality, computational time increases. Without much historical data and no baseline configuration, supersonic design is even more computationally intensive because high fidelity, physics-based analysis is needed to accurately model the vehicle performance.

2.1 Research Objectives

The goal of this research is to aid in the commercial supersonic conceptual design process and allow designers to include many different design variables while maintaining a wide design space. Active subspace method will be used to reduce dimensionality. Because an active subspace must be found within a problem, a major objective is to prove that an active subspace can be found within the design space. If this is possible, an active subspace still needs to prove its worth by buying its way onto the program. The way a method can justify use in the design process is through enabling additional design freedom by reducing computational cost. These thoughts are encapsulated in the two-part overarching research question which also scopes the research to focus on aerodynamic coefficients.

Overarching Research Question: 1) Is it possible to find an active subspace of aerodynamic coefficients in a commercial supersonic transport design space and 2) Is it worth incorporating an active subspace method into the design process?

To answer this question, active subspaces need to be further investigated with regard to the given design problem. The goal of the overarching research question is to prove that active subspaces enable a significant enough dimensionality reduction to enable larger design studies either through addition of design variables or reduction in computational time. If active subspaces can be used, then an overall research objective has been outlined to improve the commercial supersonic design methodology.

Research Objective: Develop a methodology to perform commercial supersonic conceptual design which incorporates active subspace surrogates to improve design space exploration.

If this research objective is successful then a new methodology will be outlined using active subspaces to aid the design of commercial supersonic aircraft. Due to computational limitations, this initial research will be limited in scope to only a select number of aerodynamic variables, and future work should take more variables after proving active subspaces can be applied to the given problem. To answer the overarching research question and reach the objective, specific research questions were developed.

2.2 Research Questions

Active subspaces contain the possibility of reducing dimensionality and computational time enough to enable larger design space explorations while still using high fidelity

analysis. To answer the fundamental research question, additional research questions need to be asked. These questions address the implementation of an active subspace.

2.2.1 Research Question 1

Active subspaces must buy their way into a design process, so a reduction in computational cost must be observed. A substantial component of active subspace computational cost is the number of runs required to calculate gradient values in order to calculate the active subspace variables. While Constantine outlines a recommended number of gradient values, presented in Equation 1, could better surrogates be found with a larger oversampling rate than the 10 he presents? On the contrary, is it possible to use fewer gradients than the recommended minimum oversampling rate of 2? These questions combine into research question 1:

RQ-1: How does the number of gradient values used to calculate active subspace variables impact the error of an active subspace surrogate?

This question addresses the published oversampling range of 2-10. As these are integers, it can be assumed that while the actual range may be similar, both 2 and 10 were used due to being even, understandable numbers. Because of this, it is estimated that the actual range is more fluid than the given numbers. Oversampling values less than 2 need to be tested to see the increase in active subspace surrogate error, and oversampling values greater than 10 need to be tested to see the reduction in active subspace surrogate error. If significant error reduction is observed with an oversampling value above 10, then the range must be extended beyond 10 until no additional error reductions are observed. From these

estimates, two hypotheses are presented for the low end in the range of oversampling and the high end in the range of oversampling.

Hypothesis-1.1: If cases are oversampled less than the presented $\alpha = 2$, then the error of any active subspace surrogates will drastically increase compared to active subspace surrogates within the published oversampling range.

Hypothesis-1.2: If cases are oversampled more than the presented $\alpha = 10$, then the error of any active subspace surrogates will decrease compared to active subspace surrogates created with $\alpha = 10$, and the error will continue to decrease as the oversampling value increases.

2.2.2 Research Question 2

Stemming from the idea that an active subspace must be discovered within a problem, another question arises: can multiple active subspaces be found within the same design space? Specifically, if a design space is segmented into a subset of the original design space, will the active subspace change in the range? Intuition assumes that fitting a surrogate to a smaller area in a design space would fit better than fitting to all of the data within a full design space. If this is true, then investigating how much better the local surrogate is compared to the full surrogate is of note. If data is taken in a full design space, it may be worthwhile separating the design space into segments of interest if the local segments are seen to be better fits compared to the full design space fit. This formulation developed research question 2:

RQ-2: Will an active subspace surrogate on a limited design range improve error within the limited design range compared to an active subspace surrogate of the full design space?

To address this question, the design space will need to be segmented into smaller subspaces. Contrary to intuition, if gradients are similar across both a subset and the full design space, then active subspace eigendecomposition may be the same. If this occurs, the error should be equivalent in the full design space compared to the partition of the design space. Due to the complexity of a large design space, it is estimated that different active subspaces can be found in sections of the design space. This assumption developed hypothesis 2:

Hypothesis-2: If the design space is segmented into smaller subsets of the design space, then the error of an active subspace surrogate made in this local space will show significant improvement compared to the global subspace and will show less error than a traditional surrogate made of the full design space.

2.2.3 Research Question 3

Depending on the tool used, gradients are found in different ways. While many tools contain adjoint methods to calculate gradients internally, come tools do not have this function incorporated. There are other methods to calculate gradients with one of these requiring developing a surrogate model of the design space, taking partial derivatives of this surrogate, and then calculating gradients from the partial derivatives. The additional number of cases needed to generate a primary surrogate model is impactful on the computational cost of the active subspace method. Additionally, if a surrogate is needed to

generate gradients to then make another surrogate of active subspace variables, why would the designer go through the additional process of using active subspaces if a surrogate of the design space has already been created? A question must be asked about the level of fidelity of the surrogate needed to generate gradients because if this surrogate can be a very rough surrogate of few cases per design variable, then an active subspace may still be feasible; however, if the original surrogate needs to be very detailed throughout the design space, applying the additional step of creating an active subspace surrogate would only add computational time. Through this formulation, research question 3 was developed:

RQ-3: If gradients are taken from an initial surrogate model, how does the goodness of fit of the original surrogate impact the goodness of fit of the active subspace surrogates?

A hypothesis to this question must take into account the goodness of fit of a traditional surrogate compared with the surrogate needed to develop gradients. Because partial derivatives of the surrogate equation are needed to calculate gradient values, a higher dimension surrogate is needed; therefore, it is assumed that a high goodness of fit is needed in the original surrogate. This assumption leads to hypothesis 3:

Hypothesis-3: If gradients are taken from an initial surrogate model to create active subspace variables, then as the cases per design variable used to fit the surrogate increase, the active subspace surrogate error will drastically decrease until the number of cases per design variable is equivalent to the number needed to generate a traditional surrogate.

The three research questions address details regarding implementation of an active subspace in a design process, but they do not formally ask if an active subspace should be used. Before creating a methodology, data must show that active subspace method buys itself into a conceptual design process. Even if an active subspace can be found, it may not be beneficial to implement it into the process. Impact on computational cost must be calculated to conclude whether a methodology involving active subspaces is feasible. Each of these questions need to be answered to determine the worth of the active subspace in the design methodology, and the next section outlines an approach to answer these questions.

CHAPTER 3. APPROACH

This section outlines the studies to determine which approach to take to address the research questions and the respective hypothesis. The first sections address the ways to create a distribution of many different aircraft designs and model the geometries. The following section discusses possible ways to analyze the aerodynamic coefficients of a given configuration. The last two sections explore ways to calculate gradients in the design space and finally develop active subspaces from the gradient calculations.

3.1 Design Variables

As mentioned in Chapter 2, the design variables are limited to aerodynamic variables. A major challenge in supersonic design is balancing the supersonic and subsonic performance. This is difficult because many variables want to be large in supersonic and small in subsonic or vice versa. An example of this is wing sweep. In supersonic flight, an aircraft wants a high wing sweep while subsonic wants a low wing sweep. To choose design variables for this research, traditional wing variables should be included such as sweep, chord size, and thickness to chord. In addition to this, variables that may not typically be isolated should also be included such as leading-edge radius and leading-edge droop. These variables have been shown to have an impact in subsonic design, and should be investigated to see their impact in supersonic as well.

Due to computational limitations, the number of design variables will be minimized while incorporating enough variables to see a significant reduction in dimensionality if it arises. 20 design variables were chosen including both traditional and minor design

variables. This number incorporates definition of airfoils at the root, mid, and tip chords to enable a double delta configuration. A double delta configuration was chosen to allow further parameterization of the design space. The 20 design variables are given in Table 1.

Table 1: Chosen Design Variables for Research

Variable Number	Variable Name		Variable Number	Variable Name
1	Root Chord		11	Tip Twist
2	Root-Mid Taper		12	t/c Root
3	Mid-Tip Taper		13	t/c Mid
4	Mach Number		14	t/c Tip
5	Root-Mid Sweep		15	LE Radius Root
6	Mid-Tip Sweep		16	LE Radius Mid
7	Wingspan		17	LE Radius Tip
8	Mid Span		18	LE Droop Root
9	Root Twist		19	LE Droop Mid
10	Mid Twist		20	LE Droop Tip

3.2 Design of Experiments

The first step in creating a design space is intelligently designing experiments to maximize information while minimizing experimental effort. This process is referred to by the term "Design-of-Experiments" or DoE [47]. There are many published strategies to design experiments in a way to maximize the effort; some are presented in the following sections.

3.2.1 Factorial and Fractional Factorial Designs

With multiple factors, one can conduct a factorial experiment. In this strategy, factors are varied together at given levels of each factor to calculate every possible combination of designs within a design space. A simple example is given in Figure 24 from Montgomery which shows a three-factor, two-level factorial design [48]. This means that there are three variables, called factors, and each factor has two levels, such as on and off. In the table in the figure, it is seen that for this case, there are 8 total combinations of factors and levels.

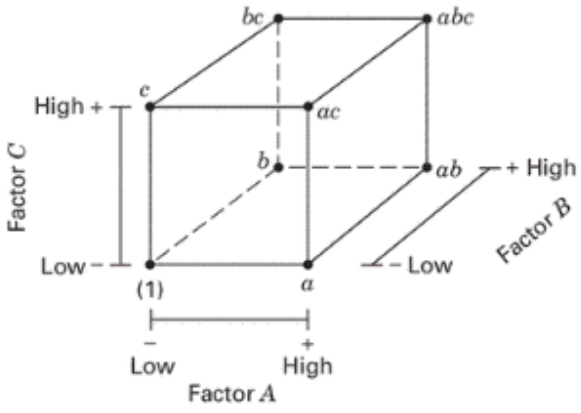

(a) Geometric view

Run	Factor A	B	C
1	–	–	–
2	+	–	–
3	–	+	–
4	+	+	–
5	–	–	+
6	+	–	+
7	–	+	+
8	+	+	+

(b) Design matrix

Figure 24: Three-Factor, Two-Level Factorial Design [48]

Factorial designs are good for addressing full design spaces, but as the number of factors increase, the number of runs also drastically increase. To address this, fractional factorial experiments are used to estimate the important factor effects and low-order interactions [49]. A fractional factorial is designed so the results can be projected to complete a factorial experiment, and this is shown in Figure 25. A fractional factorial is designed such that the impact of each level of each variable is contained within the DoE while reducing the number of cases needed to get this impact from each variable.

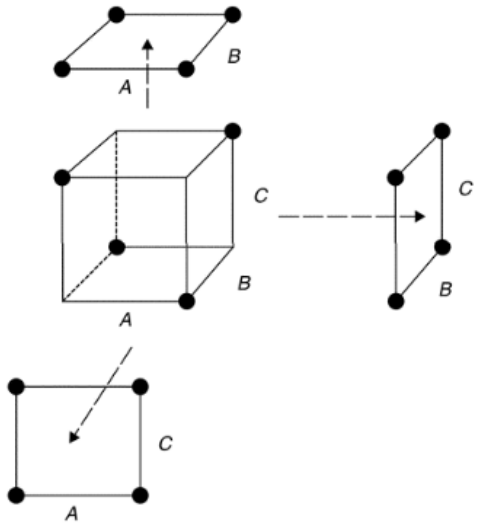

Figure 25: Two-Level Fractional Factorial Projected to Complete Full Factorial Experiment [49]

3.2.2 Space Filling Designs

If little is known about the design space or the interior of the space needs to be sampled, space filling designs can be used to sample points in between the edge cases. Three standard space filling designs are Sphere Packing, Uniform, and Latin Hypercube. These methods create points to fill the design space by maximizing separation of points, generating points

of equal space, and balancing maximum spacing and uniformity, respectively. Examples of Sphere Packing, Uniform, and Latin Hypercube designs are given in Figure 26 [47].

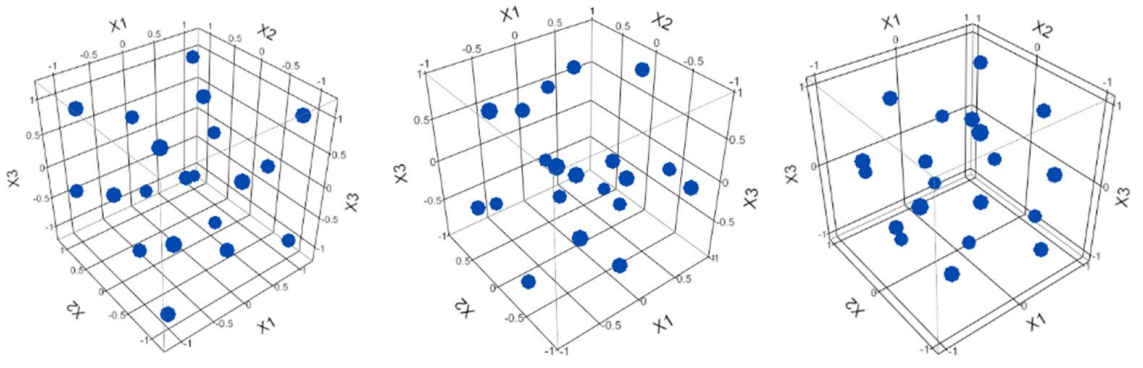

Figure 26: Space Filling Designs (from left to right) Sphere Packing, Uniform, and Latin Hypercube [47]

3.2.3 Design of Experiments Selection

For this research, a space filling design is needed as the interior of the design ranges needs to be studied in detail. Because the Latin Hypercube design balances maximum spacing and uniformity between points, this DoE design will be used for creating the design space for this research, and with enough points, this design of experiments can sample points on the edges as well as within the design space

3.3 Vehicle Parameterization

To generate enough data to analyse a full design space, many different configurations need to be run. While a designer can manually make changes and run configurations over and over, this process is typically automated to allow the human to step away while many configurations are created and analysed. This section investigates the different geometry modelling tools available and their application to parametric design.

3.3.1 Vehicle Sketch Pad

OpenVSP is a tool developed by NASA for parametric aircraft geometry. This open source tool is designed to be very easy to use and intuitive even for new users. Once a geometry is created, the program can output many different file types and formats for different engineering analyses [50]. OpenVSP can be embedded with a script to enable parameter linking and geometry parameterization. This capability is built in to the program, but a user must go beyond the intuitive user interface and script the program [51].

VSP does have limitations, particularly when preparing files for any type of high fidelity analysis. VSP can output a .stl file; however, the tessellation of the geometry does not remain consistent with the tessellation present on the geometry within VSP. Also, VSP has crashing issues when trying to export files that are medium to large sizes.

3.3.2 Engineering Sketch Pad

Engineering Sketch Pad is a geometry creation and manipulation system designed by Massachusetts Institute of Technology to support rapid analysis and design of aerospace vehicles [52]. ESP generates geometry using a set of code-based commands defined in .csm files. These files are then loaded into the program via the OpenCSM modelling system run through the terminal, and this system can be embedded into other applications. Due to the ease of text file scripting and running the geometry generation through a terminal, ESP can be scripted to read a DoE, write a .csm file, and generate a geometry without much difficulty. Another benefit that ESP has over other geometry generating software is the ability to directly control tessellation of multiple components. Tessellation parameters can be set for each part individually or a full body.

ESP has negatives specifically associated with learning the program. Because it uses its own language, while designed to be consistent with Feature Tree traversal, specific commands and inputs to commands have to be learned and are not intuitive [52]. In addition to learning the program, the time to process a .csm model to generate a geometry grows with additional geometric detail and increased tessellation. Lastly, because the geometry is defined in a separate file, changes cannot be instantaneously visualized as they can in OpenVSP or SolidWorks.

3.3.3 Detailed Computer Aided Drafting Programs

The most detailed Computer Aided Drafting (CAD) programs allow precise control over a model in a full user environment. Geometry is defined using a variety of toolbars. Each of these tools require an experienced user to operate, and the ability to change geometry is highly dependent on the sequence it was constructed. While these tools enable minute details to be added to a geometry, computational power scales with geometry detail. Difficulty in parameterizing geometry varies with program but typically requires advanced commands and definition of many variables.

3.3.4 Geometry Parameterization Tool Selection

To detemine the geometry generation tool used, important attibutes were defined for this research. Each tool was rated in these attributes as either good, average, or poor. The tool selected rated highest across all categories with as few poor values as possible. Table 2 presents the results from this decision. ESP was chosen as it enables fast and easy geometry paramterization in the loop, due to text file inputs, even with a slight learning curve. It is also available on Linux and allows direct control over geometry tesselation.

Table 2: Geometry Generation Selection Matrix

	VSP	ESP	CAD
User-Friendly			
Parametric Design			
Complex Shapes			
Easy to Learn			
Speed of Changes			
Tessellation Control			
Linux Availability			
Color Key	Good	Acceptable	Poor

3.4 Physics-Based Aerodynamic Analysis Tools

Physics based tools vary from using empirical equations based on historical data to computational fluid dynamics that solve the Navier Stokes equations across a full mesh. In this section, a variety of tools will be presented in increasing fidelity and therefore increasing computational time.

3.4.1 Vortex Lattice Codes

Vortex lattice methods are based on solutions to Laplace's Equation which assumes that the flow field is governed by a linear partial differential equation [53]. Aerodynamic bodies are segmented into their thickness and camber with no angle of attack and then flat plate at the given angle of attack. Vortex lattice methods calculate lift curve slope, induced drag, and lift distribution for an aircraft configuration, but thickness and viscosity are usually ignored [54]. To solve, the continuous bound vorticity over a wing is approximated by horseshoe vortices placed along a mesh along the geometry [55]. There are many openly available programs that use the Vortex Lattice Method to calculate lift and drag for given

configurations, but due to the way the VLM is formulated, many of these codes are limited in fidelity and cannot handle complex geometries.

3.4.2 Inviscid Computational Fluid Dynamics

While both inviscid and viscous CFD methods require a fine mesh and additional computational time to solve each point in the mesh, inviscid CFD only solves the Euler equations. Due to the simplification of the Navier-Stokes equations, inviscid techniques require approximately an order of magnitude fewer nodes and 5-10 times less storage and CPU than viscous solvers [56]. Inviscid solutions are typically accepted for use in supersonic and hypersonic flows because so much of these flows are dominated by inertial forces instead of viscous forces. The Euler equations, used in inviscid analysis, also predict the Rankine-Hugoniot shock jump conditions and provide accurate surface pressure distributions at high speeds [57]. The increasing effect of inertial forces can be seen in the equation for Reynolds number given in Equation 2, as this equation is defined as the inertial forces divided by the viscous forces. As the velocity increases, Reynolds number increases; therefore, the flow is more dominated by inertial forces [58].

$$Re = \frac{\rho_\infty V_\infty c}{\mu_\infty} \qquad \textbf{Equation 2}$$

Even though this estimation can be shown in theory, it has been tested in practice, and inviscid codes have been proven to accurately model supersonic flows. Figure 27 shows the results from Melton et al. where an advanced supersonic transport wing-body configuration was analysed at Mach 1.8 using a Cartesian grid Euler method [59]. The

comparison against experimental data clearly shows that inviscid analysis accurately models true values within the range tested.

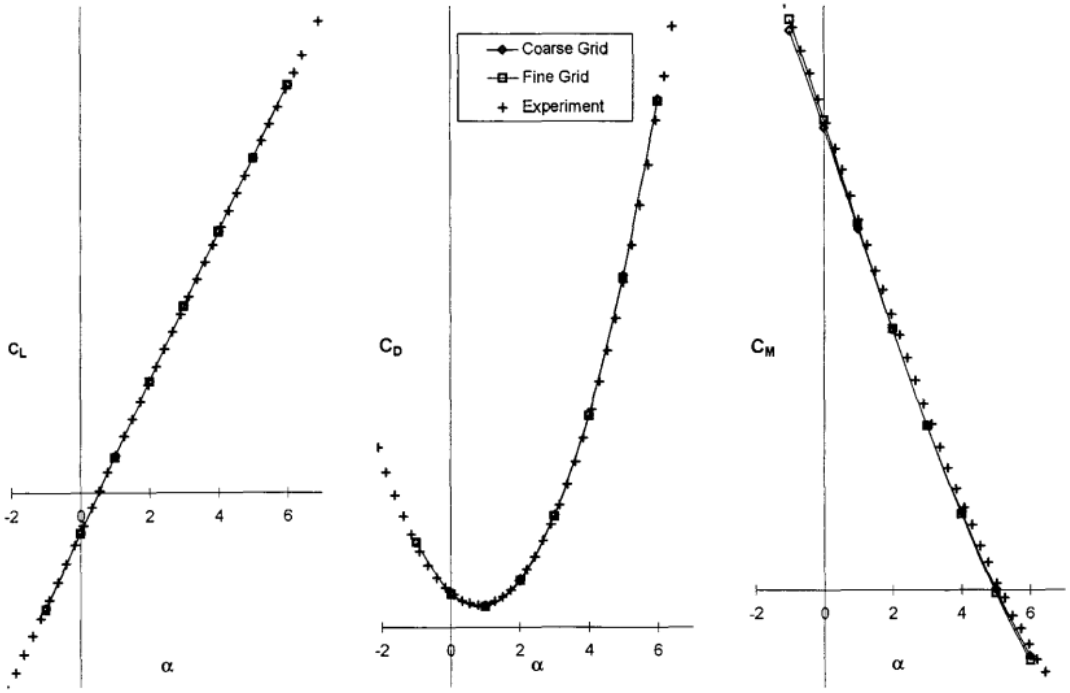

Figure 27: Inviscid Solver Aerodynamic Coefficients of Supersonic Transport wing-body configuration at Mach 1.8 [59]

A second validation case is given by Murman, Aftosmis, and Nemec in 2004 when analyzing the Langley Glide-Back Booster (LGBB) and comparing against experimental data. Figure 28 gives a comparison between experimental data, CART3D (an inviscid flow solver), and OVERFLOW (a viscous flow solver) for the LGBB at Mach 1.6 and Mach 2.2. The figure shows that lift and drag coefficients from angles of attack of -5 to 30 degrees, both inviscid and viscous solvers predict the experiment with high accuracy [60].

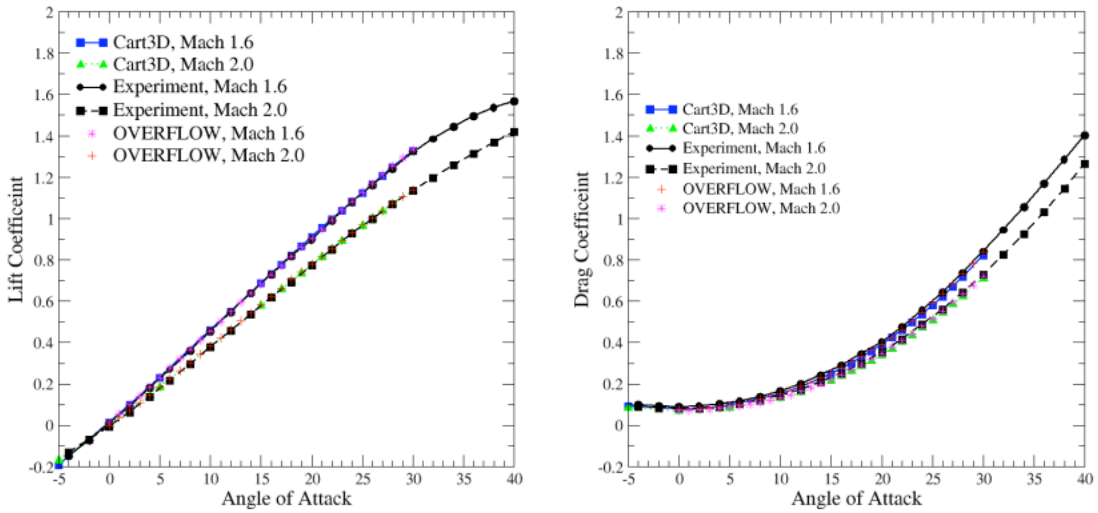

Figure 28: Comparison of Lift and Drag Coefficients for LGBB with Experimental Data [60]

3.4.3 Viscous Computational Fluid Dynamics

Viscous CFD solves the full Navier-Stokes system of equations at each grid point. Solving the full equations allows for the development of boundary layers, viscous eddies, and full separation. Many different tools have the capability to calculate viscous solutions, and these tools increase in fidelity to include turbulence models, time dependent transient models, and aerothermal applications. As complexity increases in these detailed modules, computational time also increases. Viscous CFD is significantly more costly to run than inviscid CFD, and this is shown by Rogers et al. in 2003 when, over the span of seven days, 2863 Cart3D (inviscid CFD) cases finished while only 211 Overflow (viscous CFD) cases had finished [61]. While CFD efficiency and computer hardware have increased since 2003, this ratio of computational time is still seen today.

3.4.4 Aerodynamic Analysis Tool Selection

A decision matrix was developed to select the aerodynamic analysis tool. Important qualities were determined for the research, and each tool was rated good, acceptable, or poor in each of the qualities. The best performing tool was selected; this selection matrix is given in Table 3. Inviscid CFD was chosen due to the high output detail in the regime and reasonable runtime compared to full Navier-Stokes CFD analysis.

Table 3: Aerodynamic Analysis Selection Matrix

	VLM	Inviscid CFD	Viscous CFD
Output Detail			
Complex Geometry			
Runtime			
Supersonic Analysis			
Setup Difficulty			
Mesh Size			
Stability			
Color Key	Good	Acceptable	Poor

3.5 Gradient Exploration

Active subspace theory requires gradients at each design point. While many tools can calculate gradients internally at a given design point using adjoint methods, creating a mathematical model of the full design space enables calculation of gradients at any point in the design space, including points that were not run through the high fidelity model. A good mathematical model of the design space also allows for discovery of trends in the gradients across the design space without running additional cases. However, the need for an initial surrogate requires supplementary cases and may limit the computational cost reduction. Due to this limitation, using active subspace theory when gradients are

calculated from an initial surrogate may not be beneficial to a design methodology. An active subspace may not be necessary if a full surrogate can be made using the physical design variables and may not reduce computational time. Despite this expectation, for this research, gradients will be calculated from a surrogate to perform active subspace analysis.

3.5.1 Response Surface Methodology and Higher Order Terms

With data from a Design of Experiments, a collection of mathematical and statistical techniques can be used to generate response surfaces which map the responses to the input variables. This collection of techniques is called response surface methodology or RSM [48]. A typical way to map these responses is through regression modelling. These models fit data obtained from a DoE by mapping responses to their inputs via a linear equation. Regression equations are linear with respect to the input variables, and these input variables can be expanded to include interaction, or higher order, terms. Interaction terms are products of two or more predictor variables which are included in the regression to improve the fit when there are innate interactions between input variables [49]. A typical second order regression equation with interactions is given in Equation 3, where the x_i's are the predictor variables, the β_i's are the regression coefficients, e is the error term, and y is the predicted response.

$$y = \beta_0 + \sum_i \beta_i x_i + \sum_{i<} \sum_j \beta_{ij} x_i x_j + \sum_i \beta_{ii} x_i^2 + e \qquad \textbf{Equation 3}$$

The goodness of fit of a surrogate equation can be determined by two major values: R^2 and error compared to the fit and validation data. R^2 is a mathematical measure, from 0

to 1, of how well the function measures variability of the response data. A perfect fit R^2 equals 1, but a high R^2 does not indicate that the model is a good model; however, a low R^2 is highly indicative of poor goodness of fit [47]. The more significant measure of goodness of fit are the training and validation errors, also known as the model fit error and model representation error. The training error is the discrepancy between the model's predicted value and the actual value over points with which the model was trained. The validation error is the discrepancy between the model's predicted value and the actual value over points with which the model was not trained. Typically, 25% of the data is segmented as validation data. These errors should be as close to 0 as possible, as errors of 0 show perfect model fit [62].

Goodness of fit can also be visualized using two plots: actual vs. predicted and residual vs. predicted. An actual vs. predicted plot compares the model predicted data against the actual data from the tool. A perfect fit yields a 45-degree, diagonal line from the bottom left to the top right corners of the plot. Any patterns or non-linear lines means that the data needs a transformation or higher order terms. The residual vs. predicted plot compares residuals, the error of each observation, to the predicted residual. A predicted residual is equal to zero, and a good residual vs. predicted plot shows a random pattern of residuals centered on a horizontal line at 0. If patterns appear, then either transformations or higher order terms are needed. A good rule of thumb for a residual vs. predicted plot is that if the ratio of total span of error to the minimum of the predicted is less than 10%, then the model may be valid [47].

Using these equations, the full design space can be explored by calculating points within the space that were not part of the input DoE. A limitation of DoEs and RSM is that

they cannot be extrapolated beyond the variable ranges used to fit the model, so it is important to ensure the ranges of the predictor variables are wide enough when generating the DoE.

3.6 Active Subspaces

Active subspaces identify a structure and low dimensional parameterization that a researcher can exploit to reduce dimensionality and enable previously infeasible studies of a large variable space. The task is to identify the most active direction in the design space and construct a new surrogate model in this active coordinate. To generate an active subspace, the design space must be explored and in addition to responses, the gradient must be found at each point [63]. These gradients are used to calculate a matrix, C, which is the outer product of the gradient. Using this matrix, an eigendecomposition of C is found. The eigenvectors are partitioned into two groups by size: the larger eigenvectors are used to create a new set of variables called the active variables and the variables associated with the smaller eigenvectors are considered negligible [43]. The design space is then rotated to map into the active subspace, and the response function is approximated in the active subspace by a surrogate model [46]. It is not guaranteed that a design space will have an active subspace. Because the method will not perform well if there is no decay in the eigenvalues of C, active subspaces are discovered rather than designed into a problem [64]. This method will be used to reduce dimensionality in the design space while maintaining the impact from each of the design variables.

CHAPTER 4. EXECUTION

Taking the methods developed in Chapter 3, this chapter outlines the process used in the research to address the research questions. This section is separated into an outline of the entire flow of the project, the process of data collection, data fitting through surrogate models, and active subspace analysis. Preliminary results will be presented in some sections to show the needed improvements that were made before final data could be collected and analyzed. The first section collects the tools outlined in Chapter 3 and combines them into a research methodology.

4.1 Research Methodology

Tools were selected in Chapter 3, but these tools must be combined through an intelligent methodology to collect and analyze data. To accomplish the research objective and answer all research questions, both traditional surrogates and active subspace surrogates are needed for comparison. The tools were compiled into a research methodology which allows for comparison of traditional and active subspace surrogates across a wide spread of aircraft configurations. This methodology is presented in Figure 29, and combines data collection, data analysis, and data comparison. Data collection and analysis will be further addressed in this chapter, and the details of data collection are presented next.

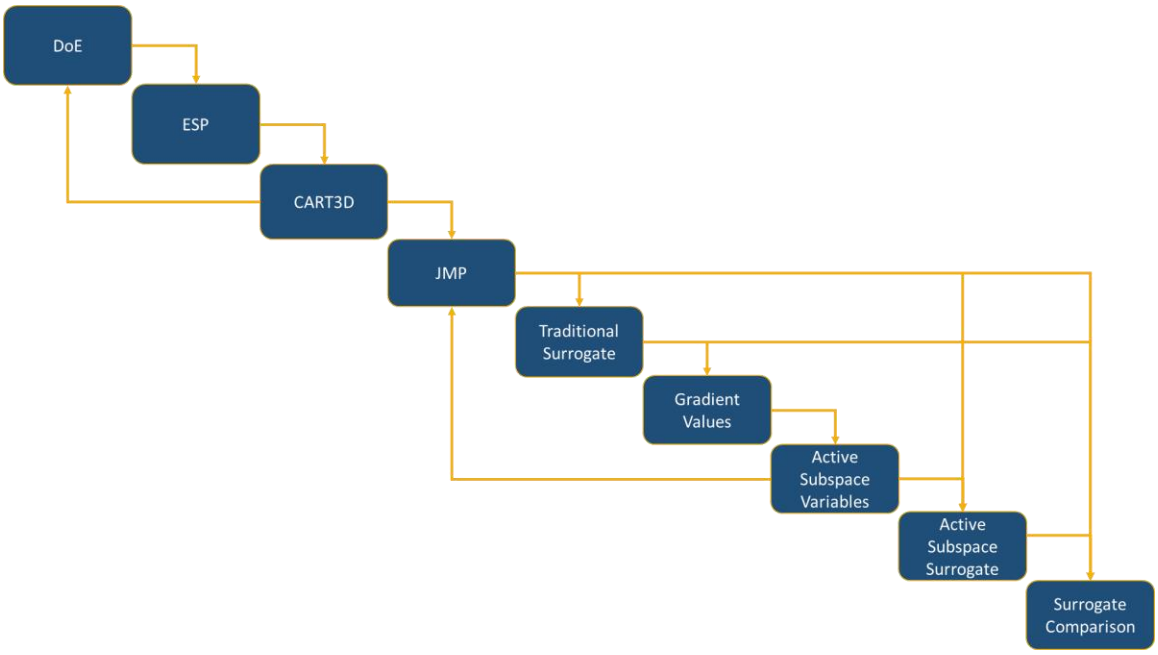

Figure 29: Research Methodology

4.2 Data Collection

All data was run on a Linux virtual machine on a 6 core Dell machine, and this computational limitation had to be taken into account. To collect data, a combination of Python and Shell scripts were created to automate the process from the defined DoE to calculating aerodynamic coefficients. The process, shown in Figure 30, begins with the DoE in a .csv file. This file is fed into ESP where the variables in the DoE case are converted into a geometry. This geometry is output as a tessellated .stl file which is fed into CART3D. CART3D transforms the .stl file into a .tri file and calculates the aerodynamic coefficients at the Mach number specified in the DoE and 0 degree angle of attack. These aerodynamic coefficients are then tabulated, the excess files are removed,

and the next case in the DoE is sent to ESP. The process repeats until there are no cases left in the DoE.

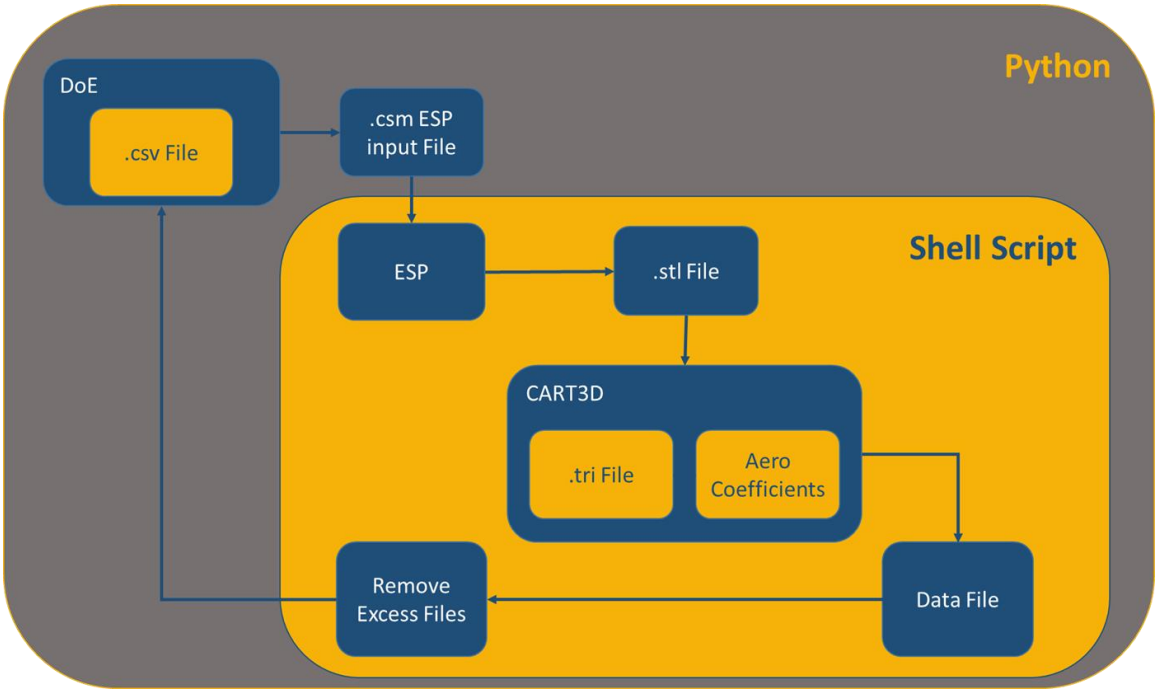

Figure 30: Code Layout to Automate DoE to Aerodynamic Coefficient Generation

4.2.1 Design Variable Selection and Ranges

Table 4 outlines the specified design variables and their maximum and minimum values. All variables except for Mach number are wing variables that may benefit supersonic or subsonic performance. Variables such as leading-edge radius and airfoil droop are included as these variables have been shown to improve takeoff and landing performance, so if they are negligible in the supersonic regime, it may be possible to benefit low speed performance without harming high speed performance.

Table 4: Design Variables and Ranges

Variable	Low	High		Variable	Low	High
Root Chord [inches]	600	1500		Tip Twist [degrees]	-6	3
Root-Mid Taper	0.3	0.7		Thickness to Chord (t/c) Root [% chord]	1.5	5
Mid-Tip Taper	0.1	0.5		t/c Mid [% chord]	3.0	6.5
Mach Number	1.5	3.0		t/c Tip [% chord]	4.5	8.0
Root-Mid Sweep [degrees]	50	70		LE Radius Root [multiplier]	0.1	2.0
Mid-Tip Sweep [degrees]	35	65		LE Radius Mid [multiplier]	0.1	2.0
Wingspan [inches]	600	1800		LE Radius Tip [multiplier]	0.1	2.0
Mid Span [% span]	30	70		LE Droop Root [degrees]	0	10
Root Twist [degrees]	-3	3		LE Droop Mid [degrees]	0	10
Mid Twist [degrees]	-3	3		LE Droop Tip [degrees]	0	10

These design variables were applied to a notional supersonic body and wing. The body was defined as an axisymmetric, cylindrical body that tapered to a tip and tail. The body was 2400 inches long with a maximum cylinder diameter of 120 inches. The nose and tail were tapered from a point to the maximum diameter over a 500-inch-long distance.

Another aspect of the geometry that was chosen was the baseline airfoil for each wing section. The airfoil was constant at each wing section, and was defined as a NACA 64A010. This airfoil does not have a sharp leading edge, and this airfoil was chosen to

study LE radius changes. The airfoil was parameterized using the Kulfan CST method functions built into ESP. The LE radius design variable was a multiplier to the first Kulfan upper and lower parameter, and thickness to chord was applied by multiplying each Kulfan parameter by the thickness to chord variable. The LE droop was applied to each section at the 10% chord of the airfoil. Figure 31 gives a notional wing and body geometry with design variables labeled, and Figure 32 shows an airfoil section with design variables labeled.

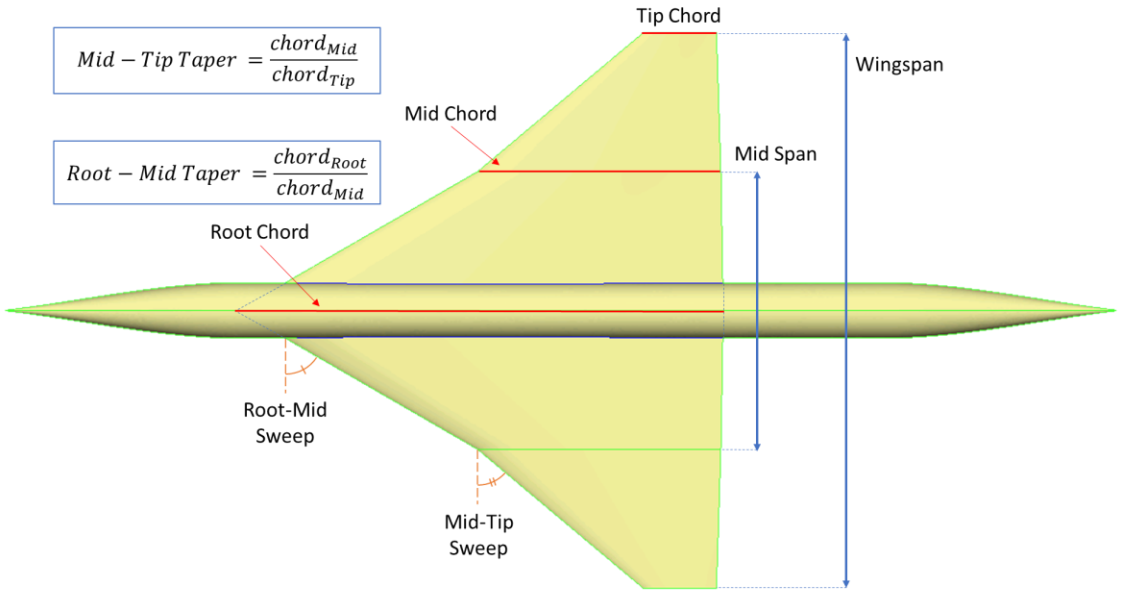

Figure 31: Notional Geometry with Planform Design Variables

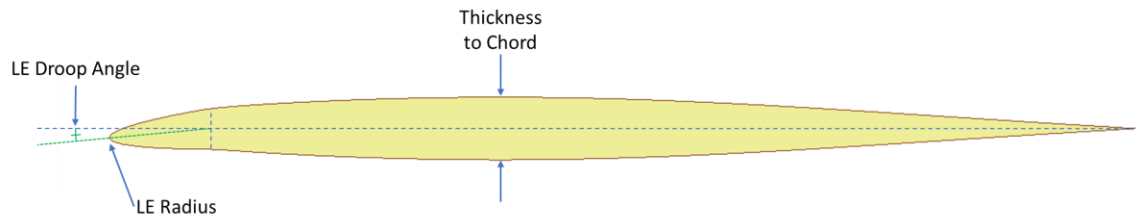

Figure 32: Notional Airfoil with Airfoil Design Variables

The ranges for each design variable were chosen to be wide enough to contain useful differences while limiting the range to realistic values. Edge cases were also checked to ensure the wing stayed within the limits of the fuselage. These variables were taken into a design of experiments to ensure the impact of each variable.

4.2.2 Design of Experiments

In order to fully map the design space, a Latin Hypercube DoE was created with 5000 cases. The Latin Hypercube design samples the interior of the design space balancing spacing and uniformity between points. The DoE uses 5000 cases in order to have as many cases per design variable while staying within the computational limits of using a single desktop computer. The large amount of cases will enable a better surrogate of the full design space which will allow more accurate gradient values at each of the points.

The design of experiments was created using JMP by SAS. This statistical software was fed the design variables, range of each design variable, type of design of experiments, and number of cases needed. Then JMP created the design of experiments with the designated number of cases within the design ranges specified. This design of experiments was then moved into a spreadsheet file and fed into a program to create the geometry of each point in the DoE.

4.2.3 Vehicle Parameterization

The vehicle was parameterized using Engineering Sketchpad. ESP takes in a text based file and generates a geometry, specifically a .stl file, to be taken into the computational fluid dynamics program. In order to parameterize the full design of experiments, the python code

read the case and values in the design of experiments, had ESP create the tessellated file, and then moved this file into CFD to run. Every geometry used the same tessellation parameters to ensure similarity. Because .stl files are large, the program also deleted the geometry before returning back to the DoE to start the next case.

4.2.4 Aerodynamic Analysis

The .stl was taken into CART3D to run the file. CART3D needs a .tri file to run, so an internal operator in CART3D was used to break the .stl and make a .tri file. This .tri file was run in CART3D at the given Mach number by using CART3D's internal grid generation and analysis tools. After the CART3D case finishes, the coefficients of lift, drag, and moment were taken and placed in a .csv file with the respective case number. After the coefficients were tabulated, all CART3D files were deleted except necessary input files.

CART3D can also perform mesh adaption when generating the mesh. To determine the number of adaptions and size of the grid needed to ensure consistent data collection, a grid study was completed with different levels of refinement. Due to the computational limitations of running on a local machine, the grid requiring the least computational time while maximizing accuracy was desired. The way CART3D changes grid size is through an input variable called maxR and the number of adaptions. The variable maxR defines the number of different sized cubes that can be used when growing the mesh off of the body and into the freestream. For example, a maxR of 10 means that the grid grows in steps moving from smallest, to second smallest, and continuing to increase until the 10^{th} cube size is present. With mesh adaption, each adaption looks for areas in the grid which needs further refinement, such as areas with shock waves present, and additional grid is added at

these points. Each adaption case requires a full run of CART3D to analyse the grid in order to make refinements. To perform the grid study, maxR and number of adaptions were changed and compared to a case using 4 million cells without adaption. The comparison for C_L and C_D is given in Figure 33 and Figure 34 respectively. The percent error for non-adapted C_L and C_D compared to the 4 million case is presented in Figure 35.

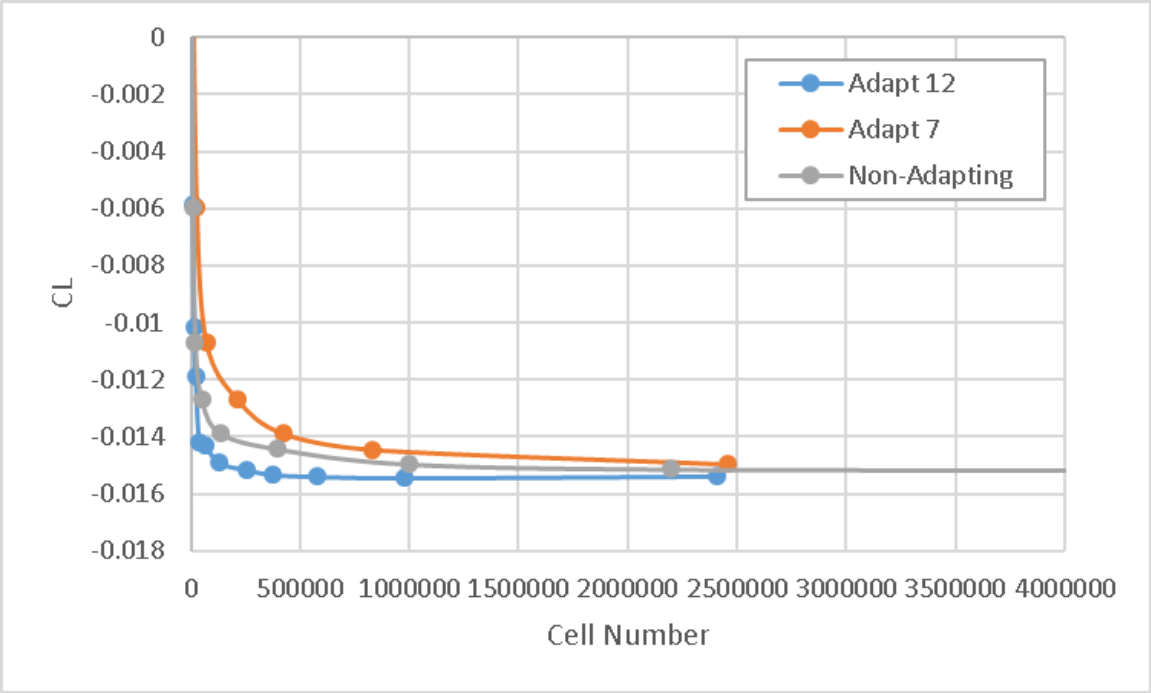

Figure 33: C_L Grid Study

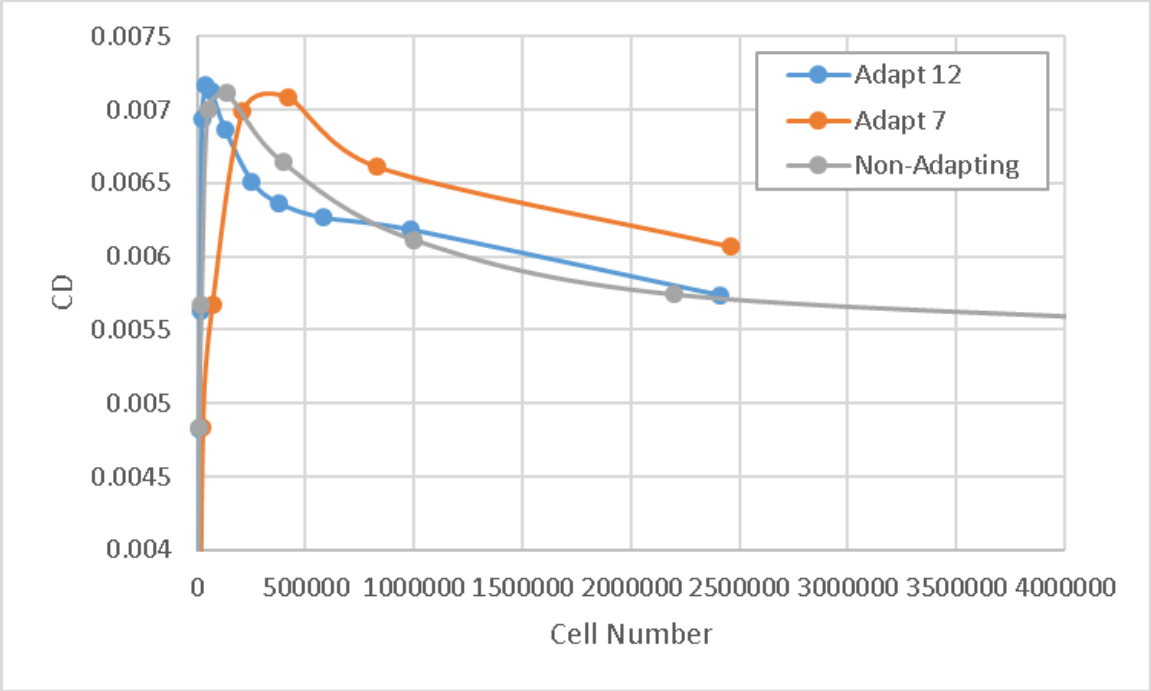

Figure 34: C_D Grid Study

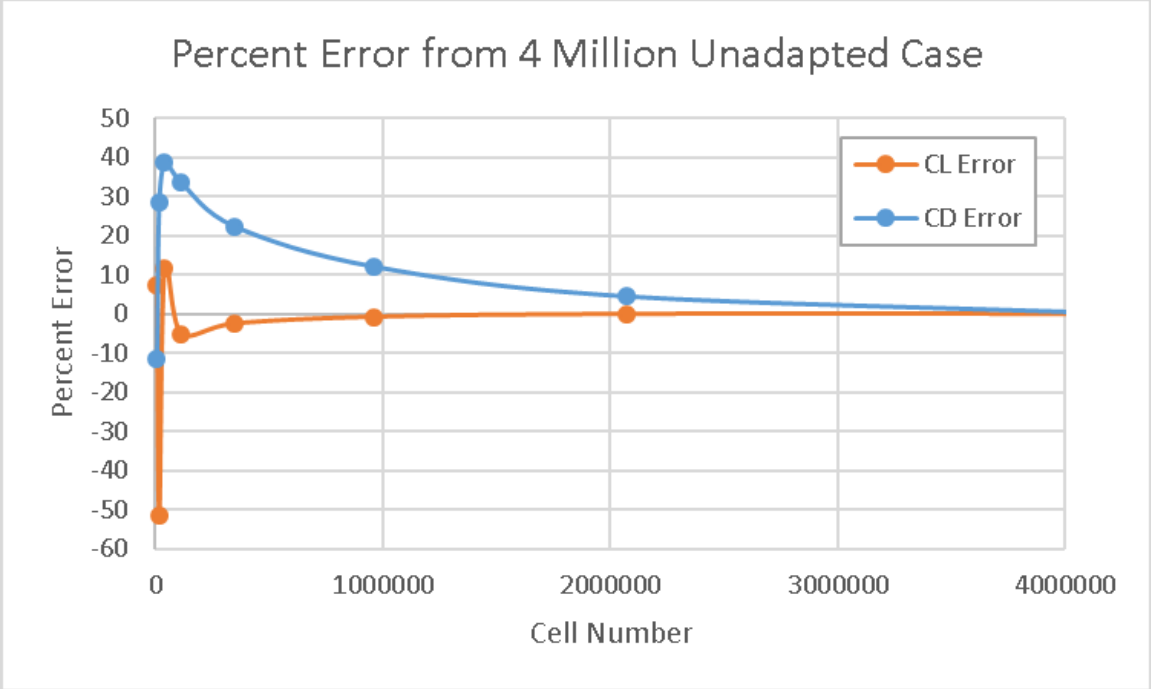

Figure 35: Grid Study Percent Error

These figures present the Adapt 7, Adapt 12, and non-adapting cases. Adapt 7 and 12 mean that either 7 or 12 adaption cycles were used to create the mesh. As more adaption cycles were used, smaller mesh growths were used to prevent the mesh from growing very large. This can be seen in the comparison of Adapt 7 to Adapt 12 as the grid points in Adapt 12 see a smaller growth in cell number than the Adapt 7 cases. The non-adapted line is generated by running different maxR values to generate a large initial mesh which is not adapted to be any larger.

Comparing the time with the accuracy, it was found that running zero adaptions with a mesh size around 2 million cells was within 5% of the 4 million cell mesh in both C_L and C_D error. This mesh size was found with a maxR of 13. While fine mesh adaption, seen in the Adapt 12 cases, saw a quicker convergence to the 4 million case, each adaption case is equivalent to running a full CART3D case. In order to get fine mesh refinement 12 CART3D cases would need to be run. While running a single large mesh takes longer than a case with a smaller mesh, it was determined that a single, larger mesh case was more computationally efficient than running multiple cases.

4.3 Baseline Surrogate Generation

After aerodynamic data was collected from the data collection flow, the data needed to be analysed. Before comparisons could be made, a traditional surrogate and active subspace surrogates needed to be created. Because gradients were calculated from a surrogate, an initial surrogate of the design space was created. From the goodness of fit section, good surrogates have a value of R^2 of 0.95 or higher, but the goal is to have 0.99 or higher. The higher the R^2, the more accurate the model will be able to match the CFD data and

interpolate the data within the design space. In addition to a good R^2 fit, the training and validation error need to be small.

The first step in surrogate generation was to take the data into JMP. The data was partitioned into fitting and validation data with validation being a random 25% of the total data set. These cases were not used to create the surrogate and were used to compare the goodness of fit of the surrogate model against points that were not included in the surrogate generation. After the validation column was created, JMP was used to create the surrogate. For the surrogates, the aerodynamic coefficients were chosen as the response variables, and the design variables were chosen as input variables. Initially a direct linear relationship was used where no interaction terms were considered. In the actual vs. predicted and residual vs. predicted plots shown in Figure 36 and Figure 37, clear trends could be seen, especially in the C_D fits, indicating poor fits and the need for high order terms.

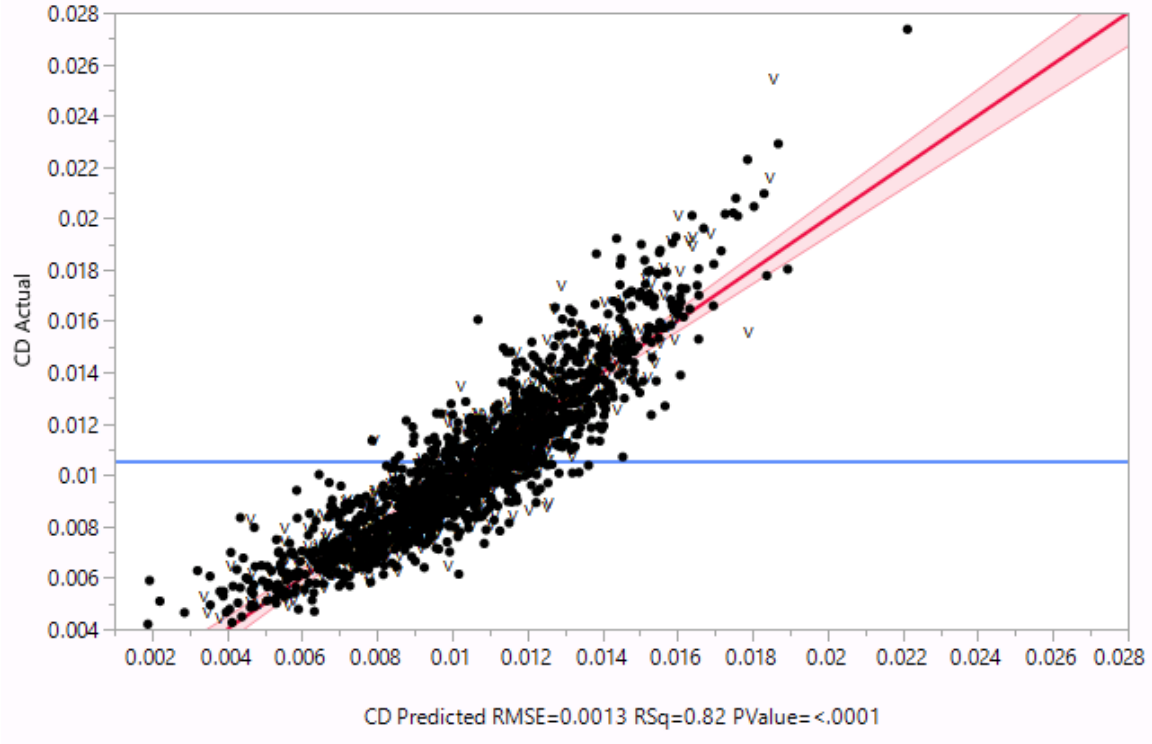

Figure 36: Actual vs. Predicted Plot for Linear C_D Fit

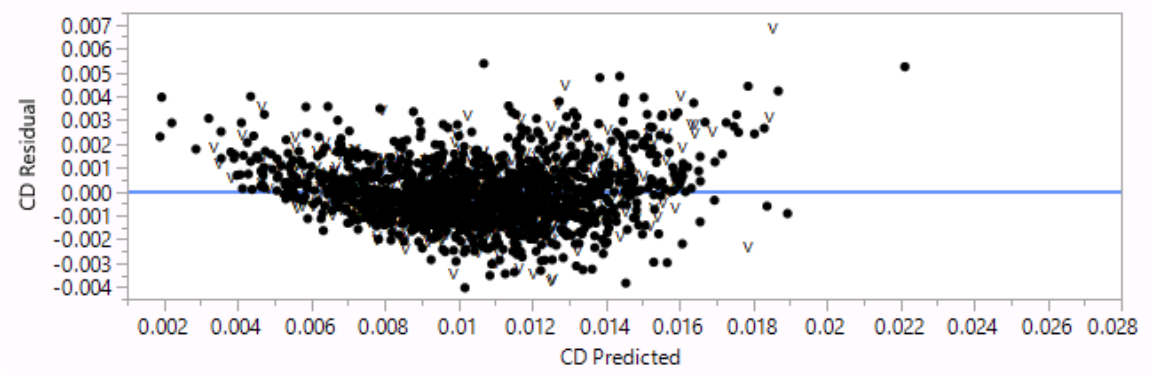

Figure 37: Residual vs. Predicted Plot for Linear C_D Fit

When extended to quadratic fits, the actual vs. predicted plot was very thick, shown in Figure 38, while a slight concave up trend can still be seen in the residual vs. predicted plot as shown in Figure 39.

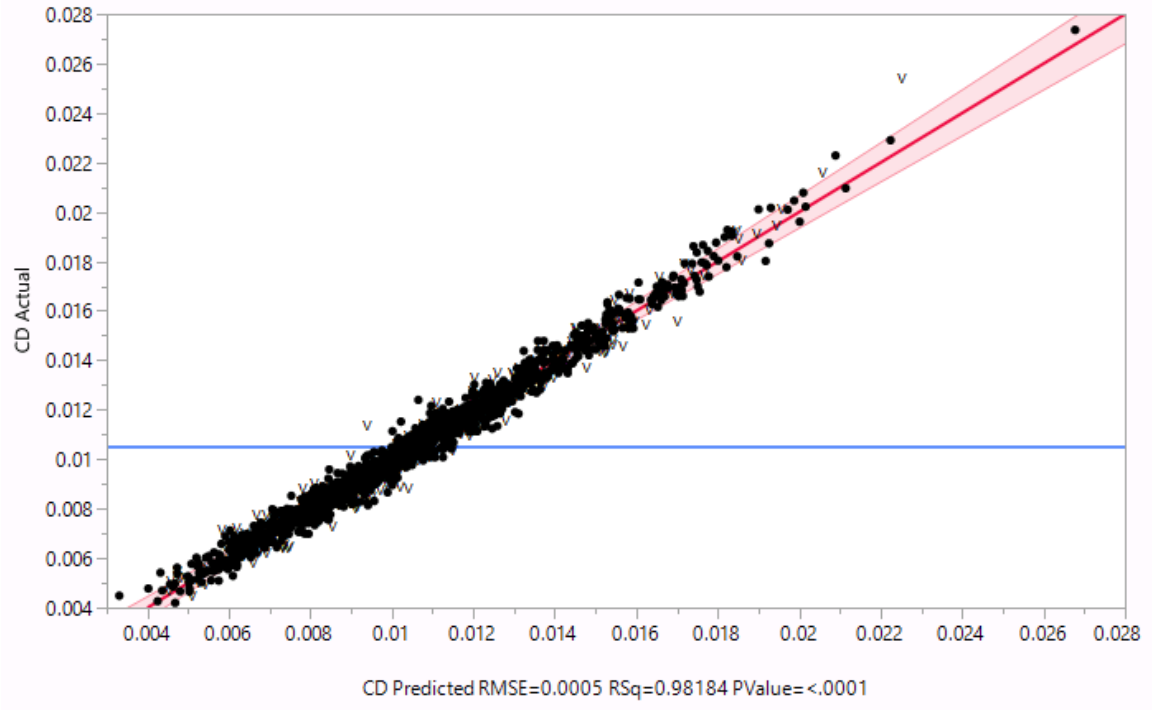

Figure 38: Actual vs. Predicted Plot for Quadratic C_D Fit

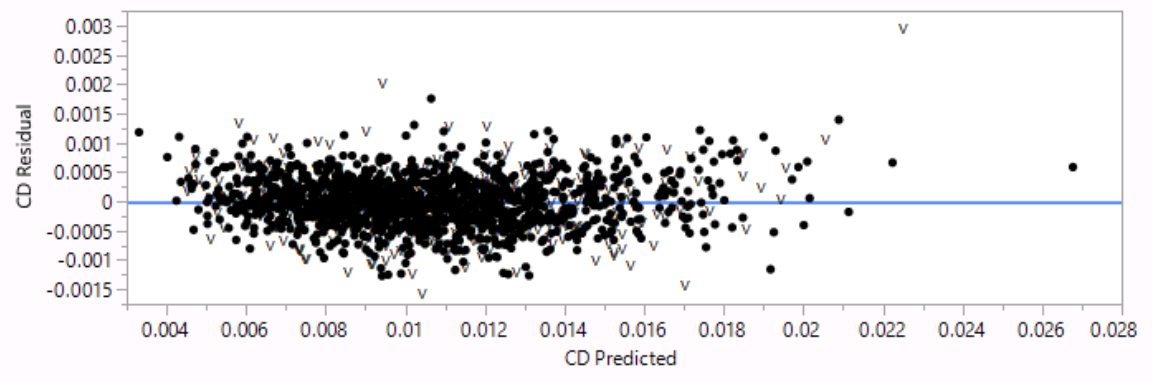

Figure 39: Residual vs. Predicted Plot for Quadratic C_D Fit

These trends usually mean that higher order terms were needed to properly model the case, so the input variables were increased to include both the pure design variables, the design variables multiplied by all the other design variables, and a third level of higher order terms. With so many extra input terms, a new method for generating surrogates was

used called stepwise regression. Stepwise regression continues to add terms until the validation R^2 begins to decrease. With the higher order terms and stepwise regression, good fits were found for both coefficient of lift and coefficient of drag.

4.4 Active Subspace Analysis

Once a surrogate model of the design space was taken, the surrogate equations were used to generate gradients. These gradients were used to develop the active subspace variables which were then used to generate active subspace surrogates with reduced dimensionality.

4.4.1 Active Subspace Variable Calculation

With good fits found from the surrogates, partial derivatives of the surrogate response equations were taken to develop gradient equations for each design variable at all points in the design space as seen in Equation 4.

$$\nabla_x f(x) = \begin{bmatrix} \frac{\partial f}{\partial x_1}(x) \\ \vdots \\ \frac{\partial f}{\partial x_{20}}(x) \end{bmatrix} \qquad \textbf{Equation 4}$$

A MATLAB script was created to calculate gradients and generate the active subspace variables. To begin generating gradients, the code was fed the C_L and C_D surrogate equations. Treating these equations as symbolic equations, internal MATLAB functions were used to calculate the partial derivatives with respect to each design variable. Using the partial derivatives, and the input data from the DoE, the gradients for each variable was found at each of the points in the DoE.

The script then combined the gradients into the C matrix and the eigendecomposition of the C matrix was performed. The decomposition was plotted to inform the user on the relative importance of each active subspace variable. The eigenvectors and values were sorted by order of importance in the eigendecomposition, and the design space was rotated into the active subspace. From this rotation, equations for the active subspace variables were created in terms of all 20 design variables.

4.4.2 Active Subspace Surrogates

With equations for the active subspace variables created, these equations were taken into JMP at each point in the DoE. JMP can apply an equation to a column of data, so each equation was input into a column in JMP. With the DoE data, each active subspace variable column is populated with the value of the active subspace at the given point in the DoE. Using the aerodynamic coefficients as responses and the active subspace variables as the inputs, surrogate equations were created in the active subspace. Using the eigendecomposition plot, the designer could intelligently select the dimensionality of the active subspace based on the importance of the eigenvalues; however, currently there is no mechanistic way to determine the number of active subspace variables needed to develop a good surrogate fit. These surrogates were generated and compared to traditional surrogates of the design space. Conclusions realized from analysing the data were used to help develop a conceptual design methodology for commercial supersonic aircraft.

CHAPTER 5. RESULTS AND DISCUSSION

This section presents the results throughout the steps outlined in the execution stage. Example aerodynamic results will be presented and the surrogate developed from these results will be given. This surrogate was used to calculate gradients which were used to calculate active subspace variables. Next, the active subspaces surrogates will be presented, and the three research questions addressed. Computational cost will then be calculated to determine the impact of active subspaces on a design methodology. Finally, from the results, a design methodology will be presented incorporating active subspaces.

5.1 Aerodynamic Results

Each case in the DoE generates a different configuration in terms of wing planform. Each wing planform was run through CART3D and the aerodynamic coefficients were calculated. Due to limited computational capacity, only 3825 cases out of the 5000 successfully provided results, and two of these cases will be given as examples. Cases 31 and 161 from the DoE are given in Figure 40 and Figure 41. These show the range of the design space. The root chord location is kept constant, but because this study is only investigating lift and drag, stability considerations were neglected.

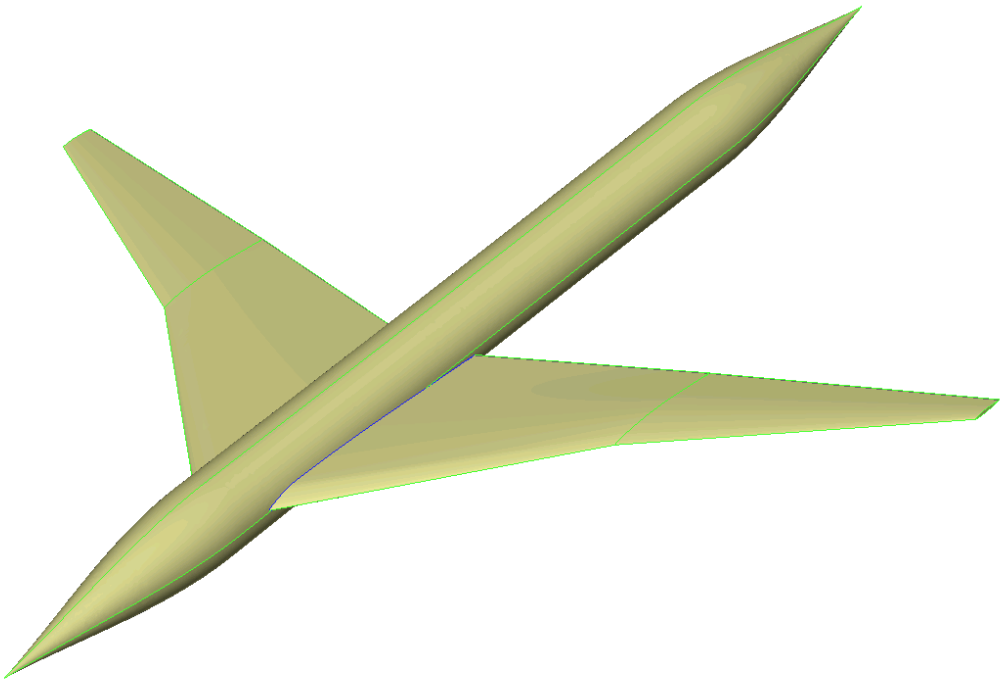

Figure 40: Case 31 Configuration

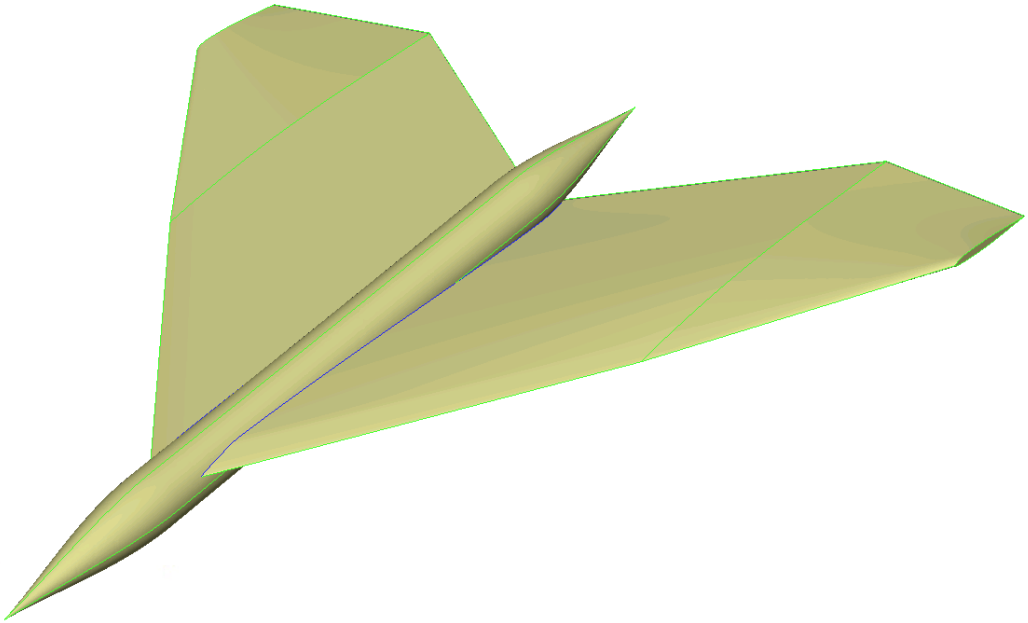

Figure 41: Case 161 Configuration

The aerodynamic results were tabulated for each run. Coefficients of lift, drag, and moment were all taken; however, only coefficients of lift and drag were used for the analysis. The design variable values as well as the coefficients of lift and drag and the L/D for the cases 31 and 161 given in the previous figures are provided in Table 5.

Table 5: Design Variables and Aerodynamic Coefficients for Cases 31 and 161

Case Number	31	161
Root Chord [inches]	622.6131	1500
Root-Mid Taper	0.434673	0.68794
Mid-Tip Taper	0.274874	0.301005
Mach Number	1.711055	1.98995
Root-Mid Sweep [degrees]	54.62312	61.55779
Mid-Tip Sweep [degrees]	42.68844	63.19095
Wingspan [inches]	1468.342	1697.487
Location of Mid Span [% wingspan]	48.8945	60.9548
Root Twist [degrees]	-1.79397	-2.8794
Mid Twist [degrees]	-2.09548	-1.37186
Tip Twist [degrees]	-1.70352	-5.72864

t/c Root [% chord]	2.9422	1.8869
t/c Mid [% chord]	5.8668	4.0025
t/c Tip [% chord]	6.9623	5.4322
LE Radius Root [multiplier]	1.723116	0.81608
LE Radius Mid [multiplier]	0.48191	0.348241
LE Radius Tip [multiplier]	1.121608	1.522613
Droop Root [degrees]	7.085427	4.522613
Droop Mid [degrees]	2.964824	1.105528
Droop Tip [degrees]	0.603015	4.170854
Coefficient of Lift	0.047419	0.179925
Coefficient of Drag	0.01035	0.015735
L/D	4.581656	11.43493

A scatterplot matrix of the C_L plotted against the C_D values for all 3825 successful cases is given in Figure 42.

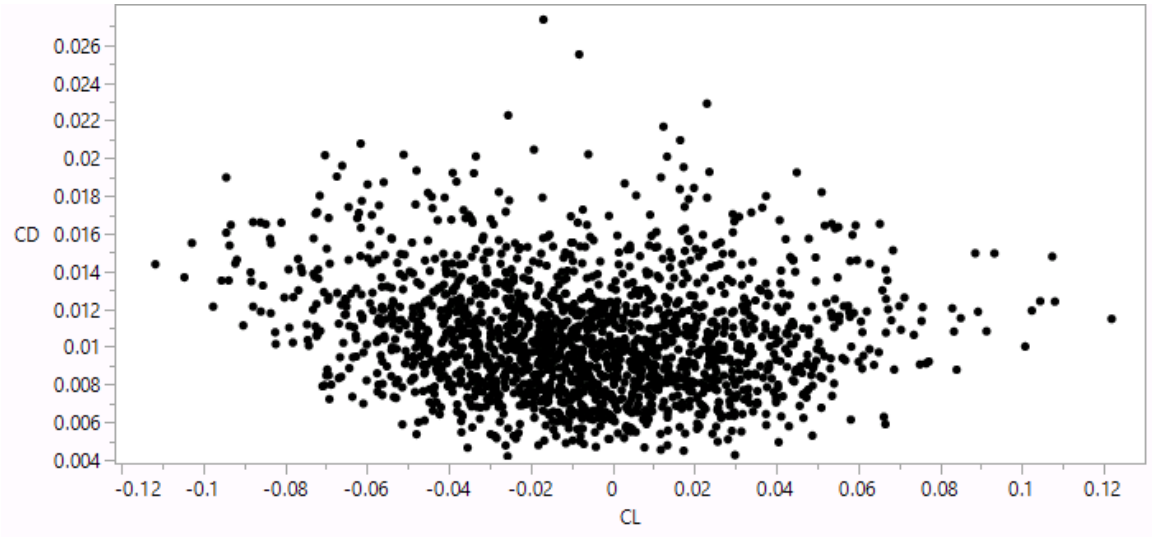

Figure 42: Scatterplot Matrix of C_L vs. C_D for the 3825 Cases

Finally, Figure 43 and Figure 44 show the distribution of the C_L and C_D over the 3825 cases. These distributions show that the C_L values are normally distributed while the C_D values are skewed left.

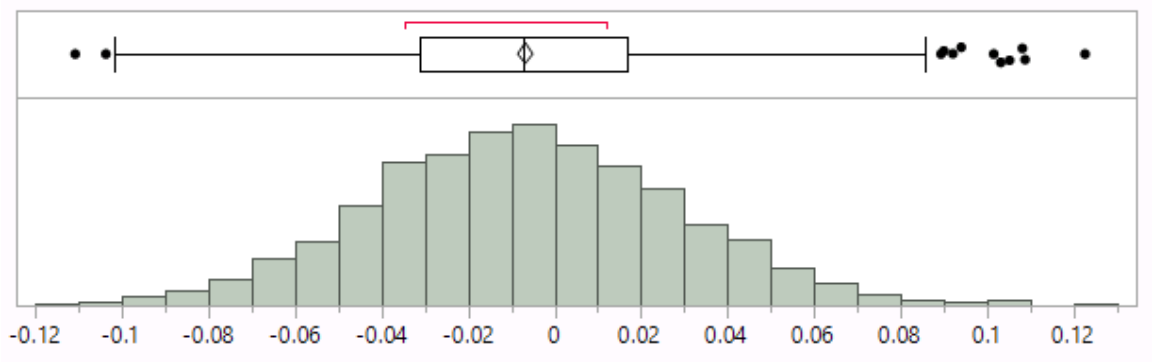

Figure 43: C_L Distribution over the 3825 Cases

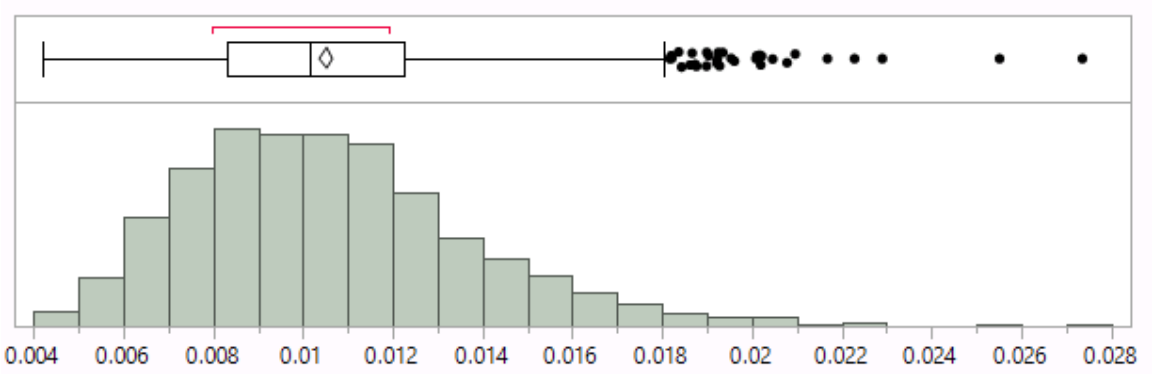

Figure 44: C_D Distribution over the 3825 Cases

5.2 Surrogate Generation Results

To generate surrogates of coefficient of lift and coefficient of drag, two transformations were needed. First, the C_L values were normalized between 0 and 1. This transformation was used to prevent very large percent errors from appearing when the expected value is near zero. Second, in order to make the C_D distribution a normal distribution, the log of the C_D data was taken. This transformation led to the data approaching a normal distribution, as shown in Figure 45.

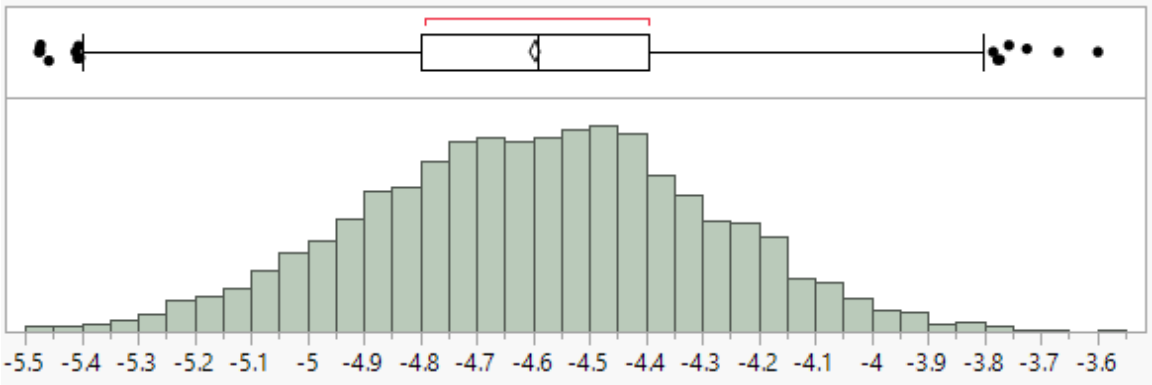

Figure 45: Log(C_D) Distribution over the 3825 Cases

With the aerodynamic coefficients transformed, surrogate models of C_L and C_D were generated over the entire design space with respect to the design variables. 75% of the data was taken for surrogate fitting while 25% of the data was separated for validation checks of the surrogate. A surrogate of L/D was not created because dividing the two results leads to additional error in the data. As mentioned in Chapter 4.2.1, the best fits were found when third order terms and stepwise fits were used. Figure 46 and Figure 47 show the actual vs. predicted plot of the surrogate models for C_L and C_D respectively. The goodness of fit values, defined by R^2, and the average fit and validation errors are given in Table 6 for both surrogates. The errors were calculated using a percent error formula comparing the surrogate-predicted value against the CFD-actual value. The validation error was calculated from the 25% of the data that was not used to fit the surrogate, and shows the accuracy of the model against points that were not used for training.

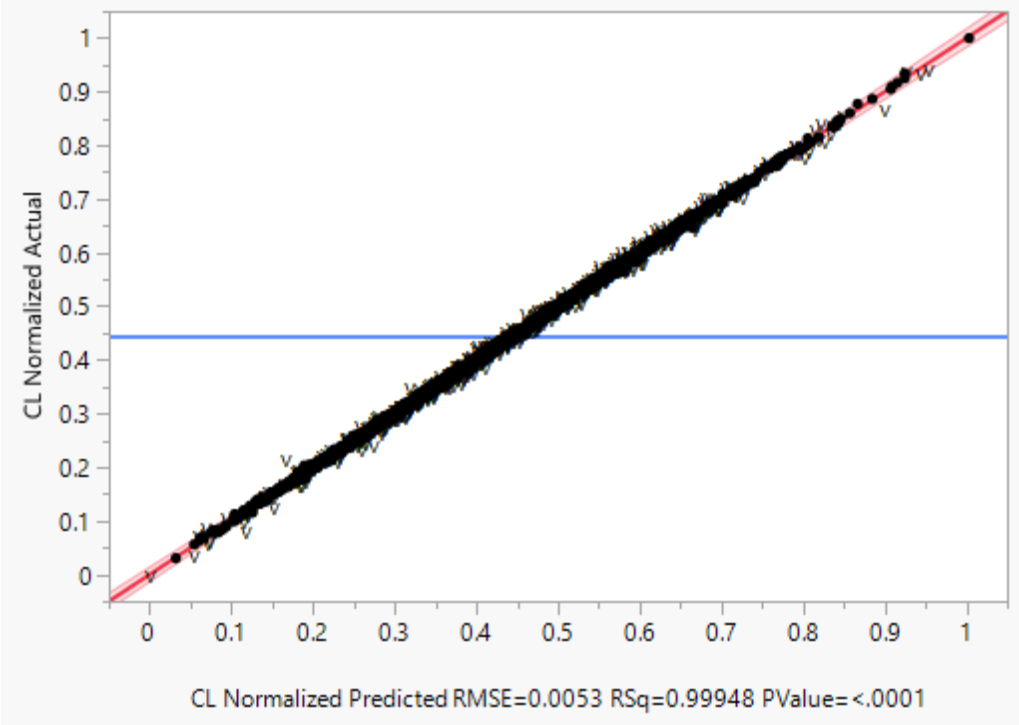

Figure 46: Normalized C_L Actual vs. Predicted Plot

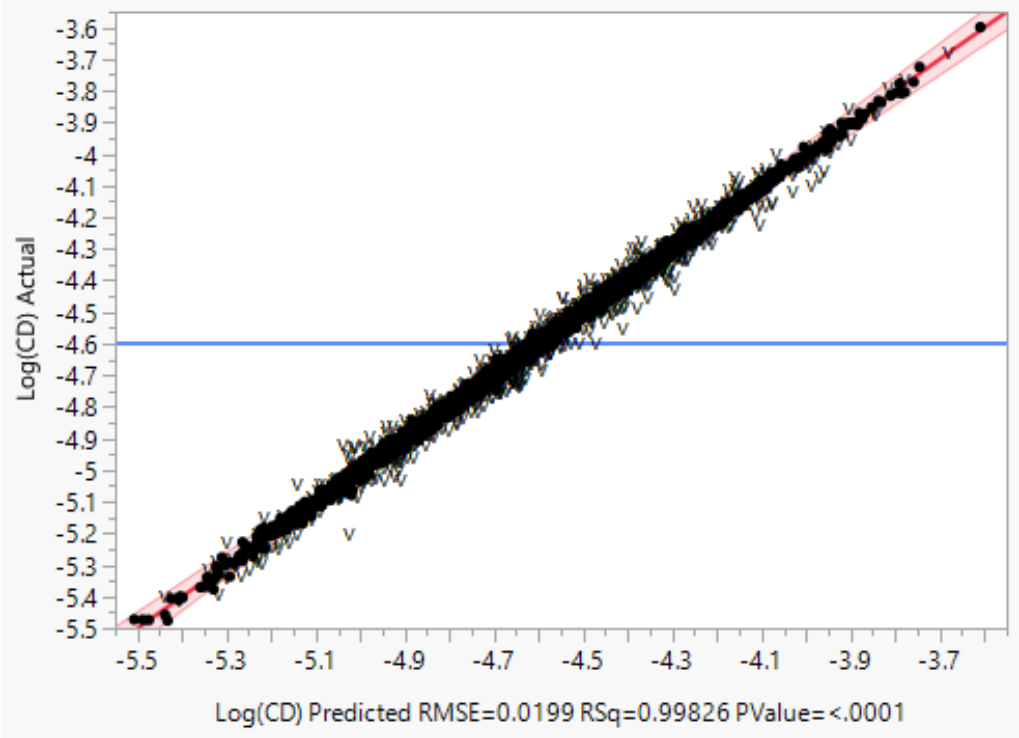

Figure 47: Log(C_D) Actual vs. Predicted Plot

Table 6: Goodness of Fit of the Surrogate Models

Surrogate	Set Used	R Square	Average Percent Error [%]
Normalized Coefficient of Lift	Training Set	0.9985	0.6751
	Validation Set	0.9974	1.8960
Log of Coefficient of Drag	Training Set	0.9983	0.9568
	Validation Set	0.9840	2.9688

An additional measure of goodness of fit is to look at the residual by predicted plot. Ideally this plot has no visible patterns with a random scatter of points throughout the plot and the range of the residual values are less than 10% of the predicted range. Figure 48 and Figure 49 show that both the C_L and C_D residual vs. predicted plots do not have a pattern and the range of the residual axes for C_L is less than 10% of the range of the predicted axes while C_D is slightly larger than 10%.

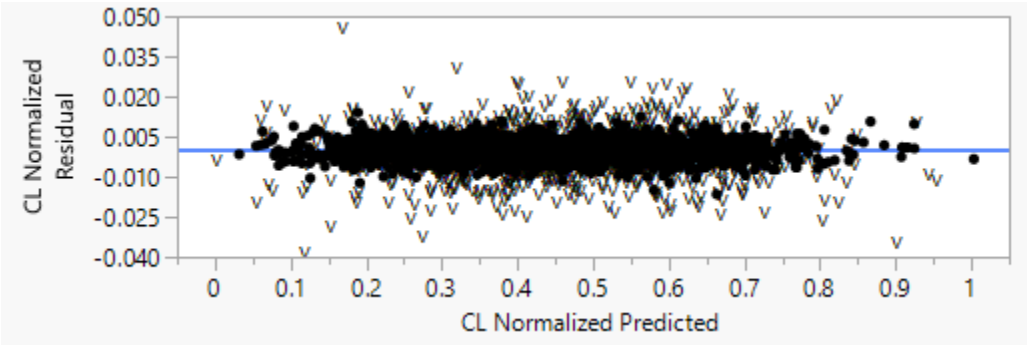

Figure 48: Normalized C_L Residual vs. Predicted Plot

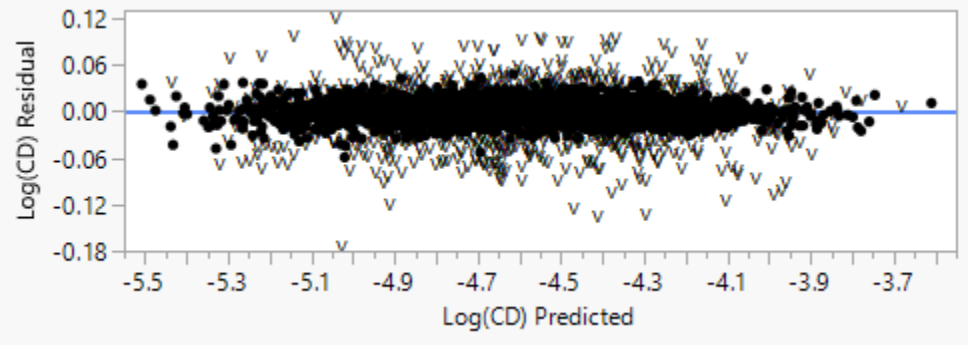

Figure 49: Log(C_D) Residual vs. Predicted Plot

From these plots and the near-one R^2 values of the surrogates, these models are good fits over the design space, and accurate results can be obtained within the design space. While additional cases could improve the surrogates, given computational limitations, these surrogates were used to find gradient values by taking first partial derivatives of the surrogate with respect to each design variable.

5.3 Active Subspace Results

5.3.1 Full space results

The first step was to see if an active subspace could be found within the design space. Using the derivatives of the surrogate equations with respect to each design variable, a matrix of gradients was created by evaluating the derivatives at all 5000 points in the original design of experiments. From the matrix of gradients, a C matrix was created for both normalized C_L and log(C_D). The eigenvalues and eigenvectors were calculated for the C matrix, and an eigenvalue decomposition was performed for both C_L and C_D to visualize

the importance of each active subspace dimension. The results from the eigenvalue decomposition can be seen in Figure 50.

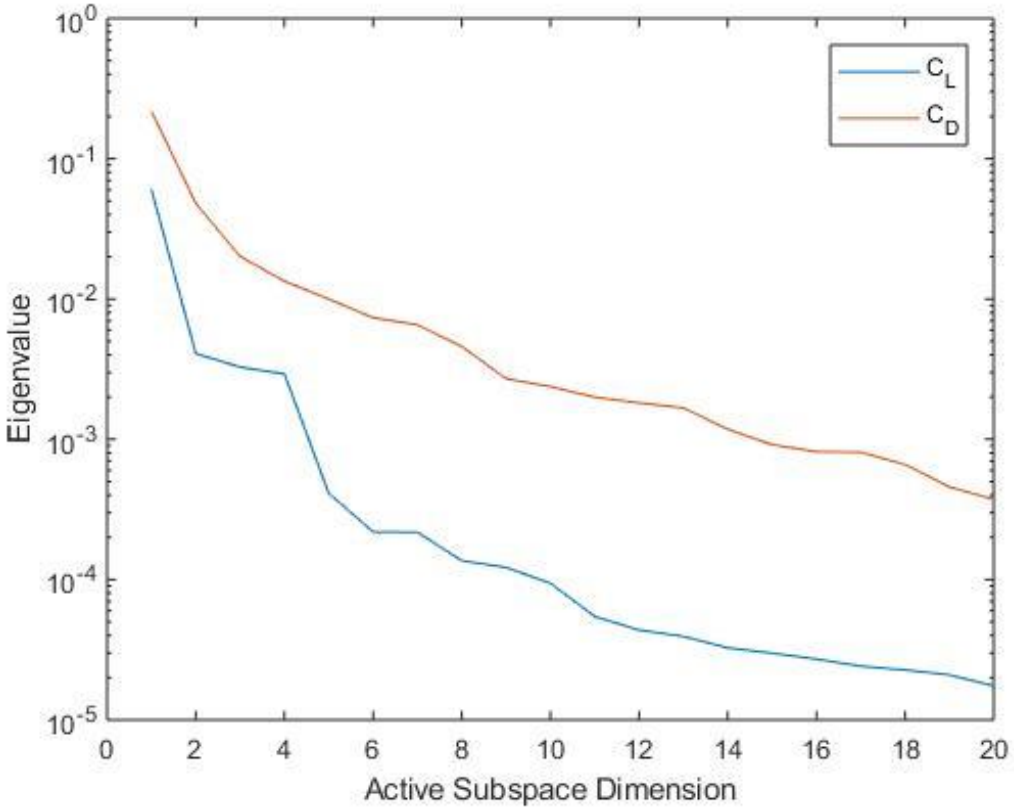

Figure 50: Eigenvalue Decomposition for C_L and C_D

To identify the importance of each active subspace dimension, large drops in the eigenvalues needed to be identified. Both C_L and C_D have a very important first dimension. After the first active subspace variable, C_D eigenvalues consistently drop from dimensions 2 to 20; however, C_L sees a second large drop after the 4^{th} active subspace dimension. From this, it is expected that C_D will have a consistent increase in goodness of fit as active subspace dimensions increase while C_L will have a large increase in goodness of fit until the 4^{th} dimension where it will begin to level off.

Choosing the dimensionality of the active subspace is determined by the analyst, and to prevent any bias, active subspace surrogates were created for all active subspace dimensions from an active subspace made only of the most important dimension to one made of all 20 active subspace dimensions. To develop these surrogates, the active subspace dimensions were taken and calculated for each point in the design of experiments. Each active subspace dimension is a combination of all 20 design variables, so each dimension contains effects from each design variable. Once the active subspace dimension variables have been calculated for each dimension, surrogates were created using the active subspace dimensions as the input variables and the calculated Norm(C_L) and Log(C_D) values as the responses. Plots of the R^2 values and average error are given in Figure 51 and Figure 52 across all 20 active subspace dimensions.

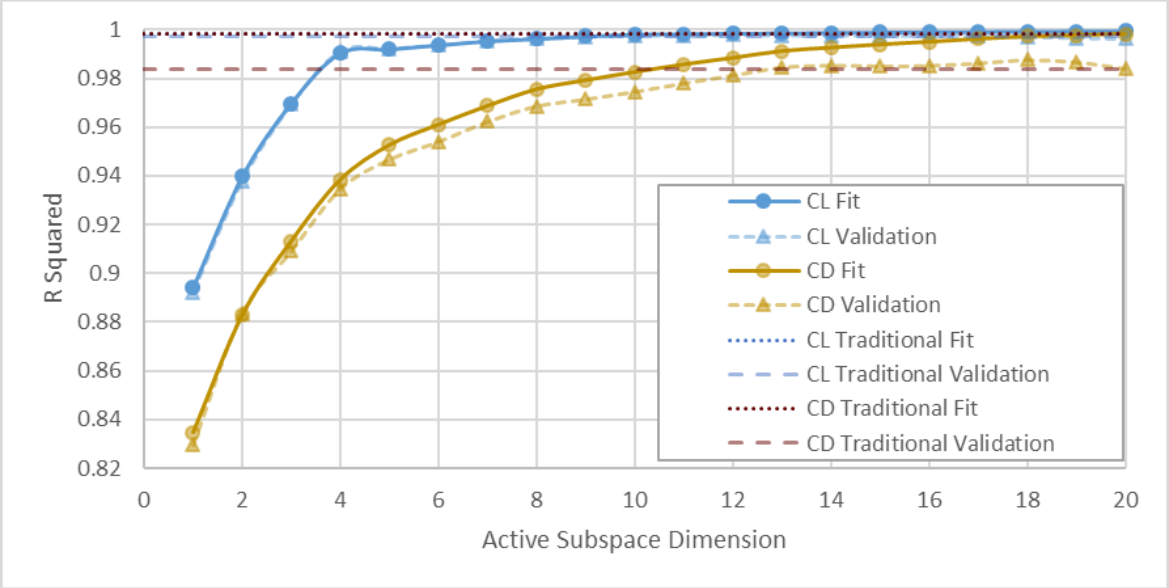

Figure 51: Goodness of Fit of Active Subspace Surrogates

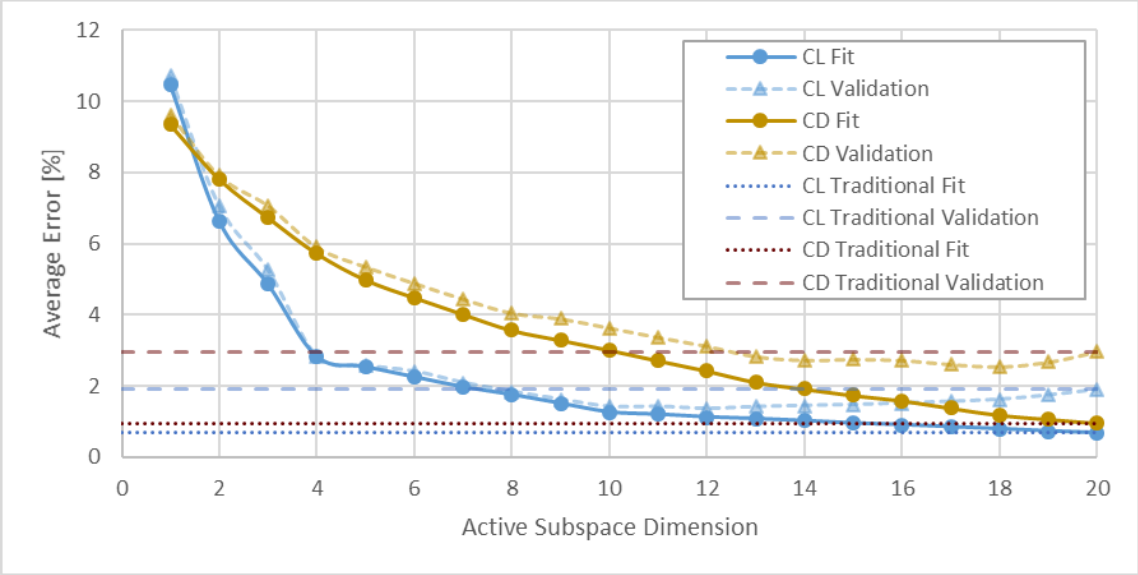

Figure 52: Average Error of Active Subspace Surrogates

In these figures, the C_L and C_D fit and validation values are plotted across all 20 dimensions, and the traditional fit and validation values are included as horizontal dotted lines. As expected from the eigenvalue decomposition plot, the error continually decreases as more dimensions are added to the C_D active subspace but the C_L active subspace sees a large decrease in error until 4 dimensions, where the error begins to taper off. One interesting observation is that both the C_L and C_D active subspace surrogates see a lower validation error that the traditional fit before rising back to meet the traditional fit at 20 dimensions. This indicates that the current traditional fit may be overfitting the data. It was expected that the active subspace surrogates would match the traditional surrogates when the dimensionality reaches 20, so this is proof that the method is working.

From these results, it can be seen that C_L will be able to reduce dimensionality more than C_D due to the rapid decrease in error from the greater importance of the first four dimensions. C_D can also see a dimensionality reduction but it does not have as large of a

separation as C_L. The benefit of using active subspaces is that even though the total number of design variables has decreased through dimensionality reduction, the design variables in the active subspace are combinations of the original design variables, so the information about the design space is not lost. To illustrate this, the first active subspace variable for both C_L and C_D are given in Equation 5 and Equation 6.

$$
\begin{aligned}
y_{1C_L} = {} & 0.06791 * Mach - 0.00465 * LEradMid - 0.00318 \\
& * LEradTip - 0.00575 * LEradRoot - 0.03816 \\
& * InSweep + 0.01369 * MidSpan - 0.01021 \\
& * MidTaper + 0.80240 * MidTwist - 0.04382 \\
& * OutSweep - 0.00341 * RootChord \\
& + 0.55853 * RootTwist - 0.02958 * TipTaper \\
& + 0.15968 * TipTwist + 0.03076 * Wingspan \\
& + 0.07853 * droopMid + 0.01344 * droopTip \\
& + 0.04642 * droopRoot - 0.00367 * tcMid \\
& - 0.00358 * tcRoot + 0.00097 * tcTip
\end{aligned}
$$

Equation 5

$$y_{1C_D} = 0.40322 * LEradMid - 0.30551 * InSweep + 0.12298 * LEradTip + 0.10069 * LEradRoot - 0.06425 * Mach - 0.34105 * MidSpan + 0.02474 * MidTaper + 0.09272 * MidTwist - 0.38125 * OutSweep - 0.30125 * RootChord + 0.07319 * RootTwist + 0.07676 * TipTaper + 0.00206 * TipTwist - 0.03432 * Wingspan + 0.24917 * droopMid + 0.04896 * droopTip + 0.13270 * droopRoot + 0.46353 * tcMid + 0.18287 * tcRoot + 0.10116 * tcTip$$

Equation 6

To further illustrate the active subspace surrogates, two are shown to visualize the goodness of fit: a C_L surrogate with 10 active subspace variables and a C_D surrogate with 14 active subspace variables. To accurately compare with the full, unique design variable surrogate, a cubic surrogate was used for all active subspace surrogates, so up to third order combinations between variables were used to create the surrogate with stepwise fits used. Figure 53 and Figure 54 provide the actual vs. predicted plots for the C_L and C_D surrogates, and Figure 55 and Figure 56 give the residual vs. predicted plots for each surrogate.

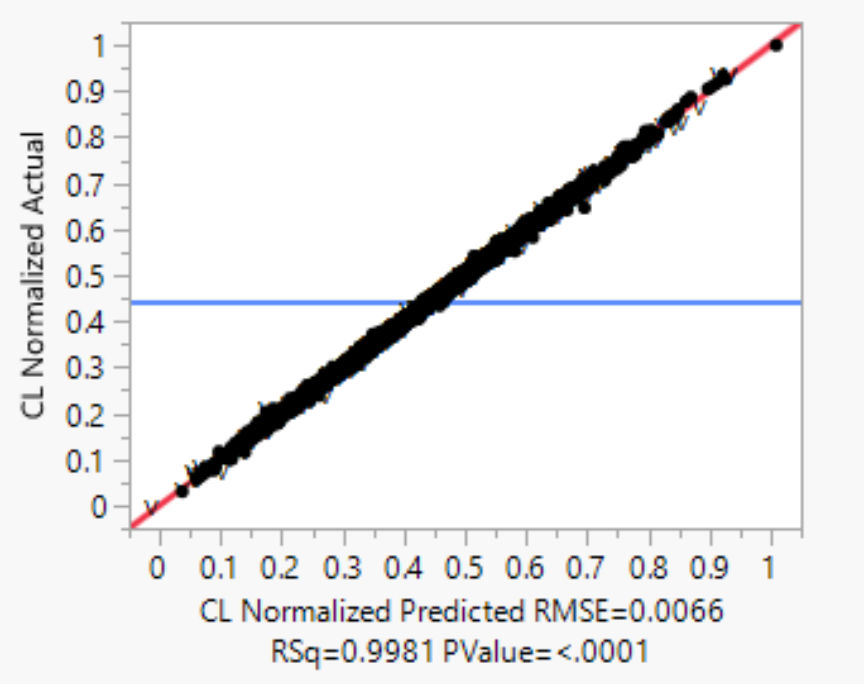

Figure 53: C_L 10 Active Subspace Surrogate Actual vs. Predicted Plot

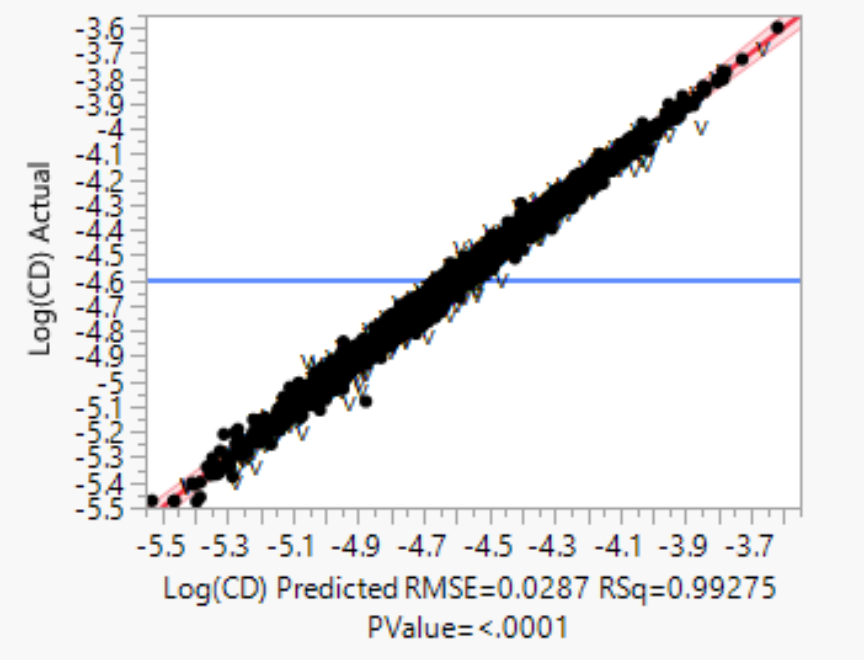

Figure 54: C_D 14 Active Subspace Surrogate Actual vs. Predicted Plot

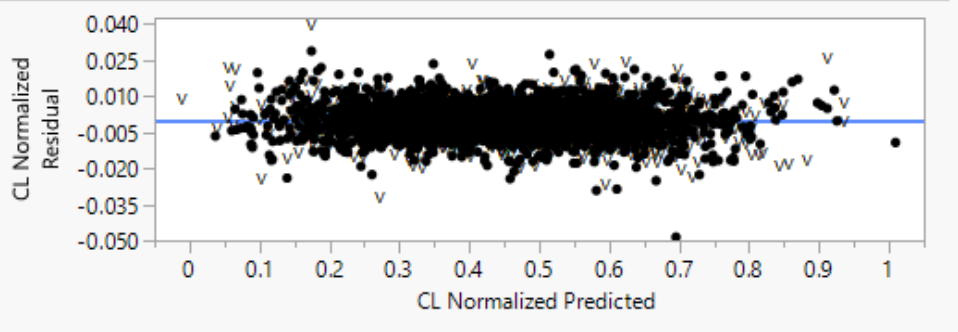

Figure 55: C_L 10 Active Subspace Surrogate Residual vs. Predicted Plot

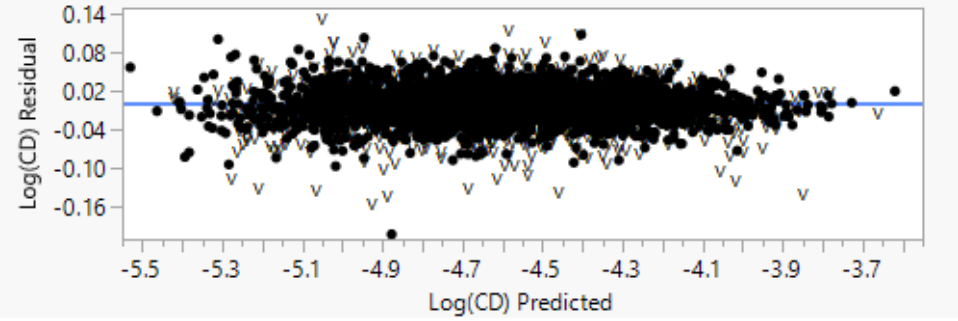

Figure 56: C_D 14 Active Subspace Surrogate Residual vs. Predicted Plot

These results show that an active subspace can be found within the design space, and active subspace surrogates can reduce dimensionality while maintaining good fit to the data. With this proven, active subspace theory was further analyzed through the specific research questions.

5.4 Research Question 1: How does the number of gradient values used to calculate active subspace variables impact the error an active subspace surrogate?

From Section 1.2.2.1, it was shown that the recommended number of cases was found by using Equation 1, which is a function of oversampling rate, number of gradients desired, and number of design variables. When initially finding an active subspace in the space, the gradients were greatly oversampled compared to this equation, as 5000 gradients were

calculated. Using Equation 1, with an oversampling rate of 2 and of 10, which are the minimum and maximum values recommended, the recommended number of cases can be calculated.

$$M(\alpha = 2, k = 20, m = 20) = 2 * 20 * \ln(20) = 119.8 \approx 120\ cases$$

$$M(\alpha = 10, k = 20, m = 20) = 10 * 20 * \ln(20) = 599.1 \approx 600\ cases$$

The recommended number of cases is a range of 120 to 600 gradients to define all 20 active subspace dimensions. This number is an order of magnitude lower than the number of gradients used to calculate the original active subspace variables.

To test the effects of over and undersampling, the number of gradient calculations were varied from 50 to 4500 runs, surrogates were created for each case, and the surrogate errors were compared for 1, 5, 10, and 15 active subspace surrogates. Each surrogate was fit with all 3825 responses. The C_L fit error is presented in Figure 57, C_L validation error in Figure 58, C_D fit error in Figure 59, and C_D validation error in Figure 59.

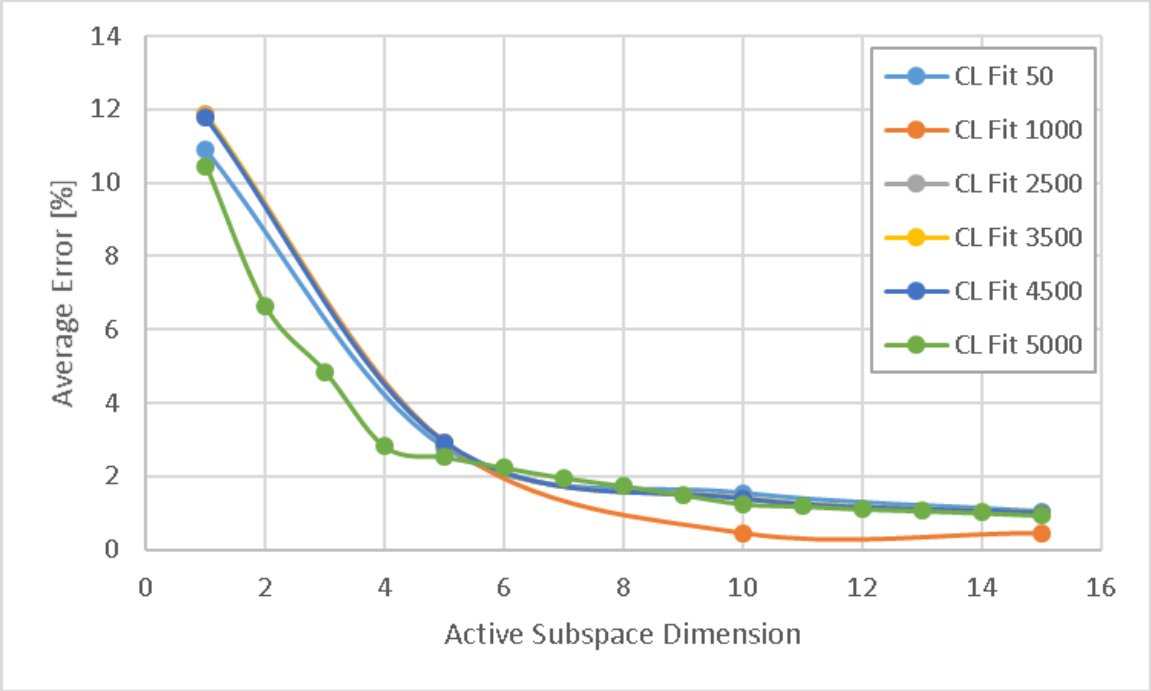

Figure 57: C_L Fit Error vs. Active Subspace Dimension for Different Number of Gradient Inputs

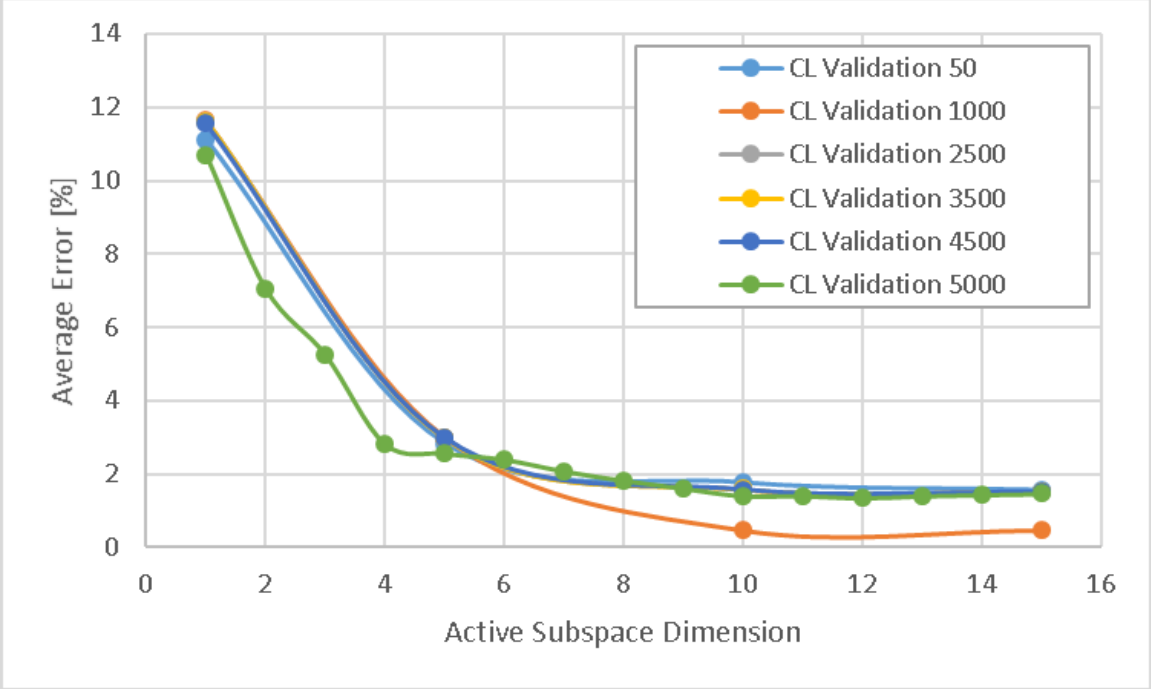

Figure 58: C_L Validation Error vs. Active Subspace Dimension for Different Number of Gradient Inputs

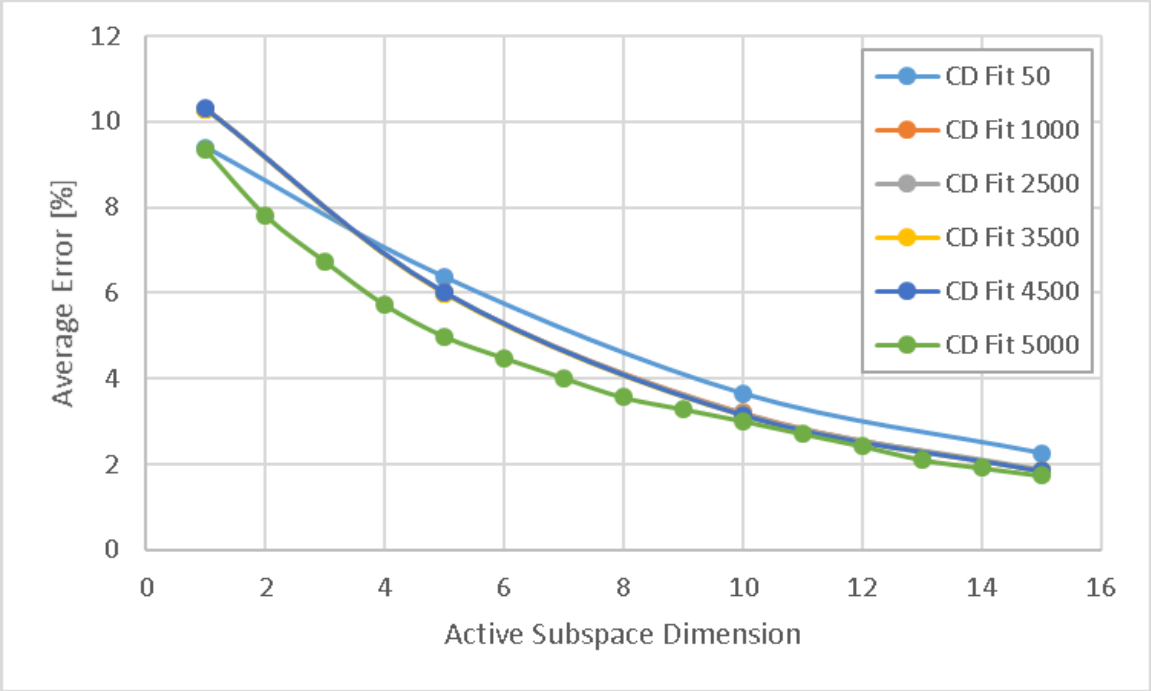

Figure 59: C_D Fit Error vs. Active Subspace Dimension for Different Number of Gradient Inputs

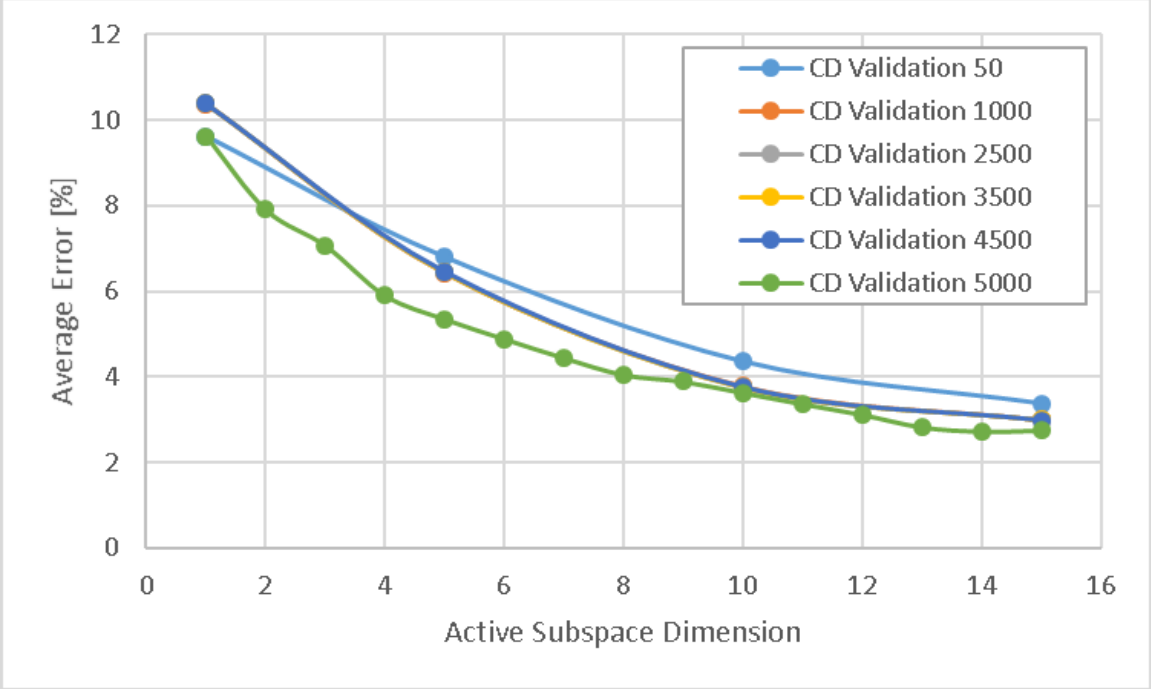

Figure 60: C_D Validation Error vs. Active Subspace Dimension for Different Number of Gradient Inputs

From these results, it can be seen that even when undersampled, the active subspace will create good surrogate fits with enough training cases. It was also shown that oversampling gradients past 10 did not improve fits as the 1000-4500 case errors were very similar for all fits. The 5000 case was very similar towards the higher dimensions but saw better errors in the lower spaces. The 1000 case also saw a very low error in the 10 and 15 active subspace dimension surrogates. Both the 5000 and 1000 case error improvements need further investigation to identify the cause of discrepancies from the other cases.

Comparing these results to hypothesis 1, the hypothesis was incorrect. As oversampling increased, it was expected that the active subspace error would continue to decrease and undersampled cases would perform much worse than cases properly sampled. The effects of over and undersampling were much less impactful to the overall error; however, this data was collected with many cases used for fitting, and the error may see a larger impact if fewer cases were used for fitting the surrogate.

5.5 Research Question 2: Will and active subspace surrogate on a limited design range improve error within the limited design range compared to an active subspace surrogate of the full design space?

The second research question addresses the improvements in active subspace accuracy within a segment of a design space compared to the full design space. In order to partition the space, gradients were initially investigated to see if there were any areas in the full space where a variable changes from being impactful to not having an impact. Due to the gradients being derived from a surrogate equation, and the surrogate only being a function of cubic inputs, the highest power of the derivatives is quadratic. A quadratic function will

not produce areas of no importance and large importance, so this method could not be used to segment the design space. Next, instead of looking at gradients, the residuals were investigated to see if there were areas in the design space where certain variables saw much larger residuals compared to other parts. This investigation yielded two design variables that saw much larger errors on one half of their value range compared to the other. Mach number showed larger errors in the lower half of its range while Mid Twist saw larger errors in the upper half of its range. The residual discrepancies can be seen in Figure 61.

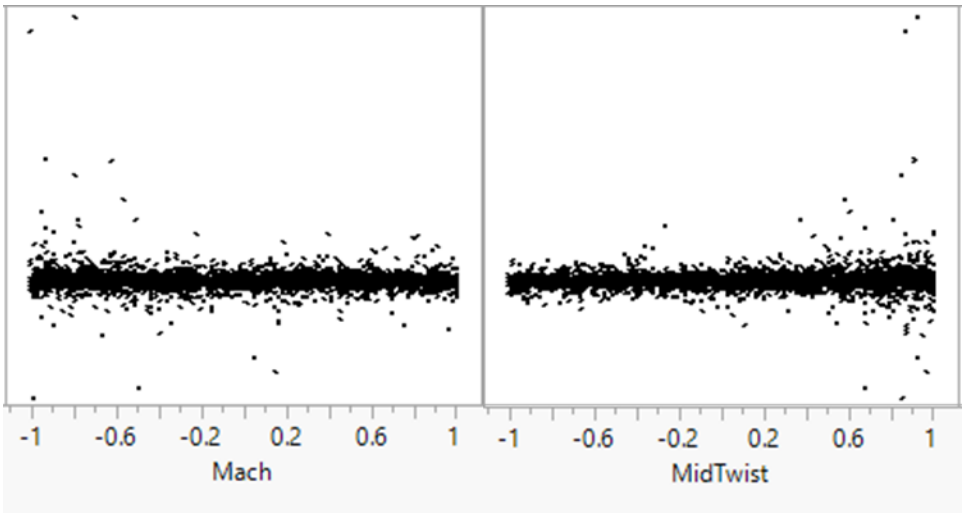

Figure 61: C_L Error vs. Mach and Mid Twist

Using this data, a smaller space within the design space was created by restricting Mach number from 1.5 to 2.0625 (-1 to -0.25 when normalized as in Figure 61) and Mid Twist from 0.75 to 3 (0.25 to 1 when normalized). This new, smaller space reduced the design variable ranges, but this reduction also led to a reduction in case responses to only 550 cases for fitting the surrogate in the local space. Using these 550 cases in the local space, a new traditional surrogate was created, and active subspace surrogates for 1, 5, 10, and 15 active subspace variables were created to compare. Figure 62 and Figure 63 show

the average errors in the C_L and C_D fits in the local space of the full traditional fit, full active subspace fit, local traditional fit, and local active subspace fit.

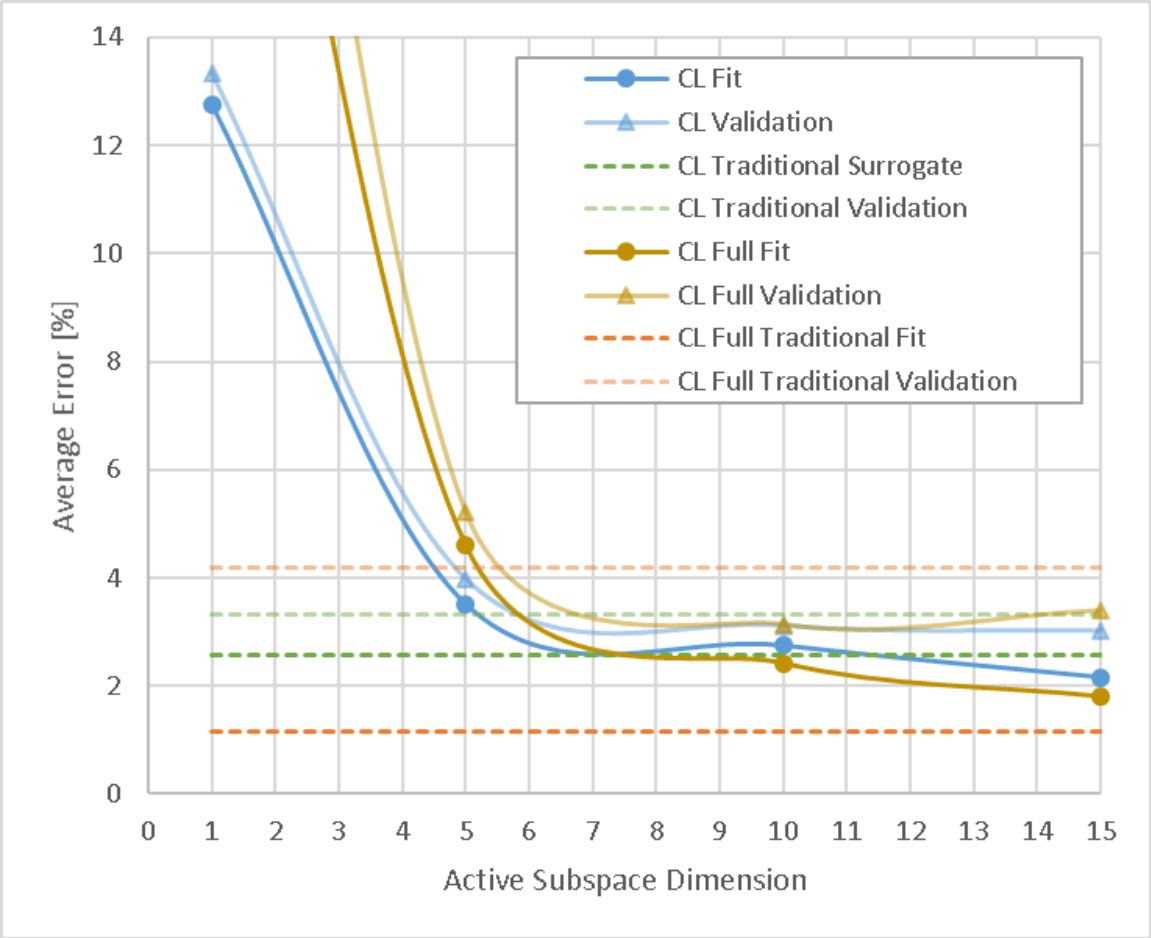

Figure 62: Local vs. Full Design Space C_L Surrogate Fit Errors

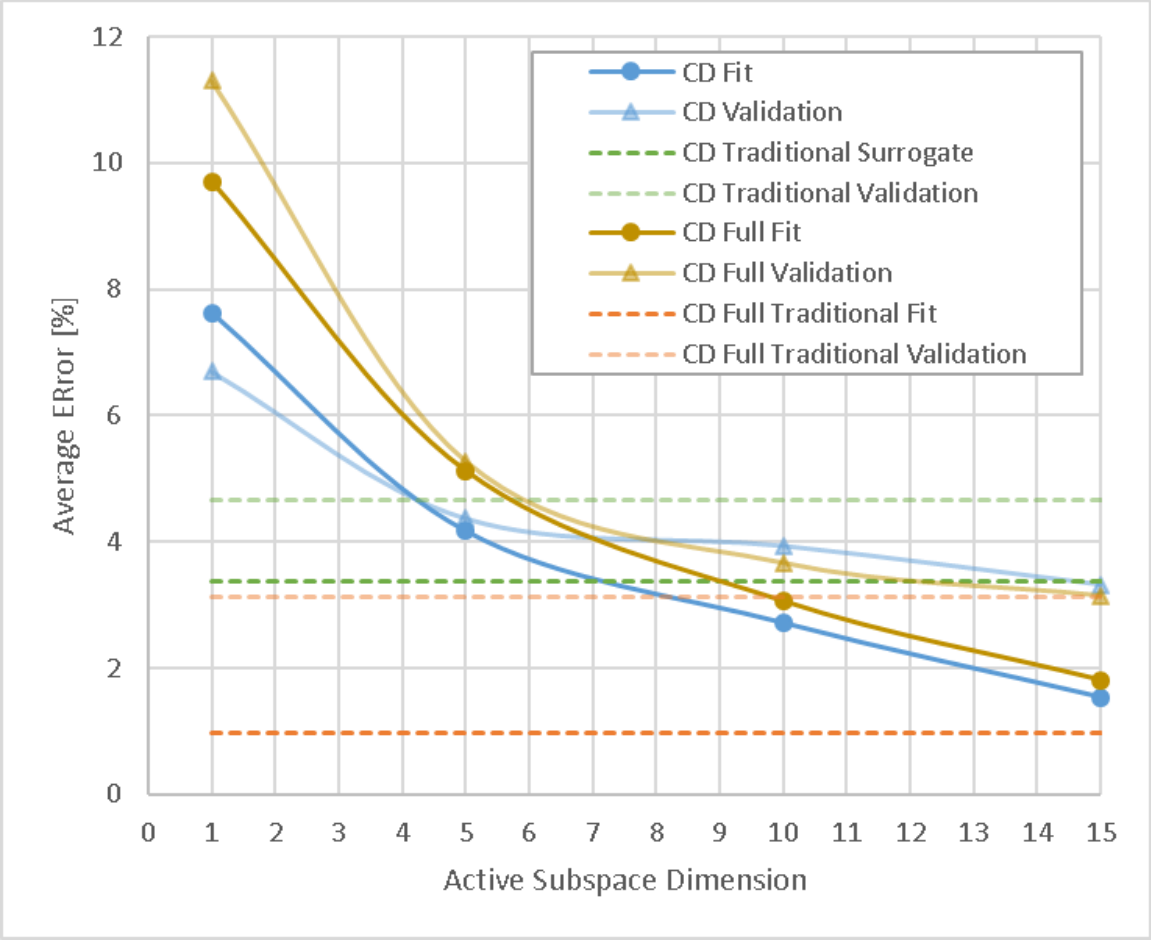

Figure 63: Local vs. Full Design Space C_D Surrogate Fit Errors

From these figures, there is an initial improvement in both local C_L and C_D active subspace surrogate errors in the local space compared to the errors from the active subspace surrogates generated from the full design space. This improvement gap closes as more active subspace dimensions are incorporated, and the C_L full active subspace fit sees lower errors than the local active subspace fit at 10 and 15 active subspace dimensions. The active subspace fits also see lower errors than the local traditional fit.

The hypothesis cannot be proven or discounted because, while this data shows initial improvement at lower active subspace dimensions, the current data does not provide

conclusive evidence that the local active subspace fits show improvement over the full design space active subspace fits. Because there were only 550 cases in the local space for surrogate fitting, the surrogates with higher dimensions could be greatly improved with more response cases. With additional cases the improvement gap between local and global surrogates could continue proving that local active subspaces map better than the global; however, additional cases and work are needed to prove this hypothesis.

5.6 Research Question 3: If gradients are taken from an initial surrogate model, how does the goodness of fit of the original surrogate impact the goodness of the active subspace surrogates?

The third research question applies to the case when a user is calculating gradients from a surrogate equation. While more accurate gradients can be calculated from adjoint methods build into many tools, some tools do not have this functionality incorporated. In these cases, it is necessary to know how good of an initial surrogate is needed to develop an active subspace because if a user is developing a surrogate already, applying active subspace theory may not be worth the extra work if the surrogate needs to be very detailed.

To address this question, five C_L and C_D surrogates were created using five different numbers of initial cases: 200, 500, 1000, 2000, and 3000. As the number of cases increase, the surrogate error is expected to decrease and the R^2 of the fit is expected to increase. To see the goodness of fit of all surrogates at each number of cases, Figure 64 plots the R^2 vs. number of surrogate cases, and Figure 65 plots the error vs. number of cases.

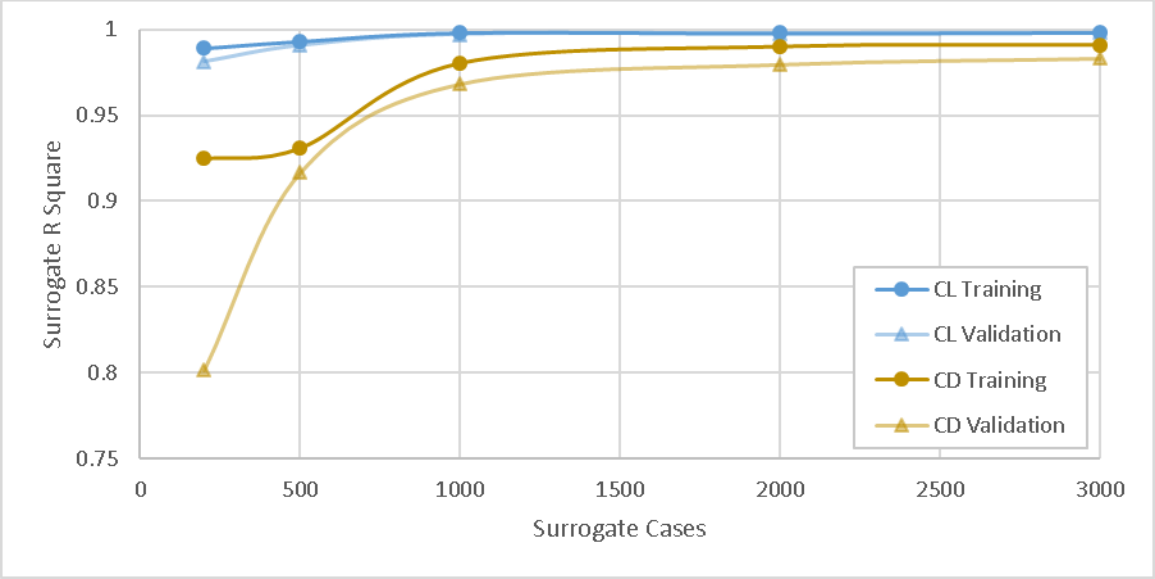

Figure 64: Traditional Surrogate R^2 vs. Cases to Develop Surrogate

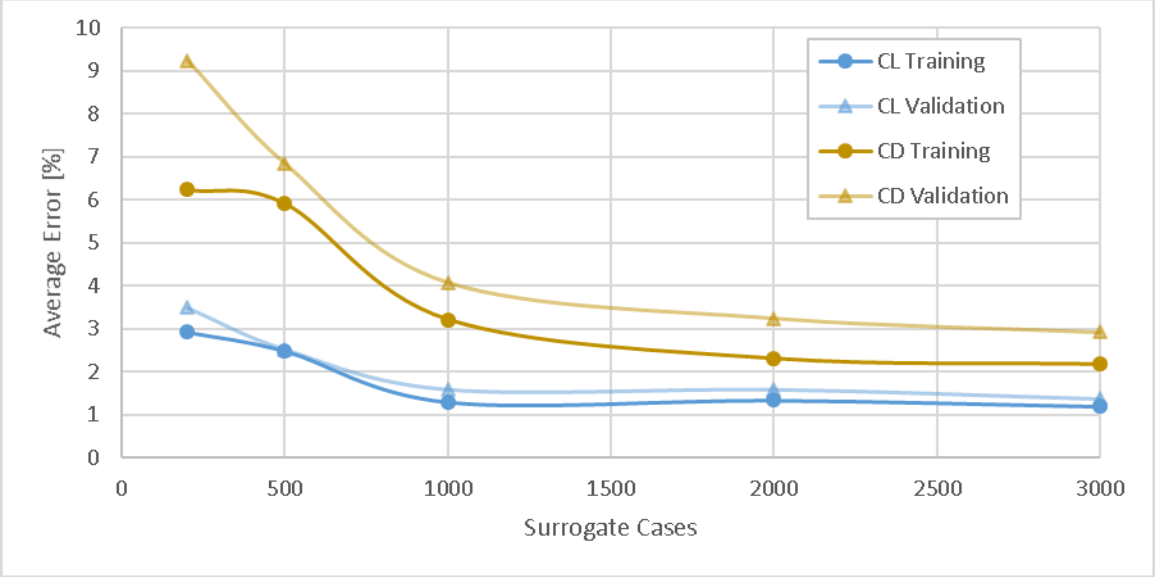

Figure 65: Traditional Surrogate Average Error vs. Cases to Develop Surrogate

From these figures, the surrogates do perform as expected with improvements in both error and R^2 as more cases are used to form the surrogate. C_L performs well with only a 3% average error with only 200 cases and sees diminishing returns after 1000 cases. C_D sees continual improvement out to 3000 cases.

Next, gradients were found from these surrogates, and the gradients were used to create active subspace surrogates. The average error of the active subspace surrogates were then compared to each other to see the impact of the goodness of the original surrogate used to generate the active subspaces. Each active subspace surrogate was created with the full 3825 responses. Figure 66 and Figure 67 show the average C_L and C_D training and validation error of the active subspace surrogates with 1, 5, 10, and 15 active subspace dimensions.

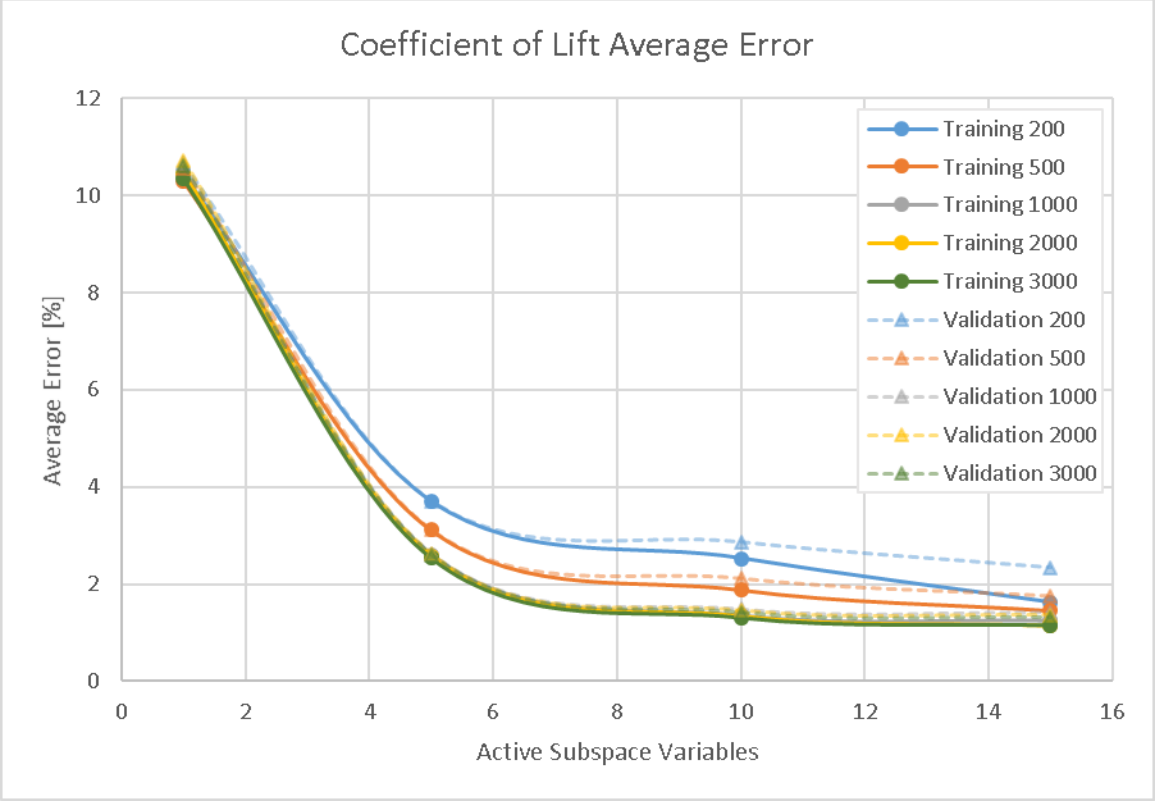

Figure 66: Average Error of C_L Active Subspace Surrogates vs. Active Subspace Dimension

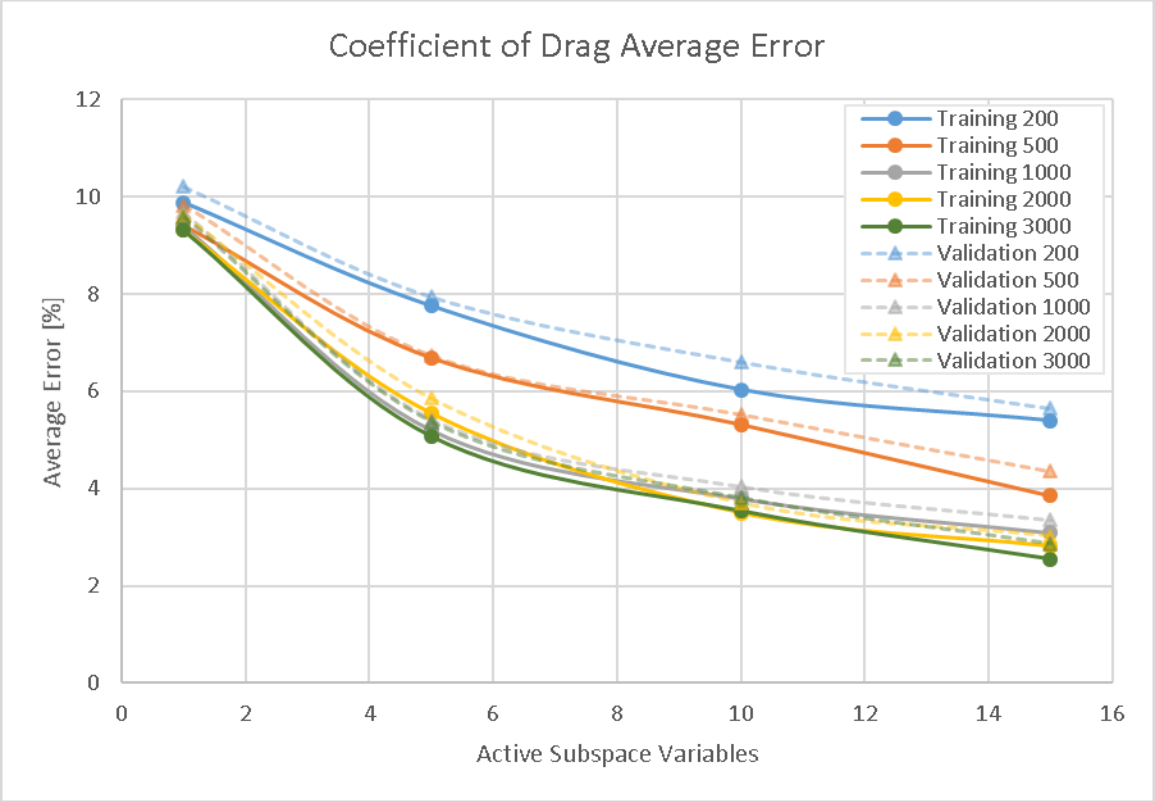

Figure 67: Average Error of C_D Active Subspace Surrogates vs. Active Subspace Dimension

From these results, after 1000 cases are used to make the initial surrogate used to calculate the gradients, the error improvement drastically decreases with additional cases. From the C_L surrogate, 500 cases could even be used if 10 or 15 active subspace dimensions are used as the errors begin to converge at higher dimensions. C_D sees a larger gap between 500 and 1000 cases, but it also does not see much improvement past 1000 cases. For this set of data, an initial surrogate from 1000 cases would generate active subspace fits with similar error to an initial surrogate from 2000 or 3000 cases. Even though the C_D surrogate generated from 1000 cases sees a larger error than both 2000 and 3000 cases, the active subspace error converges. This data partially proves the hypothesis as error did decrease as

additional cases per variable increase; however, the error stopped decreasing earlier than estimated.

5.7 Computational Cost – Should Active Subspaces be used?

The final question this research presents is whether or not active subspace theory should be implemented for a supersonic conceptual design space exploration. The basis of this research was that high fidelity analysis is necessary in the conceptual design of supersonic aircraft. To justify the use of an additional step in the design process, active subspace theory must enable a net reduction in computational cost. Computational cost will be calculated assuming two implementation methods of active subspace theory: gradients from code and gradients from surrogate. Calculating gradients from a code will require additional cases because the initial surrogate will have to be generated.

5.7.1 Gradients from Tool

The first calculations assume that gradients can be directly calculated from the tool. The total number of cases needed will represent the computational time in these analyses. With gradients given from the tool, the total amount of cases needed to create a given surrogate will be the number of gradients needed to generate the active subspace dimensions added with the number of cases needed to ensure a good surrogate fit. This calculation is written formally in Equation 7.

$$Cases = Cases\ for\ gradients + Cases\ for\ surrogate\ fit$$
$$= \alpha * k * \ln(m) + \beta * k \qquad \textbf{Equation 7}$$

In this equation, α is the oversampling rate, k is the number of gradients needed (which equates to the number of active subspace variables), m is the number of physical design variables, and β is the surrogate oversampling rate. As proven from Research Question 1, the gradient oversampling rate can be limited to 2 to 10, and two surrogate oversampling rates of 50 and 200 runs per design variable were assumed. First, Figure 68 presents the number of cases needed to get all gradients for active subspace analysis for an oversampling of 2 and 10.

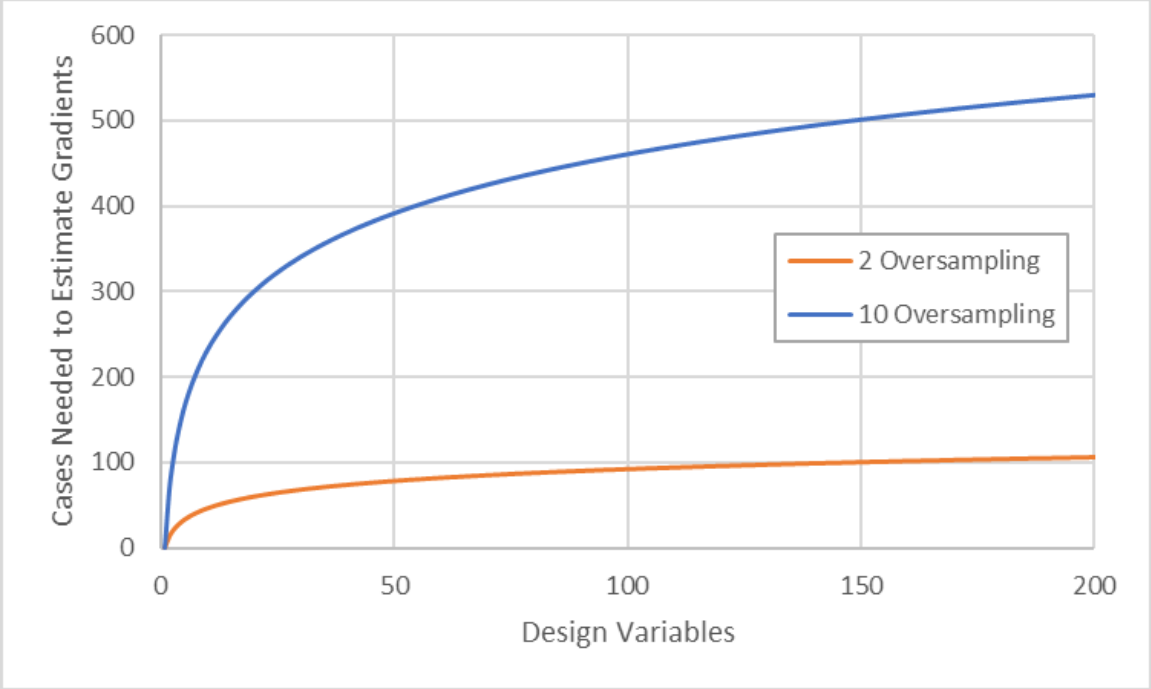

Figure 68: Number of Cases Needed to Estimate All Gradients

From this data, as design variables increase, the curves approach a plateau. This leads to the conclusion that active subspace theory greatly benefits from a larger amount of variables. Using this data, the breakeven point was found in terms of dimensionality

reduction vs. number of design variables, and Figure 69 shows this data in terms of gradient oversampling and surrogate oversampling values.

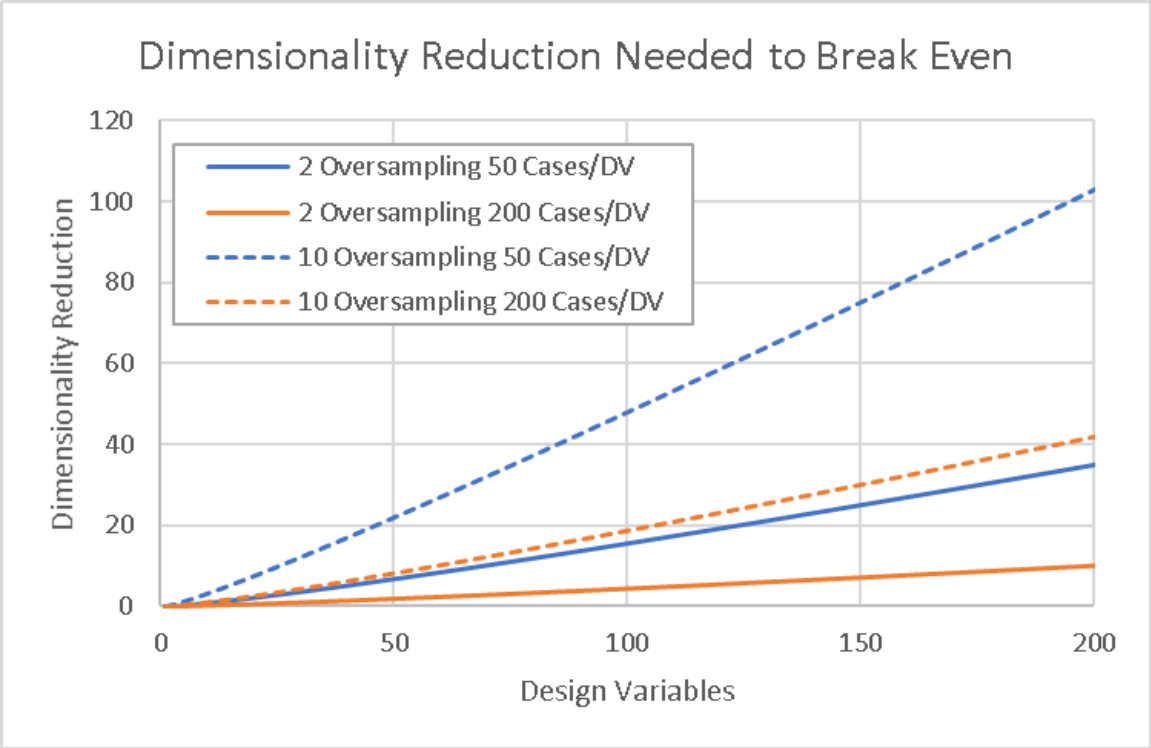

Figure 69: Active Subspace Dimensionality Reduction to Break Even vs. Design Variables

This chart shows that for an active subspace to buy its way into the design process, it must be able to reduce dimensionality by 5-50% depending on the oversampling and number of cases needed to ensure a good surrogate fit. The dimensionality reduction needed to break even increases as gradient oversampling rate increases and cases per design variable decreases. While the first makes intuitive sense, lower cases per design variable may seem opposite to expected. As the number of cases per design variable increases, the total number of cases used to create a traditional surrogate also increases; therefore, the impact of reducing a single design variable also increases. From these two factors, fewer

variables need to be removed to see the same computational time. Assuming a gradient oversampling of 2 and a surrogate sampling of 200 cases per design variable, at 100 design variables, the active subspace would need to reduce dimensionality by 5 variables. Using the worst combination of a gradient oversampling of 10 and a surrogate sampling of 50 cases per design variable, at 100 design variables, the active subspace would need to reduce dimensionality by 48 variables.

Figure 70 extends the previous calculation to show the overall reduction in cases at different active subspace surrogates. Each line represents an active subspace surrogate made of the number of active subspace variables, so the orange lines are active subspace surrogates made of 5 active subspace variables. The x axis represents the number of physical design variables in the problem, and the y axis represents the number of cases reduced where a positive number is a reduction in cases. Returning to the dashed orange line at an x value of 10; this means that there were 10 design variables originally and with an active subspace surrogate made of 5 active subspace variables there would be a reduction of 1000 cases.

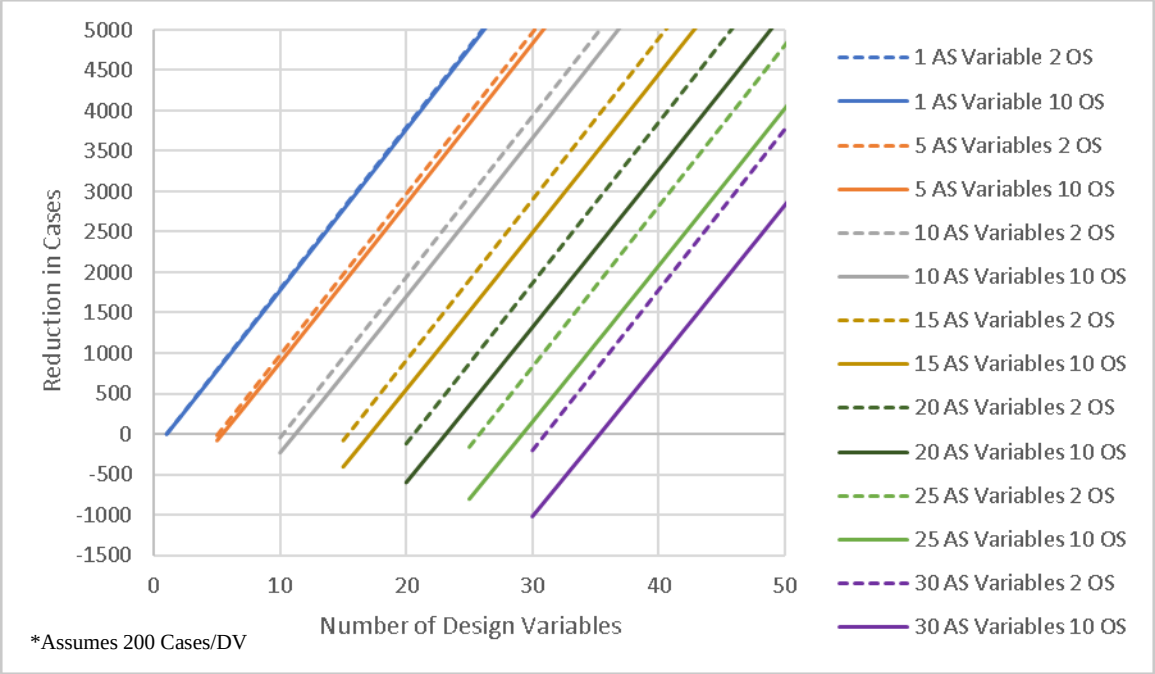

Figure 70: Case Reduction vs. Number of Physical Design Variables for an Array of Active Subspace Surrogates

This figure shows that as the number of physical design variables increases, the dimensionality reduction needs to also increase. At 30 design variables, on the x axis, with a 30 active subspace variable surrogate, the active subspace surrogate increases the amount of cases needed. This increase is due to the additional cases used to generate the gradients. It can also be seen that the larger the dimensionality reduction, the larger the reduction in cases. For example, using the solid gold line representing a 15 active subspace variable surrogate with 10 oversampling at 30 design variables, which is a 50% dimensionality reduction, the number of cases reduces by 2500. Given that the calculation assumes 200 cases per design variable, a traditional surrogate of 30 design variables would require 6000 cases, so the active subspace nearly reduces the number of cases by half.

5.7.2 Gradients from Surrogate

There is significant opportunity for computational time savings when the gradients can be calculated internally from a tool, but do these savings still appear when an initial surrogate is needed in order to calculate the gradients? In order to determine this, Equation 7 needs to be modified to incorporate the initial surrogate. Additionally, the gradient cases can be assumed to have negligible runtime as calculating gradients from a surrogate is nearly instantaneous. From Research Question 3, it was found that a 1000 case surrogate yielded similar active subspace error to the 2000 and 3000 case surrogates. From this result, it will be assumed that 50 cases per design variable is sufficient to develop a surrogate to calculate gradients. With these corrections, Equation 7 becomes Equation 8.

$$\begin{aligned} Cases = {} & Cases\ for\ initial\ surrogate\ fit \\ & + Cases\ for\ active\ subspace\ surrogate\ fit \\ & = 50 * m + \beta * \mathrm{k} \end{aligned} \qquad \textbf{Equation 8}$$

In this equation, m is the total number of design variables, β is the surrogate oversampling rate, and k is the number of active subspace surrogate variables. From this initial equation, it can be seen that if the surrogate oversampling rate is 50 for the traditional and active subspace surrogate, the active subspace surrogate will never save computational time compared to a full surrogate. If the oversampling rate is greater than 50, then the active subspace could save computational time. The first calculation performed was to find the dimensionality reduction needed to break even between a traditional surrogate and an active subspace surrogate at different β values. Figure 71 provides this data with β values

of 50 to 200 in increments of 25. At a β value of 50, the active subspace would need to see a dimensionality reduction equal to the number of design variables meaning that all variables would have to disappear in order for active subspace to work.

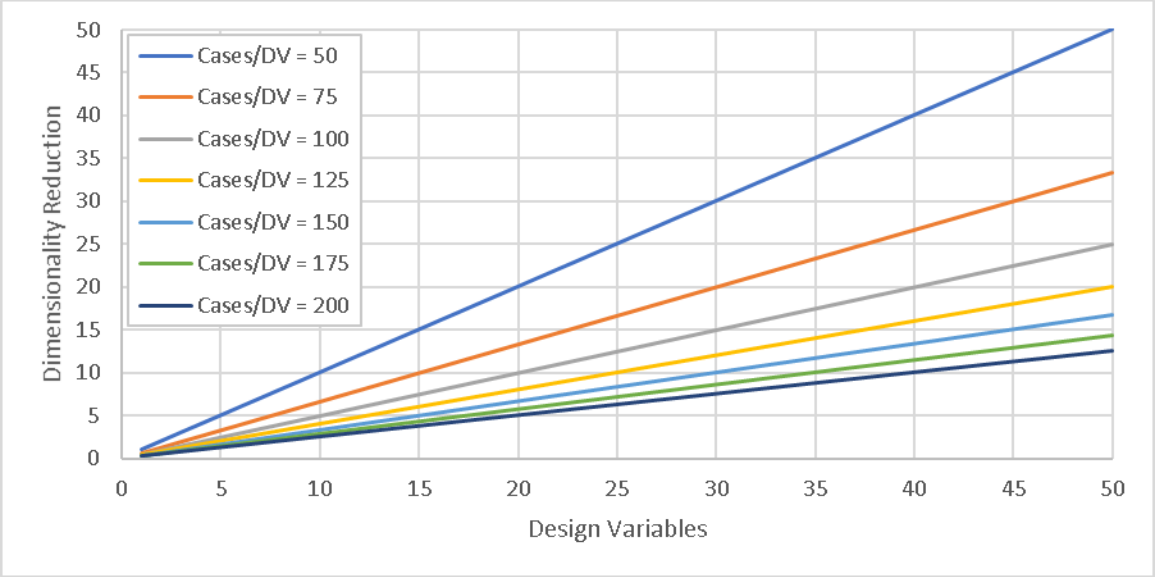

Figure 71: Active Subspace Dimensionality Reduction Needed to Break Even

The more cases per design variable used to develop a surrogate model, the less dimensionality reduction is needed to break even. Similar to the previous section, this calculation was extended to show the overall reduction in cases at different β and active number of subspace variable surrogates. Figure 72 gives the reduction in cases given an active subspace surrogate with 1 active subspace variable and an active subspace surrogate with 25 active subspace variables. The number of cases per design variable is swept from 75 to 200 in steps of 25 cases per design variable.

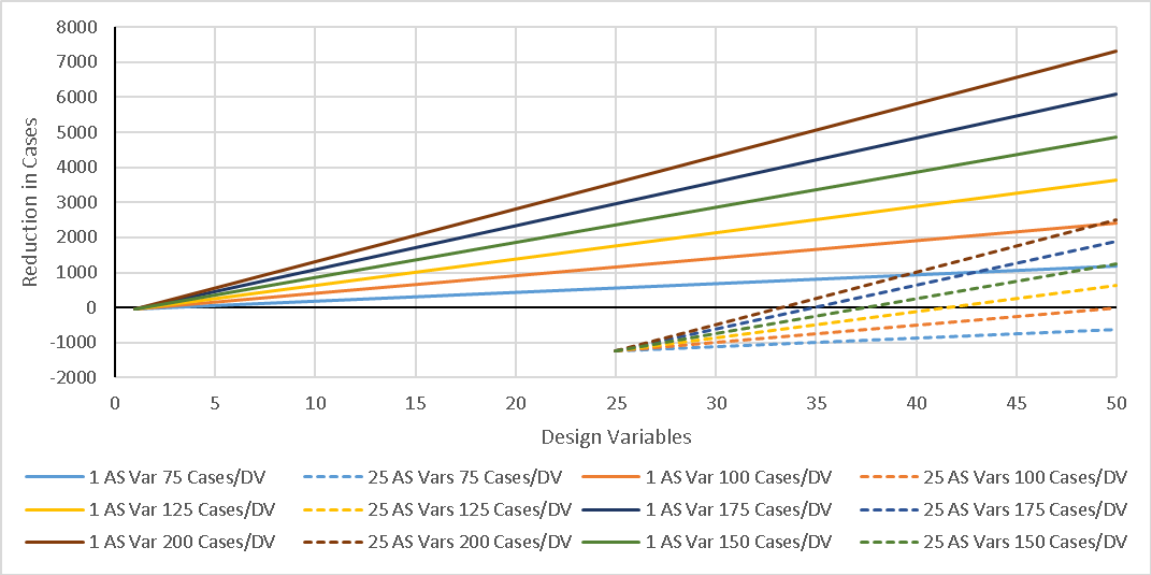

Figure 72: Reduction in Cases vs. Design Variables for Active Subspace Surrogates with 1 and 25 Variables at Different Surrogate Cases per Design Variable

This plot shows that in order to reduce computational time when using an active subspace requiring gradients from a surrogate, more dimensions need to be reduced in the active subspace. Viewing the 25 active subspace variable surrogates, if $\beta = 75$ cases per design variable, then in order to break even there need to be 75 original design variables. To benefit from an active subspace surrogate, the dimensionality would need to be reduced by two thirds. If $\beta = 200$ cases per design variable, then in order to break even, there need to be 34 original design variables. To benefit at the 200 cases per design variable mark, the dimensionality needs to be reduced by 26.5%.

From these results, it is more difficult to see a large reduction in computational cost because of the cases needed to create the original surrogate. If the cases needed per design variable to ensure a good surrogate fit is high, then active subspace surrogates can see a reduction in computational time if the dimensionality reduction is greater than 25% of the design variables. If the cases needed per design variable is towards the lower bound, closer

to 50 cases per design variable, then a substantial dimensionality reduction is needed to break even with the traditional surrogate.

In both cases, when a gradient is found in the tool and when a gradient is found using a surrogate, the computational time can be reduced. If the gradient is found in the tool, then a computational time reduction can be found with a lower dimensionality reduction. This also means that a larger computational time reduction is possible if a large dimensionality reduction is found. If a surrogate is needed to find the gradients, then a larger dimensionality reduction is needed to break even in computational time. With either of these scenarios, active subspace theory should be investigated to see if the dimensionality reduction provided as a reduction in computational time is possible.

5.8 Proposed Methodology

From the answers to each of the research questions and the computational cost calculations, a conceptual design methodology including active subspaces was created. Due to the increased possibility of reducing computational cost if gradients are found within a tool, this method is implemented in the proposed methodology. The methodology is presented in Figure 73.

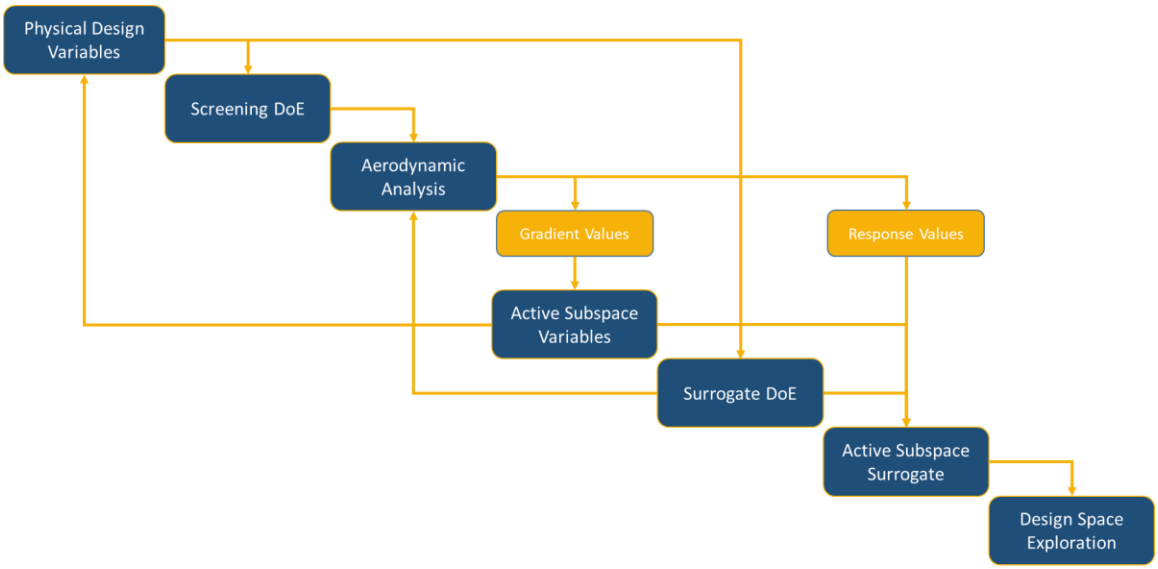

Figure 73: Proposed Conceptual Design Methodology using Active Subspaces

This methodology integrates active subspace variable calculation and active subspace surrogates into the conceptual design framework. After an initial design of experiments from the physical design variables is created, these cases are run through aerodynamic analysis, which is computational fluid dynamics for supersonic design, to calculate the gradients needed to identify an active subspace. The gradient values are found at each point in the design of experiments. The gradient values are used to calculate the active subspace variables through an eigendecomposition of the gradient matrix, and the designer selects the most impactful variables to move forward in the process, reducing dimensionality. With the active subspace variables, the method loops back to the physical design variables to create a new design of experiments in terms of the active subspace variables that captures the original range of the physical variables. This new DoE is fed into the aerodynamic analysis again to generate response values at each point. These response values are taken with the input variables to generate an active subspace surrogate. Using this active subspace surrogate, design space exploration can be performed within the

design space. This exploration will be in terms of the active subspace variables, and results need to be transformed back to be in terms of the physical design variables for any patterns to make physical sense.

Through this research, it was found that an active subspace can be found within a commercial supersonic design space, and it can also significantly reduce computational cost. A methodology has been presented to incorporate active subspaces into the design process to enable larger design exploration while still capturing the effects of a large number of design variables.

CHAPTER 6. CONCLUSION

6.1 Summary

This research has investigated the implementation of active subspace theory to a supersonic conceptual design methodology and tested extension questions on active subspace surrogates. Supersonic design is a highly interdisciplinary problem requiring many design variables early in the process. Without significant historical data and no standard baseline configuration, high fidelity analysis also needs to be included early in the design process. The combination of high fidelity analysis with many design variables leads to very large computational times which limit design space exploration. Active subspace theory, a novel dimensionality reduction technique, has been applied to different engineering problems, including a wing optimization, and it can reduce dimensionality while maintaining effects from all original design variables. This technique involves rotations of the design space into the active subspace, and then creating surrogates of a down-selected amount of these new, rotated, active subspace variables.

The goal of the research was to determine if an active subspace could be found within a commercial supersonic design space and if it was worth implementing active subspaces as an extra step in the design process. Due to computational resource limitations, 20 design variables were chosen for this study. These variables were limited to wing planform, airfoil geometry, and Mach number. The aircraft configurations had a consistent fuselage between all, but the wings were changed for each configuration through a Latin Hypercube design of experiments of the 20 design variables. These geometries were created in Engineering Sketch Pad and fed into CART3D where aerodynamic coefficients were calculated. These

aerodynamic coefficients and the respective design variables were taken into JMP to create surrogates of C_L and C_D. These surrogates were used to calculate gradients at each point in the DoE, and the gradient values were used to calculate active subspace variables. Surrogates were made from the active subspace variables.

Three additional research questions were presented to address details of active subspace implementation. Research question 1 addressed the impact of the number of gradients used to create the active subspace on the goodness of fit of the active subspace surrogate. The second research question took a segment of the design space and compared the goodness of fit of an active subspace surrogate in the local segment compared to the goodness of fit of the global active subspace in the segment of the design space. The third research question investigated the impact of the goodness of fit of the surrogate used to calculate gradient values on the error of the active subspace surrogates. Finally, computational cost calculations were performed to determine the worth of implementing an active subspace into a given design process. Using the three research questions and the computational cost calculations, a methodology was presented to incorporate active subspace theory into a commercial supersonic conceptual design framework.

6.2 Conclusions

The main questions from this research asked if an active subspace could be found in the given design problem and if an active subspace could be found, whether it would be worth implementing into a design process. While an active subspace needs to be discovered rather than created, and there may be situations where an active subspace cannot be found, an active subspace was identified in this design space. The level of dimensionality reduction

for an active subspace is determined by the user; however, the coefficient of lift surrogate saw a much larger reduction in error with fewer active subspace design variables compared to the coefficient of drag. While both could have significant dimensionality reduction, the coefficient of lift response would see larger impact. To determine the level of this impact, three research questions were asked about the implementation of active subspaces.

The first research question investigated the number of gradients needed to calculate the active subspace variables. While a notional equation is given in active subspace theory, this number was tested by over and undersampling the calculated values. The results from this question showed that even when undersampled, the active subspace created surrogate fits with enough training cases. Oversampling did not increase the goodness of fit after a gradient sampling rate of 50 gradients per design variable.

The second research question addressed the improvement in goodness of fit of an active subspace surrogate in a smaller segment of the design space compared to the full design space. The design space was segmented by reducing the range of Mach and MidTwist design variables to the locations where they had the largest errors in the coefficient of lift surrogate. An active subspace was found in this local space, although only 550 CFD responses were available for fitting the surrogates in the local space. At lower number of active subspace variables, the local surrogate sees lower error than the surrogate of the full design space; however, this error gap reduces as more variables are included in the active subspace surrogates, and at 10 and 15 active subspace variables, the local C_L error is higher than the full design space C_L error.

If a surrogate has to be used to calculate gradients, then the third research question investigated how good an initial surrogate needed to be to generate gradients good enough to create acceptable active subspace surrogate fits. It was found that after 50 cases per design variables, or 1000 cases for 20 design variables, the error did not continue to decrease. There was an increase in error when using 200 and 500 cases for the 20 design variables, but the average error for both C_L and C_D surrogates followed similar decreasing trends and did not have gross increases in errors. From this question, it was concluded that a minimum of 50 cases per design variable should be taken to ensure a good surrogate fit if gradients were to be taken.

Finally, computational cost calculations were performed. Two cases were considered: gradients taken directly from tool and gradients taken from surrogate. With gradients taken from the tool, the number of cases needed to break even between traditional surrogate and active subspace surrogates depended on active subspace gradient oversampling and surrogate sampling. To optimize the computational time reduction, a low gradient oversampling and a high surrogate sampling number is desired. At optimal conditions tested, to break even, an active subspace would need to reduce dimensionality by 5 per 100 variables; however, at least optimal conditions tested, an active subspace would need to reduce dimensionality by 48 per 100 variables. The second case, gradients from surrogate, assumed that 50 cases per design variable would be needed to generate an initial surrogate to create the gradients. The computational cost depended only on the number of cases per design variable to fit traditional and active subspace surrogates. If the cases per design variable is equal or less than the 50 per design variable needed for the initial surrogate to calculate gradients, then it is not possible to see a reduction in

computational cost. At the optimal case, to break even an active subspace would need to reduce dimensionality by 13 per 50 design variables. Due to this large reduction in dimensionality, a methodology was created implementing active subspaces only using the case when gradients are calculated from within a tool.

6.3 Future Work

This research presented an initial dive into applying active subspaces to a commercial supersonic design space. The research had limitations in computational resources. The lack of computational resources limited design variables to only aerodynamic variables and CFD cases to 3825 successful cases. While acceptable surrogates were found, with additional resources, non-aerodynamic variables need to be added to the design space to see the applicability of active subspace theory to a multidisciplinary problem. Further investigation is also needed into local active subspaces versus a full design space active subspace. Although initial error improvement was observed, there were not enough cases in the local space to conclude that the error improvement continued as higher active subspace dimensions were added. Finally, the presented methodology should be fully implemented with a tool to calculate gradients to compare the theoretical computational cost reduction to actual cost reduction. This research has shown that an active subspace can be found in the given design space, and computational cost can be reduced with an active subspace. Further work is needed to implement and test the usage of an active subspace in a design process.

REFERENCES

[1] Boeing, “Commercial Market Outlook 2019 – 2038”, Boeing.com, 2019.

[2] Airbus, "Global Market Forecast Cities, Airports & Aircraft 2019-2038," Airbus.com, 2019.

[3] Zhang, B., “A Boeing exec reveals what's in store for the 747 jumbo jet and predicts that Airbus won't be able to deliver the rest of its A380s”, Business Insider, 2018.

[4] Oestergaard, J. K., “Airbus and Boeing Report August 2019 Commercial Aircraft Orders and Deliveries”, Forecast International, 2019.

[5] Roxburgh, G., “Concorde SST: Celebrating an Icon”, 2016, concordesst.com.

[6] Ferri, A., “Possibilities and Goals for the Future SST”, *Journal of Aircraft*, Vol. 12, December 1975. https://doi.org/10.2514/3.59894

[7] Boom Supersonic, “Travel”, boomsupersonic.com/travel, 2019.

[8] Spearman, M. L., “The Evolution of the High-Speed Civil Transport”, NASA TM 109089, 1994.

[9] Sun, Y., Smith, H., “Review and prospect of supersonic business jet design”, *Progress in Aerospace Sciences*, Vol. 90, April 2017, pp. 12-38. https://doi.org/10.1016/j.paerosci.2016.12.003

[10] Aerion Supersonic, “AS2”, aerionsupersonic.com, 2019.

[11] Lockheed Martin, “Aerion And Lockheed Martin Join Forces To Develop World's First Supersonic Business Jet”, Lockheed Martin Aeronautics Company, 2017.

[12] Bogaisky, J., “Boeing To Help Aerion Develop Supersonic Jet As Lockheed Martin Exits”, Forbes, 2019.

[13] Boeing, “Boeing Partners with Aerion to Accelerate Supersonic Travel”, Boeing, 2019.

[14] Spike Aerospace, “The Spike S-512”, spikeaerospace.com, 2019.

[15] Kokalitcheva, K., “This Startup Is Developing Supersonic Planes for Virgin Group”, Fortune, 2016.

[16] Boom Supersonic, “Overture”, Boomsupersonic.com 2019.

[17] Fehrm, B., “Will Boom succeed where Concorde failed?”, Leeham News and Analysis, 2016.

[18] Welge, H., Nelson, C., and Bonet, J., "Supersonic Vehicle Systems for the 2020 to 2035 Timeframe", AIAA Paper 2010-4930, 2010. https://doi.org/10.2514/6.2010-4930

[19] "Aviation Emissions, Impacts, and Mitigation: A Primer", Federal Aviation Administration, 2015.

[20] "Electronic Code of Federal Regulations", Federal Aviation Administration, November 2019.

[21] "Airports Commission: Final Report", Airports Commission, 2015.

[22] "X-59 QueSST", Lockheed Martin Corporation, 2019.

[23] Henne, P., "Case for Small Supersonic Civil Aircraft", *Journal of Aircraft*, Vol. 42, No. 3, 2005. https://doi.org/10.2514/1.5119

[24] Chudoba, B., Coleman, G., Roberts, K., Mixon, B., Mixon, B., Oza, A., and Czysz, P.A., "What Price Supersonic Speed? – A Design Anatomy of Supersonic Transportation – Part 1", 45th AIAA Aerospace Sciences Meeting and Exhibit, January 2007.

[25] Satre, P., "Supersonic Air Transport – True Problems and Misconceptions", *Journal of Aircraft*, Vol. 7, No. 1, Jan 1970.

[26] Roskam, J., "Airplane Design: Part I: Preliminary Sizing of Airplanes", Roskam Aviation and Engineering Corporation, 1985.

[27] Mattingly, J.D., Heiser, W.H., and Pratt, D.T., "Aircraft Engine Design", 2nd Ed., American Institute of Aeronautics and Astronautics, Inc., 2002.

[28] Hamel, L., Folk, T., Jimenez, H., and Mavris, D., "Conceptual Design of an N+2 Supersonic Airliner", AIAA Paper 2009-7075, 2009. https://doi.org/10.2514/6.2009-7075

[29] Johnson, V., "A computer-assisted process for supersonic aircraft conceptual design", AIAA Paper 1985-4027, 1985. https://doi.org/10.2514/6.1985-4027

[30] Dovi, A.R., Wrenn, G.A., Barthelemy J.-F.M., Coen, P.G., and Hall, L.E., "Multidisciplinary Design Integration Methodology for a Supersonic Transport Aircraft", *Journal of Aircraft*, Vol. 32, No. 2, 1995. https://doi.org/10.2514/3.46715

[31] Sun, Y., and Smith, H., "Supersonic Business Jet Conceptual Design in a Multidisciplinary Design Analysis Optimization Environment", AIAA/ASCE/AHS/ASC Structures, Structural Dynamics, and Materials Conference, 2018. https://doi.org/10.2514/6.2018-1651

[32] Snyder, J., "CFD Needs in Conceptual Design", AIAA Paper 1990-3209, 1990. https://doi.org/10.2514/6.1990-3209

[33] Geiselhart, K., Ozoroski, L., Fenbert, J., Shields, E., and Li, W., "Integration of Multifidelity Multidisciplinary Computer Codes for Design and Analysis of Supersonic Aircraft", AIAA Paper 2011-465, 2011. https://doi.org/10.2514/6.2011-465

[34] Choi, S., Alonso, J., and Kroo, I. M., "Two-Level Multifidelity Design Optimization Studies for Supersonic Jets", *Journal of Aircraft*, Vol. 46, No. 3, 2009. https://doi.org/10.2514/1.34362

[35] Li, W., Shields, E., and Geiselhart, K., "Mixed fidelity Approach for Design of Low-Boom Supersonic Aircraft", *Journal of Aircraft*, Vol. 48, No. 4, 2011. https://doi.org/10.2514/1.C000228

[36] Chung, H., Choi, S., and Alonso, J.J., "Supersonic Business Jet Design using a Knowledge-Based Genetic Algorithm with an Adaptive, Unstructured Grid Methodology", 21st AIAA Applied Aerodynamics Conference, 2003. https://doi.org/10.2514/6.2003-3791

[37] Rallabhandi, S.K., Nielsen, E.J., and Diskin, B., "Sonic-Boom Mitigation Through Aircraft Design and Adjoint Methodology", *Journal of Aircraft*, Vol. 51, No. 2, 2014. https://doi/10.2514/1.C032189

[38] Lukaczyk, T., Palacios, F., and Alonso, J.J., "Response Surface Methodologies for Low-Boom Supersonic Aircraft Design using Equivalent Area Distributions", 12th AIAA ATIO Conference and 14th AIAA/ISSMO Multidisciplinary Analysis and Optimization Conference, 2012. https://doi.org/10.2514/6.2012-5705

[39] Nelson, A., Alonso, J.J., and Pulliam, T.H., "Multi-fidelity Aerodynamic Optimization Using Treed Meta-Models", 25th AIAA Applied Aerodynamics Conference, 2007. https://doi.org/10.2514/6.2007-4057

[40] Pawlowski, J., Graham, D., Boccadoro, C., Coen, P., and Maglieri, D., "Origins and Overview of the Shaped Sonic Boom Demonstration Program", AIAA Paper 2005-5, 2005. https://doi.org/10.2514/6.2005-5

[41] Constantine, P.G., *Active Subspaces: Emerging Ideas for Dimension Reduction in Parameter Studies*, Society for Industrial and Applied Mathematics, Philadelphia, PA, 2015.

[42] Jefferson, J.L., Gilbert, J.M., Constantine, P.G., and Maxwell, R.M., "Active subspaces for sensitivity analysis and dimension reduction of an integrated hydrologic model", Computers & Geosciences 83, pp. 127-138, 2015.

[43] Constantine, P.G., Zaharatos, B., and Campanelli, M., "Discovering an active subspace in a single-diode solar cell model", *Statistical Analysis and Datamining*,

Vol. 8, Issue 5-6, October/December 2015, pp. 264-273. https://doi.org/10.1002/sam.11281

[44] Constantine, P.G., Doostan, A., Wang, Q., and Iaccarino, G., "A Surrogate Accelerated Bayesian Inverse Analysis of the HyShot II Flight Data", AIAA Paper 2011-2037, 2011.

[45] Constantine, P.G., Emory, M., Larsson, J., Iaccarino, G., "Exploiting active subspaces to quantify uncertainty in the numerical simulation of the HyShot II scramjet", Journal of Compuational Physics 302, pp. 1-20, 2015.

[46] Lukaczyk, T., Palacios, F., Alonso, J.J., and Constantine, P.G., "Active Subspaces for Shape Optimization", 10th AIAA Multidisciplinary Design Optimization Conference, January 2014. https://doi.org/10.2514/6.2014-1171

[47] Mavris, D., "Design-of-Experiments For Practical Applications in Modeling, Simulation, and Analysis: Introduction to Response Surface Methods", Georgia Institute of Technology, Advanced Design Methods 1, 2018.

[48] Montgomery, D.C., "Design and Analysis of Experiments", 8th Ed., John Wiley & Sons, Inc., 2013.

[49] Mason, R.L., Gunst, R.F., and Hess, J.L., "Statistical Design and Analysis of Experiments With Applications to Engineering and Science", 2nd Ed., John Wiley & Sons, Inc., 2003.

[50] National Aeronautics and Space Administration, "About OpenVSP", OpenVSP, 2019.

[51] McDonald, R., "Advanced Modeling in OpenVSP", AIAA Paper 2016-3282, 2016. https://doi.org/10.2514/6.2016-3282

[52] Dannenhoffer, J. F., "ESP Overview & Getting Started", Massachusetts Institute of Technology, 2019.

[53] Mason, F., "Aerodynamics of 3D Lifting Surfaces through Vortex Lattice Methods", Virginia Institute of Technology, 1998.

[54] Budziak, K., "Aerodynamic Analysis with Athena Vortex Lattice (AVL)", Hamburg University of Applied Sciences, 2015.

[55] Bertin, J. and Smith, M., "Aerodynamics for Engineers", Prentice Hall, 1989.

[56] Aftosmis, M., "Emerging CFD Technologies and Aerospace Vehicle Design", NASA 95-28746, 1995.

[57] Ma, E., "A transonic/supersonic/hypersonic CFD analysis of the entry Space Shuttle Orbiter", AIAA Paper 1992-2614, 1992. https://doi.org/10.2514/6.1992-2614

[58] Anderson, J., “Fundamentals of Aerodynamics”, McGraw-Hill Education, 2010.

[59] Melton, J., Berger, M., Aftosmis, M., and Wong, M., “3D Applications of a Cartesian Grid Euler Method”, AIAA Paper 1995-853, 1995.

[60] Murman, S., Aftosmis, M., and Nemec, M., “Automated Parameter Studies Using a Cartesian Method”, AIAA Paper 2004-5076, 2004.

[61] Rogers, S.E., Aftosmis, M.J., Pandya, S.A., Charderjian, N.M., Tejnil, E.T., and Ahmad, J.U., “Automated CFD Parameter Studies on Distributed Parallel Computers”, 16th AIAA Computational Fluid Dynamics Conference, June 2003.

[62] Myers, R.H. and Montgomery, D.C., *Response surface methodology: process and product optimization using designed experiments*, 3rd Ed., Hoboken, N.J.: Wiley, 2009

[63] Palar, P.S., and Shimoyama, K., “On the Accuracy of Kriging Model in Active Subspaces”, 2108 AIAA/ASCE/AHS/ASC Structures, Structural Dynamics, and Materials Conference, January 2018.

[64] Constantine, P.G., Dow, E., and Wang, Q., “Active Subspace Methods in Theory and Practice: Applications to Kriging Surfaces”, *SIAM Journal of Scientific Computing*, Vol. 36, No. 4, pp. A1500-A1524. DOI: 10.1137/130916138